

Microscale analysis systems for the study of proteins and proteases

by

Kathleen Ann Sellens

B.S., McKendree University, 2012

AN ABSTRACT OF A DISSERTATION

submitted in partial fulfillment of the requirements for the degree

DOCTOR OF PHILOSOPHY

Department of Chemistry
College of Arts and Sciences

KANSAS STATE UNIVERSITY
Manhattan, Kansas

2018

Abstract

In research and industry, almost all chemical analysis methods involve the separation and detection of compounds. Typically, these separations are performed using traditional methods that require volumes in the 10 μL to 10 mL range of sample and in the 200 mL to 2 L range for solvents. These methods are not suitable for low-concentration, volume-limited samples frequently associated with biochemical studies. One way to overcome these limitations is to move the separation and detection to the microscale. The use of the microscale separation technologies enables the study of biological systems that have, until now, been out of reach due to their small volumes or low concentrations. The research presented in this dissertation will discuss two examples of this shift to microscale separation technologies which can solve some small volume sample challenges. These include the detection of protease activity in blood samples for use in cancer detection and the identification of immune system cascade proteins in the mosquito *Anopheles gambiae*.

In Chapter 2 a microfluidic method and device is proposed to monitor protease activities for cancer detection. In this method nanobiosensors are used to measure enzyme activity in biological fluids. These nanobiosensors consist of iron-iron oxide magnetic nanoparticles that are attached to peptide substrates specific for proteases through a disulfide bond. The nanobiosensors are controlled using a neodymium magnet which is attached through a 3D printed adaptor to a rotating motor for mixing and a linear stage to move the nanoparticles between different sections of the device. The separation and detection sections of the device are explained in Chapter 3.

Chapter 3 describes the fabrication and optimization of a simple device for microfluidic isoelectric focusing(IEF). IEF is a separation method in which analytes are separated based upon

their isoelectric, i.e. neutral charge, points. A reducing agent can be added to the IEF buffer to detach the nanoparticle from the peptide substrate, releasing it for focusing. IEF is also a concentration as well as separation method that will allow the peptide substrates to be focused up to 10^6 fold. It has a high peak capacity and produces reliable, reproducible separation patterns based on the isoelectric point of the peptide. To meet the detection limits required for cancer detection with proteases, scanning laser induced fluorescence is selected as the method of detection. This scanning system can monitor the separation over time to observe the parameters affecting the separation which cannot be done with typical point or imaging detection systems and allows better separation. This custom automatic detection system can distinguish focused samples of 500 fM from the background with minimal noise from the scanning system.

In Chapter 4 the identification of serine protease and inhibitor binding complexes in *A. gambiae* hemolymph using magnetic bead immunoaffinity chromatography was attempted. These proteases play a key role in the insect innate immunity system and form irreversible complexes. These complexes can be purified from a complex hemolymph sample using an antibody to one of the complex members. To separate the complexes from the hemolymph, Serpin 2 antibodies were attached to protein A coated magnetic beads and then incubated with the hemolymph. Once the purified complexes and Serpin 2 were eluted, the purified proteases were identified on Orbitrap MS. In an attempt to simplify the isolation of the complexes, a magnetic bead mixing rotor column was developed to help reduce the volume of the elution to increase the concentration. This method, however, was not robust and did not improve the concentration.

Microscale analysis systems for the study of proteins and proteases

by

Kathleen Ann Sellens

B.S., McKendree University, 2012

A DISSERTATION

submitted in partial fulfillment of the requirements for the degree

DOCTOR OF PHILOSOPHY

Department of Chemistry
College of Arts and Sciences

KANSAS STATE UNIVERSITY
Manhattan, Kansas

2018

Approved by:

Major Professor
Christopher T. Culbertson

Copyright

© Kathleen Ann Sellens 2018.

Abstract

In research and industry, almost all chemical analysis methods involve the separation and detection of compounds. Typically, these separations are performed using traditional methods that require volumes in the 10 μL to 10 mL range of sample and in the 200 mL to 2 L range for solvents. These methods are not suitable for low-concentration, volume-limited samples frequently associated with biochemical studies. One way to overcome these limitations is to move the separation and detection to the microscale. The use of the microscale separation technologies enables the study of biological systems that have, until now, been out of reach due to their small volumes or low concentrations. The research presented in this dissertation will discuss two examples of this shift to microscale separation technologies which can solve some small volume sample challenges. These include the detection of protease activity in blood samples for use in cancer detection and the identification of immune system cascade proteins in the mosquito *Anopheles gambiae*.

In Chapter 2 a microfluidic method and device is proposed to monitor protease activities for cancer detection. In this method nanobiosensors are used to measure enzyme activity in biological fluids. These nanobiosensors consist of iron-iron oxide magnetic nanoparticles that are attached to peptide substrates specific for proteases through a disulfide bond. The nanobiosensors are controlled using a neodymium magnet which is attached through a 3D printed adaptor to a rotating motor for mixing and a linear stage to move the nanoparticles between different sections of the device. The separation and detection sections of the device are explained in Chapter 3.

Chapter 3 describes the fabrication and optimization of a simple device for microfluidic isoelectric focusing(IEF). IEF is a separation method in which analytes are separated based upon

their isoelectric, i.e. neutral charge, points. A reducing agent can be added to the IEF buffer to detach the nanoparticle from the peptide substrate, releasing it for focusing. IEF is also a concentration as well as separation method that will allow the peptide substrates to be focused up to 10^6 fold. It has a high peak capacity and produces reliable, reproducible separation patterns based on the isoelectric point of the peptide. To meet the detection limits required for cancer detection with proteases, scanning laser induced fluorescence is selected as the method of detection. This scanning system can monitor the separation over time to observe the parameters affecting the separation which cannot be done with typical point or imaging detection systems and allows for better separation. This custom automatic detection system can distinguish focused samples of 500 fM from the background with minimal noise from the scanning system.

In Chapter 4 the identification of serine protease and inhibitor binding complexes in *A. gambiae* hemolymph using magnetic bead immunoaffinity chromatography was attempted. These proteases play a key role in the insect innate immunity system and form irreversible complexes. These complexes can be purified from a complex hemolymph sample using an antibody to one of the complex members. To separate the complexes from the hemolymph, Serpin 2 antibodies were attached to protein A coated magnetic beads and then incubated with the hemolymph. Once the purified complexes and Serpin 2 were eluted, the purified proteases were identified on Orbitrap MS. In an attempt to simplify the isolation of the complexes, a magnetic bead mixing rotor column was developed to help reduce the volume of the elution to increase the concentration. This method, however, was not robust and did not improve the concentration.

Table of Contents

List of Figures	xii
List of Tables	xv
Acknowledgements	xvi
Chapter 1 : Introduction	1
Analytical Separations	1
Liquid Chromatography.....	1
Separation Parameters.....	6
Plate Height.....	6
Plate Number	10
Resolution	11
Peak Capacity.....	13
Electrically Driven Flow.....	13
Electrophoresis.....	13
Isoelectric Focusing	18
Basic Principle	18
pH Gradient Formation and Carrier Ampholytes	20
Electric Field.....	24
Peptide and Protein Considerations	25
Gradient Distortion	26
Detection for IEF	27
Laser Induced Fluorescence.....	29
Microfluidics.....	30
Conclusion	33
Chapter 2 : Cancer detection via nanobiosensors using isoelectric focusing	34
Introduction.....	34
Background.....	35
Cancer	35
Nanobiosensors	37
Point of Care Devices	42

Sample Preparation and Handling	44
Separation	44
Detection	45
Automation	45
Conclusion	46
Chapter 3 : A whole channel scanning fluorescence microfluidic isoelectric focusing	47
Introduction.....	47
Materials	49
Methods	49
Linear Scanning Detection System.....	49
Fabrication of PDMS Microfluidic Isoelectric Focusing Device	50
Fabrication of Glass Microfluidic Isoelectric Focusing Device	50
Peptide Substrate and pI Markers Synthesis.....	51
pI Marker Fluorescence Labeling.....	51
Trypsin Digestion.....	52
HPLC Testing	52
Isoelectric Focusing	53
Results.....	54
Scanning Detector	54
Chip Material	56
pH Gradient Stability	58
Automated Voltage Control.....	61
pI Markers.....	61
Trypsin Digestion.....	65
Conclusion	67
Chapter 4 : Innate immune response studies on <i>Anopheles gambiae</i> via immunoaffinity chromatography and mass spectrometry	68
Introduction.....	68
Background.....	70
Malaria	70
Immune Response.....	71

Serpin Inhibition	71
Affinity Chromatography.....	73
Immunoaffinity Chromatography	74
Co-immunoprecipitation	75
Magnetic Bead Chromatography	75
Mass Spectrometry.....	77
Trypsin Digestion.....	79
Standard Biochemical Techniques.....	80
Methods	81
Insect rearing.....	81
Hemolymph Sample Collection	82
Purification of Serpin 2 Antisera	82
Procedure for In-tube Immunocapture and Separation.....	83
Mass Spectrometric Analysis.....	84
Database Searching.....	84
Criteria for Protein Identification.....	85
Online Immunocapture and Separation Device	85
Procedure for Rotor Immunocapture and Separation	86
Results.....	87
Hemolymph Sample Collection	87
Detergent effects on Non-Specific Binding	88
MALDI-TOF Contamination Testing.....	90
Immunoaffinity Western Blot Results	91
Mass Spectrometry Results.....	91
Initial Magnetic Bead Column Formation	92
Magnetic Bead Rotary Column	93
Conclusion	97
Funding	97
References.....	98
Appendix A : IEF Protocols and Programs.....	108
IEF on Chip Procedure	108

Trypsin Digestion of Peptides.....	109
Igor IEF Data Analysis Procedure	109
Igor Procedure Loader Code.....	112
Igor IEF Analysis Code	114
Appendix B : IEF and Microfluidic Protocols.....	118
Glass Etching for Microfluidic Devices	118
Photolithography Procedure	123
Appendix C : Mass Spectrometry Results for Serpin2 Co-IP Experiments	127
Appendix D : Figure Permissions	129

List of Figures

Figure 1.1: A plot of the van Deemter curves for the determination of optimum flow rate.	7
Figure 1.2: This figure shows how the electric double layer created by the negatively charged silica surface creates an excess of positive analytes near the surface that are then moved to the cathode when an external field is applied and thus create bulk fluid flow (EOF)	16
Figure 1.3: Shows magnitude of the electrophoretic and electroosmotic mobilities as well as the overall magnitude of the total mobility.	17
Figure 1.4: A schematic diagram showing the motion of charged molecules upon the application of an electric field in a pH gradient.	19
Figure 1.5: A graph of the continuous pH gradient that is formed upon application of an electric field in a channel filed with carrier ampholyte of the range of pH 3-10.	21
Figure 1.6: Chemical schemes for the synthesis of Ampholine™. ⁷	23
Figure 1.7: Chemical schemes for the synthesis of Servalyt™. ⁷	23
Figure 1.8: Schematic of pressure induced mobilization of IEF focused bands for single point detection.	28
Figure 1.9: Simplified epi-illumination laser induced fluorescence schematic.	29
Figure 2.1: Mechanistic scheme of the “light switch effect” upon proteolytic cleavage: the fluorophore is switched on due to the increase in distance between the Fe/Fe ₃ O ₄ core/shell nanoparticle, leading to decreased Förster Energy Transfer (FRET), k ₁ , and dipole-surface energy transfer (SET), k ₂ . Reproduced from Ref 41 with permission of The Royal Society of Chemistry. ⁴¹	38
Figure 2.2: Schematic for the design of peptide substrates for protease activity studies.	39
Figure 2.3: Diagram of the reducing agents (Left) Tris(3-hydroxypropyl) phosphine and (Right) Dithiothreitol.	40
Figure 2.4: A point of care device to diagnose and monitor neonatal jaundice in low-resource settings. Copyright 2017 National Academy of Sciences. ⁶⁰	42
Figure 2.5: (A) Sample and nanobiosensors are mixed and incubated; (B) Magnet moved nanobiosensors to the washing chamber; (C) Magnet moved to IEF chamber and disulfide linkage is reduced; (D) Magnet moved out of IEF chamber and IEF separation and detection is performed.	43

Figure 3.1: The prototypes IEF device with LabView control and automation for the detection of fluorescent peptides.	54
Figure 3.2: 3D printed PDMS blank hole punching with alignment tool.....	57
Figure 3.3: Scans of microfluidic chips made of PDMS channels (left) and glass channels (right)	57
Figure 3.4: Focused pI markers 3.99, 4.5, 6.86, and 9.5 in a glass chip at 5 nM concentration each. Sample (20 mM Arg, 0.11% Brij 35, 1% Servalyte Carrier Ampholyte, 0.4% Methyl Cellulose), $V_{\min}=300, V_{\max}=3300, V_{+}=600$, 10 $\mu\text{A/V}$ sensitivity, 100 Hz.	62
Figure 3.5: A graph of pI markers 3.99, 4.5, 6.86, and 9.5 in a glass chip at 5 nM concentration each. Sample (20 mM Arg, 0.11% Brij 35, 1% Servalyte Carrier Ampholyte, 0.4% Methyl Cellulose) to study the drift of the focused peaks over time.....	63
Figure 3.6: 3D graph of pI markers 3.99, 4.5, 6.86, and 9.5 in a glass chip at 5 nM concentration each. Sample (20 mM Arg, 0.11% Brij 35, 1% Servalyte Carrier Ampholyte, 0.4% Methyl Cellulose), $V_{\min}=300, V_{\max}=3300, V_{+}=600$, 10 $\mu\text{A/V}$ sensitivity, 100 Hz.	64
Figure 3.7: Graph of the LOD of pI 9.5 marker.....	65
Figure 3.8: Trypsin 4hr digestion results with pI markers 3.99 and 9.5 in a glass chip at 5 nM concentration each. Sample (20 mM Arg, 0.11% Brij 35, 1% Servalyte Carrier Ampholyte, 0.4% Methyl Cellulose)	66
Figure 3.9: HPLC results of Trypsin Digestion samples	66
Figure 4.1: A diagram of the transmission and lifecycle of the malaria parasite. Center of Disease Control. (2016). Global Health- Division of Parasitic Diseases and Malaria. About Malaria. Retrieved May 3, 2018, from https://www.cdc.gov/malaria/about/biology/ ⁷⁹	70
Figure 4.2: X-ray crystal structure of the covalent complex serpin and a protease. The serpin is rendered in orange and protease in red with the reactive center loop in blue. Reprinted with permission from Gettins, P. G. W., Serpin structure, mechanism, and function. Chemical Reviews (Washington, DC, United States), 102 (12), 4751-4803. Copyright 2002 American Chemical Society. ⁸⁹	72
Figure 4.3: Flowchart of general steps of the mosquito melanization cascade.	73
Figure 4.4: The standard immunoaffinity protocol with Serpin complexes as the antigen.	74
Figure 4.5: Schematic of MALDI desorption	77
Figure 4.6: A diagram of the Western blot procedure.	81

Figure 4.7: Left is the magnified side of a mosquito with the injection point labeled and right is the hemolymph collection after incubation into 1x Roche protease inhibitor	82
Figure 4.8: In-house mixing device for axis rotation.....	83
Figure 4.9: Left magnetic rotor for the mixing of magnetic beads and right diagram of the magnetic bead mixing device.....	86
Figure 4.10: A picture of the Western Blots used to determine which immune system challenge gave optimum complex formation.	87
Figure 4.11: A picture of a Western Blot of a sample that was collected with the optimized sample collection procedure. Using Image J, it was determined that each mosquito contained 1ng Serpin complex and 2.5ng Serpin 2.....	88
Figure 4.12: A Western Blot and Silver Stain of the detergent washes and elution of the immunoaffinity protocol with four different methods of detergent washes. The methods were PBS, PBS + n-octyl- β -D-Glucopyranoside (Og) 0.7%, PBS + Og 0.35%, and PBS + TWEEN-20(PBST).	89
Figure 4.13: Western blot showing enrichment of serpin and complex from lane 5 and 7.....	91
Figure 4.14: This graph shows the consistency of the mass spectrometry results with the new sample collection and detergent washes.	92
Figure 4.15: Left the initial magnetic bead column creation. Right the initial setup for the simple magnetic bead column	93
Figure 4.16: The bead trap device used in for SISCAPA Peptide Enrichment. A) side view; B) schematic diagram; C) top view. This figure was originally published in Molecular & Cellular Proteomics. N. Leigh Anderson, Angela Jackson, Derek Smith, Darryl Hardie, Christoph Borchers and Terry W. Pearson. SISCAPA Peptide Enrichment on Magnetic Beads Using an In-line Bead Trap Device. Mol Cell Proteomics. 2009; Vol: 995–1005. © the American Society for Biochemistry and Molecular Biology. ¹²²	94
Figure 4.17: The setup of the mixing device with the camera in place with a 10x magnification lenses for visualization.....	95
Figure 4.18: Western blot of the comparison of the in-tube elution to the rotor elution.	97

List of Tables

Table 2.1: 5 Year Survival Rates for Pancreatic and Breast Cancers	35
Table 3.1: Peptide sequences and pI's for IEF	51
Table 3.2: Analysis of background and noise of the detection system	55
Table 3.3: Analysis of the signal to noise ratio of different microfluidic chip materials	56
Table 3.4: Drift analysis of different compositions of anolyte and catholyte solutions	59
Table 4.1: Lane identifications for the study of detergent effects on the IEF separation	89

Acknowledgements

I would like to thank the Department of Chemistry, Kansas State University, for offering me admission to the Chemistry graduate program and supporting me as a Graduate Teaching Assistant at Kansas State in which I gained valuable experience in teaching chemistry. Thank you for the grants and scholarships that comfortably saw me through the graduate program.

I would also like to thank my advisor, Dr. Christopher Culbertson. Thank you for the opportunity you gave me to work in your group. I appreciate the opportunities I had to learn so many analytical techniques and the time I was given to follow my ideas to improve my project by learning new skills. Thanks for all the opportunities you provided.

I would also like to say thank you to the Culbertson group members, past and present, (including all of the undergraduate researchers and summer interns) who have made the lab a fun place to work. Thanks to Jay for all of the conversations about each of our separate projects. We came up with so many ideas that I don't think either of us would have come to on our own.

I would not have been able to follow through with my out of the box ideas without the time and experience that Ron, Tobe and Jim provided, so thanks for all your help.

I would like to thank Dr. Stefan Bossmann and his group members for all of their help with the peptide synthesis and the optimization of that process. I also appreciated all of the conversations that helped me come up with ideas to improve the IEF separation.

I would also like to thank Dr. Kristin Michel and Prof. Mike Kanost for allowing me to work in their labs and for providing direction and ideas with the insect hemolymph experiments. I am particularly grateful to their post-doctoral fellows: Drs. Maurine Gorman, Neil Dittmer, and Xin Zhang, for training me in hemolymph collection and routine biochemistry procedures (SDS-PAGE, gel staining, etc) and all the helpful discussions we had.

Chapter 1: Introduction

Analytical Separations

The ability to separate, detect, and quantify compounds is vitally important for most scientific research as well as in most industries. Healthcare and environmental studies are of great interest to scientists thus new methods for investigating biological samples are of significant concern. The separation of biological compounds is typically performed via either chromatographic or electrophoretic methods. These methods include liquid chromatography, affinity chromatography and isoelectric focusing. Analyte detection after separation is most often performed by spectroscopy including absorbance, fluorescence or mass spectrometry. When choosing an analytical method, the speed, ease and convenience, skill required of operator, cost and availability of equipment, and per sample cost must be considered.¹ The method must also be robust, sensitive, selective, accurate, and precise. In the subsequent chapters the development of a device for the early detection of cancer using nanobiosensors and microfluidic isoelectric focusing with scanning laser induced fluorescence will be discussed that has the potential to fulfill many of the requirements stated above. Also, the method development and results for the identification of protease and inhibitor complexes in *Anopheles gambiae* hemolymph using immunoaffinity chromatography will be described in Chapter 4.

Liquid Chromatography

One of the most widely used of the traditional methods of separations for biological compounds is liquid chromatography. This is due to its sensitivity, robustness, ease of automation, suitability for separating non-volatile and thermally fragile biological analytes, ability to integrate a variety of detection systems, and the capability of quantification.¹ High performance liquid chromatography (HPLC) is a method that is used to separate, identify, and quantify each

component in a mixture of analytes and contaminants. The key components in the separation of analytes by HPLC are the stationary phase and the mobile phase.

Some considerations that must be accounted for when developing a separation method, include that the separation should generate a baseline separation of the analytes and have a sufficient peak capacity to separate all analytes and contaminants. This is done by maximizing the differential transport between the species. This differential transport most often arises from interactions between analyte molecules and the stationary phase. These varying interactions are due to the differences in the intrinsic properties of the molecules which include mass, charge, intermolecular and intramolecular forces. In the case of high performance liquid chromatography, the main forces that are exploited are London dispersion forces and the hydrophobic character of the molecule.

The most commonly used type of HPLC column used is reversed phase. In this case, the stationary phase coating is nonpolar, and the mobile phase is polar. The stationary phase most commonly consists of long chain alkyl groups, such as octadecyl groups (C18), coated on a porous silica stationary phase support. The stationary phase support often consists of spherical particles that are 2-5 μm in diameter and are tightly and uniformly packed to create the column. The particle pore size is measured in angstroms (\AA) and generally ranges between 100-1000 \AA . 300 \AA is the most popular pore size for proteins and peptides and 100 \AA is the most common pore size for small molecules. The mobile phase is generally composed of two components consisting of water (component A) and an organic (component B) which is commonly acetonitrile for peptide samples. Additionally, an acid such as formic acid or trifluoroacetic acid is added at low concentrations of 0.1%. This improves the chromatographic peak shape as an ion pairing reagent. The addition of an acid also provides a source of protons in reverse phase LC-

MS. This acid is required for mass spectrometry as the molecules must be ionized and for protein and peptide analysis the positive ionization mode is used. Thus, the acid in the mobile phase is used to create positive ions. The acidic pH is also used to minimize the interactions between the analytes and free silanol on the stationary phase support.

The two components, A and B, are mixed to create the mobile phase for the separation.

Typically, to achieve high resolution, the composition of the mobile phase is altered using a gradient from aqueous (hydrophilic) at the beginning of the separation to organic (hydrophobic) at the end of the separation. This allows increased retention on the hydrophobic stationary phase at the beginning of the separation and complete elution of the most hydrophobic analytes at the end. Further explanation is available in the resolution section that follows.

HPLC's are typically modular in design and generally include the solvent reservoir(s), a mobile phase pump, injector-autosampler, column and detector. The instrument has special fittings that allow for high pressure and thus higher flow rates which often increases the resolution of the separation.

One of the main criteria for liquid chromatography is that the sample must be soluble in the mobile phase at all solvent compositions. If it is not soluble, another method or solvent system must be utilized. Another concern is the presence of solid particles in the solvent and injected sample. If there are particles in the solvent, the pump head can be scratched and cause cavitation in the flow. This would generate unstable flow and decrease the resolution of the separation through excessive band broadening. Solid particles in the system, if they reach the column, can also disrupt the flow of the column which would cause problems in the separation as discussed in the next section. However, there are typically short guard columns in place to prevent this from

occurring. Also, to prevent these issues solvents are purchased prefiltered and all samples are filtered with a 0.2- 0.5 μm syringe filter.

The main advantages for HPLC are the moderate speed (minutes or seconds), high resolution, high sensitivity, high accuracy, the ability to modify the selectivity using mobile phase and stationary phase changes and the use of automated systems (unattended operation, from sample prep to report generation).²

When considering detection methods for any separation, there are four main figures of merit that must be considered for the technique. Sensitivity is the ratio of the detector response to the amount of analyte introduced. The best detector choice should be sensitive to the analyte and small differences in concentration should result in measurable differences in detection signal. Related to the sensitivity, the limit of detection (LOD) is the amount of analyte that results in a peak that is 3 times higher than the noise of the system.³

The third figure of merit that should be considered when choosing a detector is the selectivity of the system. Selectivity is a measure of which components such as functional groups, atoms, or other properties make the detector respond. The option when choosing a detector is between a universal detector or a selective detector. A universal detector can detect all molecules, but if the sample is complex there will be many peaks that are not of interest. However, if a selective detector is chosen then minimal information is gathered on other molecules in the sample other than the analytes of interest and contaminants cannot be detected.

The final figure of merit is the dynamic range of the detector. The dynamic range is the concentration range over which the detector provides a linear response. This ranges from the LOD to the point at which the response becomes non-linear at high concentrations.

The most common detector in most HPLC systems is absorbance based. This is simple and rugged detector as all that is needed is a light source, prism or diffraction grating to choose the wavelength and a photodiode array for detection. Beers law (Equation 1)² is used to calculate the concentration of a known molecule. Either a calibration curve must be created to calculate the molar absorptivity or there must be a literature value with the same conditions as the measurement and molecule in question.

Equation 1: $A = -\log T = \log \frac{P_0}{P} = \epsilon bc$, where A is the absorbance, T is the transmittance, P₀ is the incident light power, P is the transmitted light power, ϵ is the molar absorptivity, b is the pathlength and c is the concentration.

The main limitation with absorbance-based detection is that it is not a universal detector and for visible wavelength detection the analyte must contain a chromophore. UV detection is more universal but often the materials that the system is made of, as well as many common solvents, absorb light at wavelengths below 190 nm which can limit the usefulness when detecting compounds like peptides. Also, the typical LOD for absorbance based detection is in the range of 10^{-5} - 10^{-6} mol/L (μ M) which limits the system to detection of more concentrated analytes.

HPLC with absorbance detection is often used to purify compounds as absorbance is a non-destructive detection method that allows for collection of the separated and purified compounds. This technique is commonly used for the purification of proteins and peptides that are synthesized in a laboratory setting. These compounds can be detected at 205 nm for the peptide backbone (double bond character) and 280 nm for the detection of tyrosine and tryptophan (aromatic ring character).

Separation Parameters

There are many parameters that are used to describe the extent of separation from a method. Some of these parameters are the height equivalence of a theoretical plate (H), number of theoretical plates (i.e. separation efficiency, N), variance (σ^2), resolution (R_s), selectivity (α), sensitivity and peak capacity (n).

Plate Height

The term plate height (H) was developed in a theoretical study by Martin and Synge. In this study, they described a distillation column where plates were defined as the imaginary zones of narrow layers where the analyte moves from the stationary phase of the separation to the mobile phase.⁴ The smaller the plate height for the separation, the more plates there were and the larger the separation between adjacent analytes and thus the better separation efficiency. In a packed separation column, such as those found in HPLC, one of the most useful equations is the van Deemter equation. This equation categorizes band broadening phenomena into three classes/types. These phenomena include band broadening due to column packing, diffusion, and mass transfer. When the variables of the van Deemter equation are optimized, the separation between two species can be increased (Equation 2)². The equation can also be used to examine the factors that affect band broadening in open tubular columns such as gas chromatography as well as capillary electrophoresis.

Equation 2: $H = A + \frac{B}{u} + (C_s + C_m)u$ where H is the height of theoretical plates, A is the influence of column packing, B is the influence of diffusion, C_s is the influence of the resistance of mass transfer from the stationary phase, C_m is the influence of the resistance of mass transfer from the mobile phase and u is the linear velocity or flow rate.

Often either the volumetric flow rate or linear velocity are variables used in the van Deemter equation, but the linear velocity is not often a measured value in HPLC. A more commonly

reported variable is the flow rate which is proportional in a given column to the linear velocity as seen in Equation 3.²

Equation 3: $F = uA_c$ where F is the flow rate, u is the linear velocity and A_c is the cross-sectional area of the column

The linear velocity can also be calculated chromatographically by measuring the retention time of an unretained compound and then using Equation 4²

Equation 4: $u = \frac{L}{t_M}$ where L is the length of the packed column and t_M is the retention time of an unretained solute.

The van Deemter equation (Equation 2) is often used to determine the ideal flow rate for a separation by plotting H as a function of u as seen in Figure 1.1.⁵

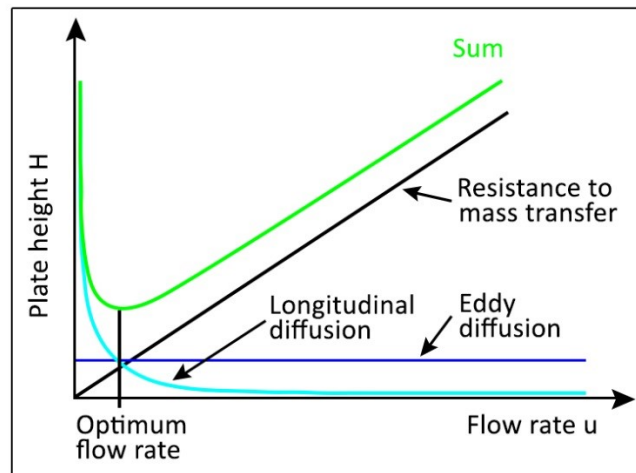


Figure 1.1: A plot of the van Deemter curves for the determination of optimum flow rate. To maximize the separation efficiency, the plate height must be minimized which results in tall, narrow peaks. To minimize the plate height each of the terms of the van Deemter equation should be as small as possible.

The A term, also known as the multipath term, comes from the multitude of paths that an analyte can travel throughout a packed column. Since the length of these paths can differ significantly, the molecules of analyte will exit the column at various times. This causes a broadening of the

eluted peak and the process is otherwise known as eddy diffusion. The magnitude of the multipath term depends upon the quality of the column packing as well as the diameter of the particles with Equation 5² showing the relationship between these factors.

Equation 5: $A = 2\lambda d_p$ where λ is a constant that depends of the quality of the column packing at d_p is the diameter of the particles in cm.

To minimize the A term, smaller particles should be used, and they should be packed as tight as possible. However, the smaller the particle the higher the pressure at a given flow rate ($\Delta P \propto \frac{1}{d_p^2}$ and ΔP at $u_{opt} \propto \frac{1}{d_p^3}$) therefore, there is an upper pressure limit set for most instruments to prevent leaking in valves and connections. If this upper pressure limit is reached, then the more modern instruments will automatically set off an alarm and turn off the mobile phase pump to prevent system damage.

The second term, $\frac{B}{u}$, is known as the longitudinal diffusion term. This term describes the diffusion of molecules from areas of high concentration to low concentration.² This diffusion leads to an injected band of molecules forming into a gaussian shape over time. On either side of the highly concentrated band the molecules diffuse into the mobile phase which is of lower concentration and thus the Gaussian shape is formed.² The standard deviation of the band, σ is equal to the distance from the center of the Gaussian profile to the point of inflection and the base width is approximately 4σ . The relationship between the width of the band and the time over which diffusion is occurs is the variance (σ), and is given by the Einstein-Smoluchowski equation².

Equation 6: $\sigma^2 = 2Dt$ where D is the diffusion coefficient and t is time.

Equation 7: $D = \frac{kT}{6\pi\eta r}$ where k is Boltzmann's constant, η is the viscosity, T is the temperature in Kelvin and r is the radius

When calculating the plate height, the B term is inversely proportional to the flow rate because if the flow rate is faster, then the molecules will reside in the column for a shorter time and thus there will be less time available for the spreading of the band. From Equation 8² it can be determined that a small diffusion coefficient would be preferable, however this is difficult to minimize in HPLC as the easiest method to lower the diffusion coefficient is to increase the viscosity of the mobile phase.

Equation 8: $\frac{B}{u} = \frac{2\gamma D_M}{u}$ where γ is the obstruction factor that arises from packed columns and D_M is the diffusion coefficient in the mobile phase

Increasing the viscosity of the mobile phase would be detrimental to all the other factors that affect the separation and thus is not typically done. Since the B term is divided by the flow rate a larger flow rate also minimizes the plate height, however as discussed before there is a limit to how high the flow rate can be for any given instrument.

The C_s term, also called the mass transfer of the stationary phase term, relates to the sorption and desorption of the solute into and out of the stationary phase. As the solute partitions into the stationary phase, the flow is still proceeding which continues to move the remaining solute through the column. When the solute desorbs out of the stationary phase it is the further away from the band of the most concentrated molecules. This leads to band broadening which is detrimental to the separation.

Equation 9: $C_s = \frac{8}{\pi^2} \frac{k}{(1+k)^2} \frac{d_f^2}{D_s}$ where k is retention factor, d_f is the average film thickness of the stationary phase and D_s is the diffusion coefficient in the stationary phase

To minimize the effects of the C_s term the film thickness should be thin to increase the kinetics.²

The C_m term, also called the mass transfer of the mobile phase term, relates to the sorption and desorption of the solute into and out of the mobile phase. Individual solute molecules may spend

more time in the slow-moving regions of the column and arrive at the column exit after another molecule that was, on average, in the higher velocity regions. This solute dispersion is decreased by fast lateral diffusion which causes better mixing between flow streams, and less zone broadening. The equation that describes these phenomena is known as the Golay equation and it relates the diameter of the column(d_c) to the retention factor(k) and the diffusion of the solvent in the mobile phase(D_M) (Equation 10)².

Equation 10:
$$C_m = \frac{(1+6k+11k^2)d_c^2}{96(1+k)^2D_M}$$

From Equation 10 it can be determined that small diameter columns minimize broadening because the mass transfer distances are relatively small. Similarly, large diffusion coefficients promote mixing and decrease broadening.²

Overall to decrease the plate height for packed columns the most important variables to decrease are the diameter of the particles and the thickness of the film that make up the column packing. Otherwise, the main parameters to optimize are the flow rate and the mobile phase composition which will be discussed in the next section.

Plate Number

To relate the plate height to the overall length of the column, the number of theoretical plates is used. This value can be calculated via Equation 11.⁶

Equation 11: $H = \frac{L}{N}$ where **H is the plate height, L is the column length and N is the number of theoretical plates.**

The number of theoretical plates is related to the number of times the solute partitions in and out of the stationary phase over the length of the column. Therefore, the higher the number of plates the greater the degree of separation of the method. To calculate the number of theoretical plates

experimentally Equation 12¹ can be used to relate the retention time of the peak (t_r) to the width of the peak at half of its height ($W_{1/2}$).

$$\text{Equation 12: } N = 5.54 \left(\frac{t_r}{W_{1/2}} \right)^2$$

Equation 12 is an approximation and only works for gaussian shaped peaks without any skew in the form of peak fronting or tailing however, it is very useful to use when examining a separation after completion of the method as well as examining other researchers results.

Resolution

In addition to the plate height and number, there are a few other parameters that are often used when analyzing and developing a separation method. One example is the resolution of a separation which is defined by how well adjacent peaks are separated. In a chromatographic separation the distance between the peaks and the width of the peaks are used to calculate the resolution.

Equation 13: $R_s = \frac{2(t_{r1}-t_{r2})}{(w_1+w_2)}$ where t_{r1} and t_{r2} are the respective retention times of two adjacent peaks and the w_1 and w_2 are the corresponding base line widths.

Another option to calculate the resolution is to use the capacity and selectivity factors. This is a more theoretical method which is useful when analyzing the effects of multiple variables on the resolution. The capacity factor (k') describes the velocity of the analyte relative to that of the mobile phase.¹

Equation 14: $k' = \frac{t_r - t_o}{t_o}$ where t_r is the retention time and t_o is the solvent elution time

If the capacity factor is less than one, then the retention time of the analyte would be too small for exact determination as it would elute with the unretained solute (t_M). If the value of k' is large, the analyte will move very slowly and take more time to elute thus the method will use an

excessive amount of the instrumentation time and one of the optimum criteria for a separation is that it should be fast. The ideal value for capacity factor is between one and five.¹ Other books suggest that the ideal values are between two and seven as this allows for more separation at the beginning and wider peaks at the end of the separation.

The selectivity factor for a given separation describes the relative velocity between two analytes and gives a measure on how well the method discriminates between the two species.

$$\text{Equation 15: } \alpha = \frac{k'_2}{k'_1} = \frac{t_{r2} - t_o}{t_{r1} - t_o}$$

When the capacity and selectivity factors are used, the resolution can be defined as in Equation 16¹ which shows that the capacity factor has a significant effect on the resolution of the overall separation method.

$$\text{Equation 16: } R_s = \frac{\sqrt{N}}{4} (\alpha - 1) \left[\frac{k'}{1+k'} \right]$$

This equation explains the general elution problem where if a separation is optimized so that early eluting compounds have small k' then the later eluting compounds will have excessive band broadening and thus poor resolution. Also, in reverse if the separation is optimized for late eluting compounds then the early compounds will have poor resolution. This problem is overcome in HPLC by creating a gradient over the course of the experiment that decreases k' for the later eluting compounds. This is typically done in HPLC by changing the composition of the mobile phase.⁵ The mobile phase for reverse phase typically starts with high percentage water to help retain compounds on the hydrophobic stationary phase. As time proceeds in the separation, the amount of organic modifier (typically acetonitrile) is increased to release the hydrophobic compounds from the stationary phase, as they will then have a higher affinity to the mobile phase.

Peak Capacity

The last main parameter that is often used when describing a chromatographic separation is the peak capacity. Peak capacity is defined by the maximum number of peaks that can be separated in a column of defined length L as seen in Equation 17.¹

Equation 17: $n_c = \frac{L}{w} = \frac{L}{4\sigma}$ where n_c is the number of peaks and w is the peak width

Often peak capacity is a better parameter to report in complex samples as it defines how many analytes can be separated rather than just the separation between two peaks. The peak capacity can be used to give an approximation of the number of components (analytes and contaminants) that can be separated under a specific set of conditions, if this peak capacity is lower than the number of components in a sample, then the method is incapable of producing a chromatogram with all peaks resolved from one another.

Electrically Driven Flow

Electrophoresis

Biological molecules can also be separated through the use of electrophoresis.

Electrophoresis is the movement of charged particles within an applied electric field and is a commonly used method of inducing separation in capillary and microfluidic devices.

Electrophoretic separation is based on differences in mobility that analytes exhibit in an applied electric field due to size and charge differences among the analytes. It can be used to separate proteins, nucleic acids, amino acids and carbohydrates and works particularly well with large molecules.

To perform electrophoresis the analytes are placed in a conductive buffer. An electric field is then applied axially along a capillary channel by placing electrodes in the buffer reservoirs on either side of the capillary. The high electric field generates electrostatic forces on the ionic

species in solution causing them to migrate toward the electrode that is opposite their charge. i.e. positively charged species (cations) move toward the cathode, and negatively charged molecules (anions) move toward the anode. The electrostatic force on a charged species can be described using Equation 18.¹

Equation 18: $F = qE$ where F is the force, q is the charge of the ions and E is the applied field strength

The field strength is determined by the voltage applied along the channel and the length of the channel as shown in Equation 19.

Equation 19: $E = \frac{V}{L}$ where V is the voltage applied and L is the length of the channel

In addition to the electrostatic force, a drag force is also exerted on the migrating species. The drag force is oriented in the opposite direction to the electrostatic force and is due to the friction from the species moving through the medium. The magnitude of the drag force (described by Equation 20)¹ depends upon both the velocity of the ionic species (v_{ep}) as well as the viscosity of the medium (η).

Equation 20: $F = 6\pi\eta r v_{ep}$ where η is the solution viscosity, r is the particle radius and v_{ep} is the electrophoretic velocity

When the electric field is applied, the species accelerate to their electrophoretic velocity and the magnitude of the drag force is then equal to the electrostatic force. Thus, the two equations can be set equal to each other and rearranged to solve for the electrophoretic velocity.

Equation 21: $v_{ep} = \frac{qE}{6\pi\eta r}$

The constant terms on the right side of the equation can be grouped into a new term called the electrophoretic mobility which is given in Equation 22⁵

Equation 22: $\mu_{ep} = \frac{v_{ep}}{E} = \frac{q}{6\pi\eta r}$, where v_{ep} is the migration velocity, E is the electric field strength, q is the ion charge, η is the viscosity of the medium, and r is the radius of the ion.

The electrophoretic mobility μ_{ep} is directly proportional to the charge and inversely proportional to the molecule's effective hydrodynamic radius. Therefore, a smaller molecule with higher charge will have a higher electrophoretic mobility than a larger molecule with a lower charge and a lower mobility. This difference in mobility can induce a separation, however, in an electrophoretic separation there is a major secondary force that affects the motion of molecules in the channel.

This secondary force is the electroosmotic flow (EOF) in the channel. EOF arises from the fact that most channel materials carry a charge. In the case of glass, the surface is negatively charged above a pH of 3 due to the presence of deprotonated silanol groups. These negative ions attract cations from the solution and create an electric double layer. The electric double layer, according to the Gouy-Chapman model, consists of two main components. The Helmholtz (fixed) layer is made of adsorbed cations along the negatively charged wall of the channel. The second layer is the diffuse layer which is mainly cations in the solution. This layer decays rapidly (typically 1 nm to 100 nm wide) into the bulk solution where standard electroneutrality laws are observed. The diffuse layer next to the charged surface contains more positive charge ions than the bulk solution, and thus the positive charges are attracted to the cathode. The viscous drag from this motion of ions causes bulk flow to the cathode.

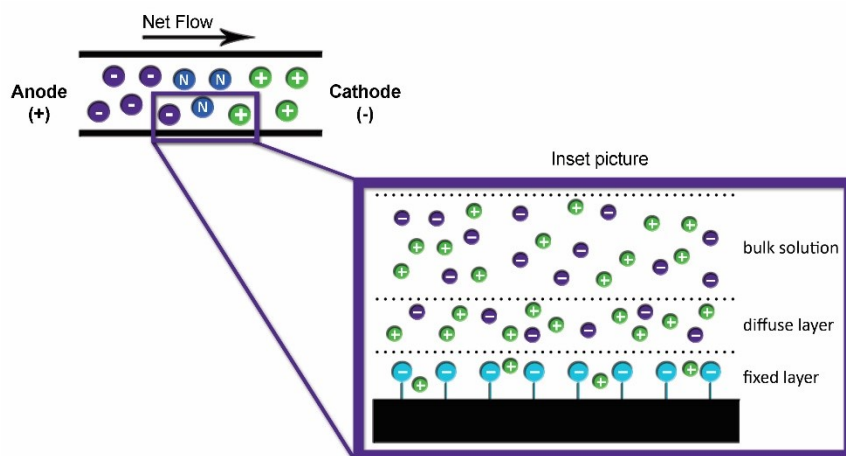


Figure 1.2: This figure shows how the electric double layer created by the negatively charged silica surface creates an excess of positive analytes near the surface that are then moved to the cathode when an external field is applied and thus create bulk fluid flow (EOF)

The EO mobility can be calculated using Equation 23 by determining the velocity of a neutral compound.

Equation 23: $v_{EOF} = \mu_{EOF}E = \frac{\epsilon\xi}{\eta}E$, where v_{ep} is the EOF velocity, E is the electric field strength, ϵ is the dielectric constant, ξ is the zeta potential of the buffer and η is the viscosity of the buffer.

The electroosmotic mobility does not depend of the charge of the molecule as seen in Equation 23 ⁵, therefore all molecules in the same channel will have the same μ_{EOF} . Whereas the electrophoretic mobility is highly dependent on both the charge of the molecule for the direction of mobility, and the magnitude of the charge for the magnitude of the mobility as q is in the numerator of Equation 22.

As seen in Figure 1.3 when the two main mobilities of electrophoresis (EP and EOF) are added together, in the cases of a glass channel, the mobility of the EOF from the bulk flow will overcome the electrophoretic mobility for the negatively charges molecules so that the total mobility will move all of the ions towards the cathode for detection and separation. Thus, single-point detector can be used to detect molecules of all charges in most cases.

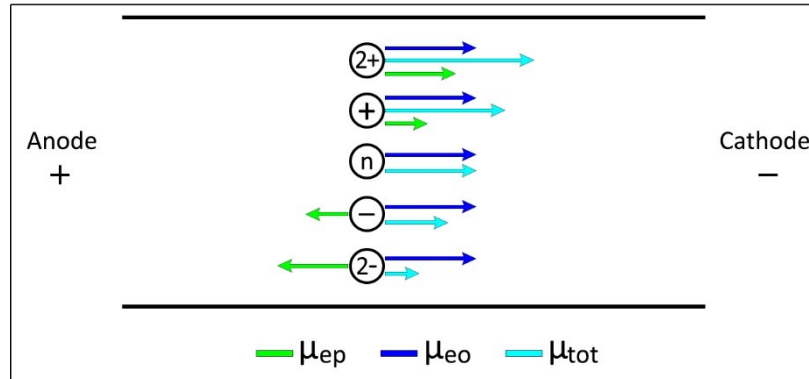


Figure 1.3: Shows magnitude of the electrophoretic and electroosmotic mobilities as well as the overall magnitude of the total mobility.

The EOF can be diminished in a glass channel by using a buffer of low pH that is less than four so that the silanol groups are protonated. This is not an option with protein studies as many proteins can denature at low pH and therefore lose function. The other option is to chemically modify the surface with hydrophobic functional groups to suppress EOF, however, these modifications typically have poor long-term stability. A dynamic coating of a polymer can also be used to create a viscous layer, and the viscosity of the run buffer can be increased. Surfactants can also be used to modify the surface charge at low concentrations below the CMC and used to increase or decrease EOF.

Band broadening is the spreading out of a group of the same molecular species as they move through a chromatography column. In many cases the main source of band broadening is diffusion, however, the main cause of excess band broadening and therefore loss of resolution in electrophoresis is a phenomenon known as Joule heating. Joule heating occurs when the current passes through the running buffer and there is a voltage drop. The power lost from this effect can be calculated from the voltage drop using Equation 24.⁵

Equation 24: $P = (V_A - V_B)I$ where P is the power converted from electrical to thermal energy, $V_A - V_B$ is the voltage drop across the element and I is the current through the element

This heating causes a temperature gradient across the cross section of the channel and can cause convective flow of the buffer which can lead to band broadening of the analytes. If the temperature reaches the boiling point of the buffer, then there will be excess bubble formation which is detrimental to the separation. To mitigate these temperature effects the electric field can be decreased to thus decrease the current, or a lower conductivity buffer can be used to which would also decrease the current. Another option is to choose geometries of the separation channel to have large surface-to-volume ratios to allow the channel material to dissipate the heat. Most materials used in microfluidic applications are partially chosen for their heat sink capabilities along with other favorable material properties.

A subtype of electrophoretic separations is isoelectric focusing which combines electrophoresis as well as pH gradient formation to separate zwitterionic biological compounds.

Isoelectric Focusing

Basic Principle

Isoelectric focusing (IEF) is an electrophoretic method that typically is performed under static conditions with minimized EOF. The underlying principle of IEF is the separation of analytes such as proteins based on their characteristic isoelectric point (pI), or the pH at which the molecule is neutrally charged. An approximation of the isoelectric point of a simple compound is determined from the average of its constituent pKa's as shown in Equation 25.

Equation 25: $pI = \frac{1}{2}(pK_i + pK_j)$, where pK_i and pK_j are the dissociation constants of the ionization steps involved. ⁵

Most compounds that are separated with IEF are peptides and proteins for which there are online calculators such as pepcalc.com to assist with the more complex calculations involved.

The way this calculator works is by determining the charge at pH 7 using Equation 26, then if the charge is positive it computes the charge at pH of 10.5, and if the charge negative then the charge at pH 3.5 is checked. This is repeated, using increments/decrements to halve the size of the previous pH, until the charge found equals 0, or is sufficiently close to 0 at which time the pH is then determined to be the pI of the peptide.

Equation 26: $Z = \sum_i N_i \frac{10^{pKa_i}}{10^{pH} + 10^{pKa_i}} - \sum_j N_j \frac{10^{pH}}{10^{pH} + 10^{pKa_j}}$ where N_i is the number, and pKa_i is the pKa values of the N-terminus and the side chains of Arginine, Lysine, and Histidine. The j-index pertain to the C-terminus and the Aspartic acid, Glutamic acid, Cysteine and Tyrosine amino acids.

There are a few limitations to this calculation. The residues are assumed to be independent of each other, only free termini and the 20 naturally occurring amino acids and their D-forms are considered, all others are ignored, and the resulting net charge depends on the pKa values from the CRC Handbook of Chemistry and Physics, 87th edition.

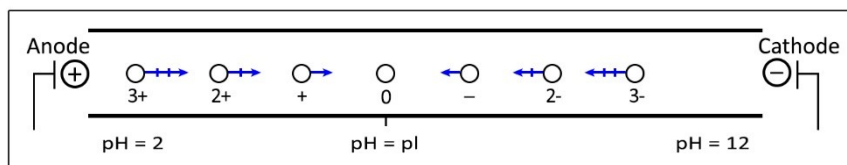


Figure 1.4: A schematic diagram showing the motion of charged molecules upon the application of an electric field in a pH gradient.

Isoelectric focusing of a peptide occurs when a sample that contains the analyte (often peptides or proteins) is placed in a channel that has reservoirs containing an acidic analyte at the anode and a basic catholyte at the cathode and an electric field is applied. If the peptide is in a pH region below its pI, then it will be positively charged and will migrate towards the cathode as seen in Figure 1.4. As it migrates through the gradient of increasing pH, the peptides overall charge will decrease until it is neutrally charged at the pH that is equal to its pI. When this occurs, the peptide will no longer move, in any appreciable manner, and the peptide will form a

sharp gaussian shaped focused band. If the peptide diffuses out of the band, it will become charged again and the electrophoretic motion of the peptide will move the peptide back into its neutral pH and it no longer has electrophoretic mobility. This process causes sharpening of the peaks and leads to very high resolution of the separated bands.

pH Gradient Formation and Carrier Ampholytes

There are a few methods by which the pH gradient can be formed. The first method that was developed used the electrolysis of water to create the acidic anode and basic cathode. In this process the buildup of acid and base diffused into the separation channel to create the pH gradient, however these gradients were not stable nor linear.⁷ A pH gradient for isoelectric focusing should be stable over time, reproducible, continuous, exist in a conductive medium and its shape, slope and range should be controllable. To stabilize and create linear pH gradients carrier ampholytes (CA's) were developed. They are called such as they carry charge and buffering capacity while also having defined pI's arising from possessing both basic and acidic functional groups.⁷

A CA is an amphoteric compound that under the electric field will migrate toward the electrode of the opposite charge. As this occurs, the H^+ from the anolyte and the OH^- from the catholyte travel toward the opposite electrode and a pH gradient develops. Slowly, as carrier ampholytes move into the gradient, they reach their pI and become neutrally charged, stop moving and concentrate. As the CA has a high buffering capacity at its pI (one of the criteria for a good carrier ampholyte), it will form a small pH plateau around its maximum concentration in a gaussian shape. If there are multiple CA's these pH gaussian distributions will overlap with other CA pH distributions and a continuous and stable pH gradient will be formed as shown in Figure 1.5.⁸

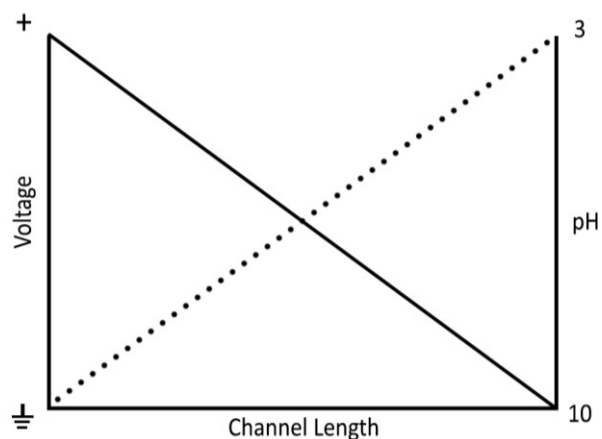


Figure 1.5: A graph of the continuous pH gradient that is formed upon application of an electric field in a channel filed with carrier ampholyte of the range of pH 3-10.

A good CA should have very high buffering capacity such that the $pI-pK$ should be less than 0.5 pH units. This small difference indicates sharp iso-ionic points. The iso-ionic point is the pH value at which a zwitterionic molecule has an equal number of positive and negative charges and no adherent ionic species. This need for sharp iso-ionic points means that virtually all amino acids are poor carrier ampholytes. For example, only glutamine and histidine would be acceptable, but glycine with a charge of zero over the range of pH 4-8 would not.⁹

The CA's should also have stable conductivity across the gradient to prevent thermal convection from Joule heating. The conductivity is again dependent on the carrier ampholyte being isoelectric between two closely spaced pK values and if the conductivity is particularly low between two carrier ampholytes then a high potential difference will form which will lead to heating in that area and thus loss of resolution.

Typically, these carrier ampholytes are used at concentrations of 2-4%(w/v) of the total sample or solution. This small amount is sufficient to stabilize the pH gradient while also keeping the conductivity low and thus allowing the application of higher electric fields without the loss of resolution from Joule heating.

The difference between proteins, which are the typical analytes in IEF, and the carrier ampholytes is that the proteins have a much lower buffering capacity and a much larger molecular weight than the typical CA. Therefore, since the buffering capacity per unit weight of proteins is much lower than the carrier ampholytes there is minimal pH gradient perturbation by the focusing of proteins overall in the system.

One aspect of IEF to consider is the resolving power which can be described by ΔpI (pI difference between two proteins that can be reasonably well resolved) in Equation 27.

Equation 27: $\Delta pI = 3 \sqrt{\frac{D(\frac{dpH}{dx})}{-E(\frac{du}{dpH})}}$ where D is the diffusion coefficient of the protein, E is the field strength (V/cm), dpH/dx is the pH gradient at the zone location and du/dpH is the (negative) mobility slope at the pI.

Good resolving power should be obtained with analytes with a low diffusion coefficient and shallow pH gradient as they are in the numerator in Equation 27. In addition, high electric field and high mobility slope are advantageous as they are in the denominator in Equation 27.

Furthermore, the high resolution possible with IEF depends primarily on the magnitude of the field strength as well as the number of different carrier ampholyte species present in the formation of the gradient. When the field strength is higher, then the electrophoretic velocity of the species is higher. This can be determined when Equation 22 is rearranged to show that the velocity is directly related to the electrophoretic mobility and the electric field. However, the field strength has a limitation in that the higher the field strength the more current and thus additional Joule heating. Due to the carrier ampholytes there can be variations of conductivity and thus voltage drops along the gradient and which can cause Joule heating and thus peak broadening in areas of the gradient. This can lead to loss of resolution in those areas. The

resolution also depends of the CA's that are chosen for the stabilization of the pH gradient. The higher the number of different individual carrier ampholyte species the smoother the pH gradient and thus the higher the capacity of the separation and the better the resolution. To separate two analytes of interest there must be at least one carrier ampholyte species with a pI in-between them. Otherwise the analytes will co-focus in the gaussian distribution of that pH. To increase the number of carrier ampholytes used in a separation multiple purchased CA's can be mixed as there are three different methods for their creation.

CA's are typically purchased commercially, but the simplest, AmpholinesTM, are made by reacting polyamine mixtures with acrylic acid to form a complex mixture of polyamino polycarboxylic acids which have pI's in the range of 3-10 Figure 1.6.

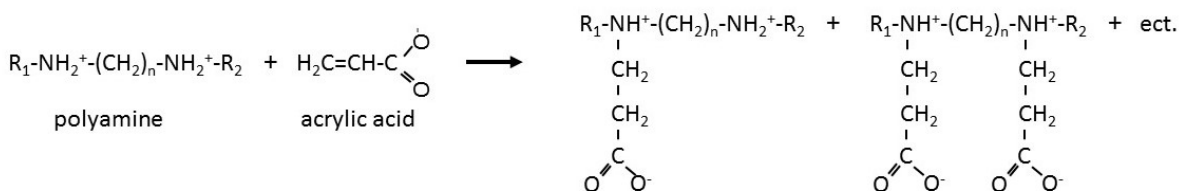


Figure 1.6: Chemical schemes for the synthesis of AmpholineTM. ⁷

This method is the most straightforward as many carrier ampholytes are made at the same time in a one pot method. Another type, ServalytTM, are made by reacting polyamines with either propane sultone or chloromethylenephosphonic acid (Figure 1.7).

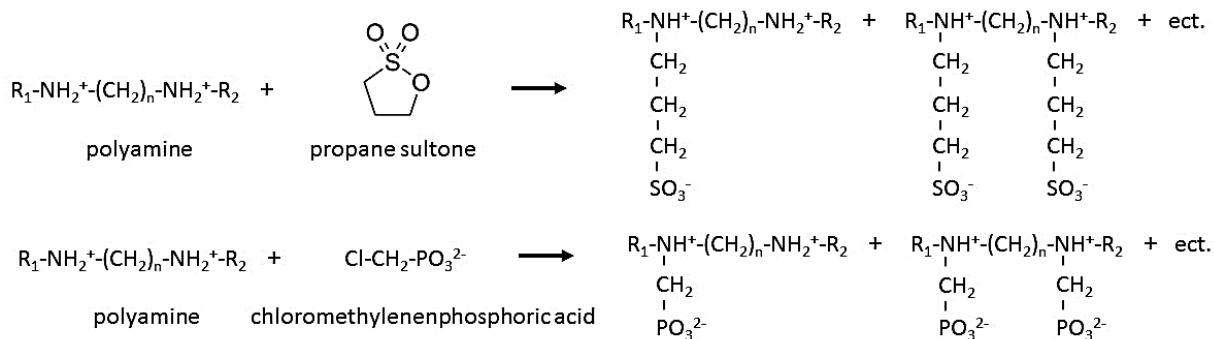


Figure 1.7: Chemical schemes for the synthesis of ServalytTM. ⁷

The third most common type is Pharmalyte™ which is made by co-polymerization of amines and amino acids with epichlorohydrin. However, this method produces more narrow cuts of the pH range and if a wider gradient is required then the product from multiple reactions must be mixed together to form a gradient from pH 3-10.

Often when using IEF as the first stage in a series of separations the sample will need to be recovered without the CA's thus it is frequently advantageous that the CA's are of low molecular weight, so they can be removed by filtration or dialysis. However, if collection is not required higher molecular weight CA's can be advantageous as they tend to have better buffering capacity therefore smaller concentrations can be used. This leads to an overall lower conductivity and thus higher electric fields can be applied which results in higher resolution.⁹

Electric Field

In a conventional IEF experiment the current is very high initially, but as the CA's lose charge when they migrate through the pH gradient and focus at the isoelectric points, the current decays. If the experiment is run in constant voltage mode, then the voltage must be limited to prevent Joule heating from the high current at the beginning of the separation. If the system is run at constant current, the voltage will decrease as the separation proceeds which will negatively affect the resolution of the separation. One way to avoid these problems is to apply the electric field in constant power mode which is often done in gel IEF.

Equation 28: $P = IV$, where P is the power applied to the system, I is the current and V is the voltage.

When constant power is used as the basis for the electric field the voltage will be lower when the current is higher and then will increase as the current decreases (Equation 28) which allows a higher resolution and shorter times than either of the above-mentioned methods. Another method

is to use voltage programming to increase the voltage as the separation proceeds and thus allow lower current at the beginning of the separation, but higher resolution once the analyte is focused. However, most modern capillary and microfluidic IEF separations run at constant voltage as programming can be difficult to implement and optimize.

Peptide and Protein Considerations

When developing peptides for pI markers one consideration should be the differences of pKa among the amino acids within the peptides. When the differences in pKa's are smaller the peptide has a higher effective mobility when away from the pI because it is fully dissociated over a larger pH range.⁷ When a peptide is fully dissociated it has a higher velocity in an applied electric field which leads to quicker focusing of the peptide.

A typical complication with protein IEF is that at the pI a protein frequently has decreased solubility due to the reduction of intermolecular interactions in the uncharged state. To help prevent precipitation of these proteins nonionic surfactants are often added in 0.1-5% concentrations to increase peptide and protein solubility by adding amphiphilic molecules to the sample solution.

These surfactants can also contribute other positive effects because, as shown in Kang et al., non-ionic surfactants can also reduce adsorption/absorption of fluorescently labeled peptides onto/into PDMS microfluidic devices which is important as when IEF is executed, the high concentration in the focused peaks can stain hydrophobic PDMS and cause limited reusability of the devices.¹⁰

The other main additive to increase protein solubility is 3-5 M urea which breaks hydrophobic bonds and disrupts hydrogen bonds. In gel electrophoresis denaturing agents like mercaptoethanol and dithiothreitol also be used to disrupt disulfide bonds of intact peptides to

help improve solubility. However, when measuring intact proteins, the additives other than surfactants can affect the resultant pI measurement.

Gradient Distortion

Gradient distortion is the most frequent problem when performing IEF. There are many potential causes of gradient distortion, but gradient drift from electroosmotic flow is the most commonly discussed. EOF arises from the material from which the channel is formed. If the material is glass, then there will be a negatively charged surface from the ionized silica molecules which will cause the formation of a positively charged rigid Stern layer and a diffuse layer of mobile cations that extends into the bulk solution as discussed in the previous section. If the bulk solution has low ionic strength, then the diffuse layer is larger. Typically, the diffuse layer ranges from nm to μm in thickness. When the electric field is applied along the channel the bulk solution will flow to the cathode. This process also works with materials of opposite charges in the same manner.

There are many techniques that are used to reduce EOF with the most common being surface modification or coatings. Polyacrylamide is one of the most commonly used surface modification coatings used in capillary IEF¹¹⁻¹⁶ along with dynamic coatings of methylcellulose^{8, 17-20}, polyvinylpyrrolidone²¹⁻²³, or hydroxypropylcellulose²⁴. These coatings work by shielding the charge on the channel material to prevent the formation of the Stern and diffuse layers. In addition to the pretreatment with polymers to create the dynamic coating, the polymer is often included in the sample as well to reduce degradation of the coating as well as increase the viscosity. The increased viscosity reduces the overall conductivity of the sample and reduces the EOF. This is because in Equation 23 the η term is viscosity, and if it is increased then the EOF decreases as it is in the denominator. Another common option to reduce EOF is to pretreat the

channel with an amphipathic surfactant which can also reduce the surface charge of the channel and thus decreases the ξ potential. However, this technique does not work as well as the coating is less viscous than the polymer and some EOF will still occur.

Another source of gradient distortion can come from thermal mixing from Joule heating. This can happen in a few cases. If the applied voltage is too high at the start of the experiment, then the current will be very large due to the increased resistance from the charged ampholytes that are unfocused. Equation 29 is also known as Ohm's law and describes the relationship between voltage(V), current(I) and resistance(R).

Equation 29: $V = IR$

When the heat sink capabilities of the channel forming material are overcome then thermal mixing will occur. When the buffer is heated then the conductivity increases which then causes more heating. It is possible that the liquid can boil in the channel which causes bubble formation and thus failure of the experiment.

Conductivity differences in the carrier ampholyte mixture can also cause Joule heating which cause high field strengths in a portion of channel and thus low field strengths in the rest. This causes low resolution in the remainder of the channel which can be overcome by the previously mentioned voltage ramping or constant power operation.

Detection for IEF

There are two common detection strategies for IEF including whole column imaging and mobilization of the focused bands over a stationary detection point. Whole column imaging is typically absorbance based and uses a CCD camera to image the entire column of focused analytes at one time. The main advantage is that there is no perturbation of the focused bands and the imaging can occur while the electric field is applied. Due to these reasons there is no

additional band broadening and the imaging can be repeated over the course of the separation to monitor the method over time. The main limitation to this method is that the limit of detection is in the micromolar range due to imaging limitations.^{8, 17, 22, 23} Also, sensitive CCD cameras are quite expensive in the \$5,000-\$10,000 range and the excitation light must be spread out with even illumination which requires costly optical components.

The other typical detection method for IEF is mobilization of the focused bands over a detection spot. This can be done by changing the reservoir solutions to cause chemical mobilization under the applied electric field. The other main method is to apply pressure to one side of the channel which causes parabolic flow of the separated bands (Figure 1.8). Both methods require the use of an anodic pI spacer to prevent focusing in part of the channel so that highly basic compounds can be detected as typically the detection spot is on the cathodic end of the channel.

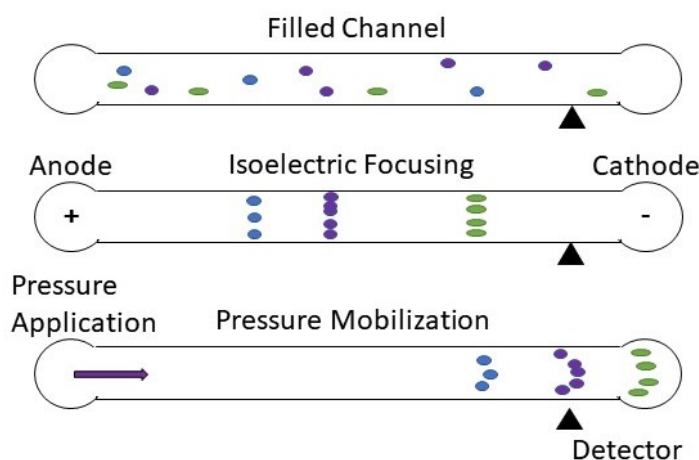


Figure 1.8: Schematic of pressure induced mobilization of IEF focused bands for single point detection.

As the bands are moved, diffusion disperses the separation and causes a loss of resolution.

However, this method is highly compatible with traditional optics and absorbance and fluorescence detection methods that are used with other types of separations. Therefore, for most laboratories these methods are less expensive to implement as detection systems can be repurposed from other systems.

Laser Induced Fluorescence

Laser induced fluorescence (LIF) is the most sensitive of the common analyte detectors with a typical LOD in the range of 10^{-16} mol/L (fM). LIF is also a very selective method due to the need of a fluorophore. Most analytes of interest are not fluorescent at typical wavelengths and therefore must be conjugated to a fluorescent molecule. This leads to increased cost and preparation time in most cases. The advantage of LIF is the method's selectivity as there are minimal background affects in comparison to other methods. This is where the very low LOD of LIF arises. The instrumentation for this type of detector consists of three main parts: the light source, filtering optics and light detector.

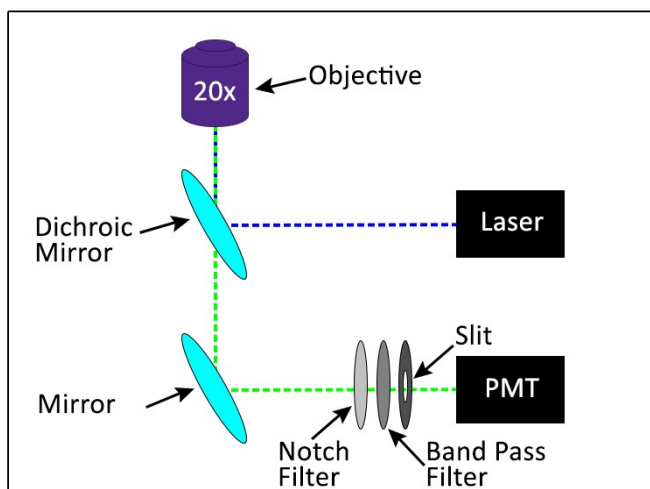


Figure 1.9: Simplified epi-illumination laser induced fluorescence schematic.

The traditional light source for LIF has typically been a mercury arc, xenon arc, metal halide, tungsten or deuterium lamp.³ Lasers then became more popular with the use of the argon ion and helium-neon systems. Current research is turning more toward solid state laser diodes and LEDs as the power output is easily tuned and they are much less expensive with comparable intensities and sufficient peak width resolution and coherency.

The second element for LIF is the optical components for the filtering of the light and the control of the beam as seen in Figure 1.9 which is a schematic of a epi-illumination LIF system. The main parts are a dichroic mirror to reflect the incident light and transmit the fluorescence (i.e. emitted light). Then there is a combination of notch, long pass and bandpass filters to reduce the background light noise and the amount of incident light that reaches the detector. A notch filter only prevents a small wavelength range of light from passing through the filter and is often used to reduce the incident light from the laser used for excitation. A long pass filter only allows light above a set wavelength to pass through the filter and thus can also be used to reduce the light from the excitation laser as the emission wavelength is always longer than the excitation. A long pass filter can also be used to prevent noise from ambient sources of lower wavelengths from reaching the detector. The bandpass filter allows a small wavelength range of light to pass through is typically used before a detector in a LIF system to allow only the fluorescence light to pass through. Often there is also a pinhole or slit to reduce the total amount of light and the area of the channel that the detector samples. There also is an objective, or set of lenses, that are used to focus the incident and emission light. The final component is a photon detector. The most common are the charge-coupled device (CCD) which captures images or the photomultiplier tube (PMT) which results in a current spike for each photon. These results are often graphed as the light intensity vs either the channel length or the pH gradient.

Microfluidics

Traditional separations involve substantial amounts of solvent and relatively large samples or high sample concentration. One way to overcome these challenges is to move to the microscale. Microfluidics is the design and fabrication of devices that have channels and features with at least one dimension less than 1 mm. The devices go by many names including: micro total

analysis devices, lab-on-a-chip devices, and even just chips and are used in many areas of research such as cell analysis²⁵, peptide analysis²⁶, fluid flow studies^{27, 28}, drug studies^{29, 30}, and even environmental studies^{31, 32}.

The advantages of microfluidics as a platform for traditional separation techniques are the faster analysis times, lower reagent consumption and thus minimal waste generation, low sample volume and the ease of automation. These devices can perform multiple analysis processes rapidly and in a parallel manner as a result of the small size and minimal reagent consumption. Due to the size and methods of fabrication available, multiple channels can intersect with different purposes in one device to perform all the steps that would traditionally be undertaken using lab bench scale instrumentation. There are three main geometries that are of importance for microfluidic separations. The T-junction where a perpendicular channel is at the end of another, and this is used typically for mixing. Another type of junction is the cross, which is useful for valving and fluid switching. Lastly is the straight channel which is typically where the main separation and detection occurs.

The traditional fabrication method for microfluidics is wet chemical etching to create channels in glass substrates (typically microscope slides). This is done through the use of photolithography to create patterns of the channels and buffered hydrofluoric acid etchant to then remove the exposed glass material.³³ The glass slides can then be bonded together via high temperature to create closed channels.

Another method used to fabricate microfluidic devices is soft lithography using elastomeric polymers, typically PDMS. This method uses photolithography with a standard negative tone photopolymer such as SU-8 as the mold onto which PDMS is poured (more information and protocols are located in Appendix B).³⁴

There are even some new casting methods that use acrylic³⁵ or polystyrene³⁶ to create microfluidic devices. These materials have advantages in that they are more amenable to large scale production methods, however, they can be difficult to implement as many are not optically transparent at the required wavelengths for detection. There is also less research that has been performed in modifying the surface properties for EOF and staining concerns.

However, hybrid devices are of particular interest as the best properties of each material can be chosen to create an ideal device for a particular application with respect to ease of fabrication and functionality of the channel surface.³⁷

The most common method of separation for microfluidic devices is electrophoretic as the small channel sizes require smaller voltage applied to reach similar electric fields that are used in capillary electrophoresis (CE). This arises from Equation 19 as the electric field is dependent on the length of the channel and in microfluidic devices the channel length is must shorter than the typical CE capillary length. Also, microfluidic devices have high heat dissipation as typically the channels are created inside larger solid substrates. Often glass slides are used as a platform for microfluidic devices as the increased mass compared to CE capillaries allows for larger heat dissipation from the microfluidic channel. This large heat dissipation allows for higher electric fields to be applied in microfluidics as the increased Joule heating can be absorbed into the bulk of the material. Higher electric fields correlate to higher electrophoretic velocity and thus faster separations from microchip electrophoresis as per Equation 22. This also is the same when comparing capillary IEF to microfluidic IEF in that a higher electric field can be applied which correlates to a faster separation with higher resolution.

To be used in a clinical setting the microfluidic device must have low reagent and energy consumption, high reliability, low maintenance and good robustness in the hands on not-

analytically trained personnel.³⁸ This is a goal for the development of a microfluidic based cancer detection device that is introduced in Chapter 2

Conclusion

The fundamental basics of analytical separations have been discussed as well as specific information about liquid chromatography and electrophoretic separations. Also, detection methods for these types of separations have been presented. In addition, microfluidics has been introduced as a platform for these types of separation and detection methods that have advantages over the traditional platforms. In the subsequent chapters the initial steps in the development of an automated system for studying enzyme activity via peptide substrate nanobiosensors for the detection of cancer will be discussed. Also, in Chapter 3 the development and optimization of a microfluidic device that uses isoelectric focusing and a scanning laser induced fluorescence detector is presented. In Chapter 4 a separate project on the Innate immune response studies on *Anopheles Gambiae* via immunoaffinity chromatography and mass spectrometry will be introduced and the optimization steps and results will be analyzed.

Chapter 2: Cancer detection via nanobiosensors using isoelectric

focusing

Introduction

At early disease stages cancer detection requires a fast and accurate response with minimally invasive sample collection, however there are currently no techniques or devices that meet these criteria. A method that may be able to meet these goals for detecting cancer, is to monitor up or down regulation of proteases that are related to cancer proliferation. One option for measuring protease activity is to use a peptide substrate that will be recognized and cleaved by the protease. Protease activity may then be quantified by measuring the ratio of the cleaved and uncleaved peptide substrate. The main complications of such analysis in biological samples arise from the complex matrix that these proteases are located within, as well as the low concentration and possible low activity of the proteases. Thus, sample preparation is critical to minimize the matrix effects for the separation without reducing the concentration or activity of the proteases.

To improve sample preparation, nanometer-sized magnetic nanoparticles can be utilized as the substrate to which to attach the peptides for the reaction and sample handling. The peptide substrates can be bound to the nanoparticles through a reducible disulfide bond and still be biologically accessible for protease cleavage. The other advantage is that nanoparticles are highly compatible with microfluidic devices and thus can be moved throughout the device with an external translating magnet.

The overall operation of the device that is proposed in this chapter will consist of channel filling, enzyme reaction, sample preparation and handling, peptide release, IEF separation, and scanning LIF detection. Chapter 3 will discuss the results from the development of the instrumentation for the separation of peptides by IEF and detection with scanning LIF.

Background

Cancer

Cancer is a collection of diseases that are defined by the uncontrolled growth and spread of abnormal cells. This growth and spread can lead to death if not detected and managed at preliminary stages. About 1.7 million new cancer cases are expected to be diagnosed and about 600,000 Americans are expected to die of cancer in 2018.¹

Stages are used to describe the degree of the spread of cancer at the time of detection. With many cancers there are different therapies used based on the stage of cancer, thus it is important to understand how stages are classified. For most cancers, the stage is defined by the size and spread of the primary tumor. For example, stage zero is *in-situ* (cancer cells are present only in the layer of cells where they developed and have not spread), stage one is early where the spread is local and stage four is advanced with distant spread of cancerous cells. Stages two and three are in between and defined by the regions of spread and the cancer type.

Cancer Stage when Detected	Pancreatic Cancer*	Breast Cancer**
0-1	13%	100%
2	7%	93%
3	4%	72%
4	1%	22%

*National Cancer Data Base (1992-2004, statistics last revised on 09/15/2016)

**National Cancer Data Base (2007-2013)

¹ Estimated new cases are based on 2000-2014 incidence data reported by the North American Association of Central Cancer Registries and estimated deaths are based on 2001-2015 US mortality data, National Center for Health Statistics, Centers for Disease Control and Prevention.

The stage at which the disease is initially detected has a large effect on the 5-year survival rates for most cancers (see Table 2.1). For instance, breast cancer survival rates decrease by a factor of 4.5 when detected at stage 4 as opposed to stage 1. This decrease in survival rates can be attributed to better therapies that are available before the disease has spread throughout the body of the patient. Therefore, early, relatively inexpensive, and noninvasive cancer detection is a critical area of research to increase survival rates of many cancers.

Currently the principal method of early cancer detection with liquid biopsies uses PCR to detect genetic mutations that are frequently overexpressed in tumors. These methods often require the sequencing of entire sections of the patient's genome and are labor intensive and take a great deal of time. Very recently, a new method for using cancer detection was published in the journal *Science*.³⁹ This technique is called CancerSEEK and can detect eight common cancers by assessment of the levels of circulating proteins and cell-free DNA. The theory behind this method to discover cancer is based on the detection of mutations in the DNA based on the amplification of 1933 gene positions. This is different than typical DNA based cancer discovery that is based on genome wide sequencing. Only scanning for certain point mutations allows for greater sensitivity of the sequencing method. The system then probes for eight specific peptides with a bead-based immunoassay to determine the tissue source of the cancer. While this method is very intriguing, it does require a large amount of sample preparation and is therefore not amenable for low-cost, point of care detection. Therefore, more research is still needed to take cancer detection using blood samples from the laboratory to the clinic.

Nanobiosensors

An interesting option to reduce the required sample preparation for many methods is to use nanobiosensors as a platform for the reaction. Nanoparticles are frequently used as a substrate for biosensors due to their very high surface to volume ratio (specific surface area) which allows for many molecules to be attached to each nanoparticle. This results in a high concentration of sensors for a given volume of material. Another advantage of using nanoparticles as a substrate is that they can be made from materials with magnetic properties to allow for easier sample handling. When designing these magnetic nanoparticles, increasing the size from 5 to 50nm increases the magnetism and allows for easier capture and transfer of the particles via external magnets. However, the increased size decreases the surface-to-volume ratio and, therefore, decreases the number of biosensors per mass of nanobiosensor. These competing characteristics must be balanced when creating the nanoparticles.

Nanobiosensors consist of sensors that are attached to a nanoparticle to study specific types of biological interactions. Some common interactions to study are enzymatic in nature such as kinases and proteases which can be monitored through the use of peptide substrate sensors. A peptide substrate reporter contains a recognition sequence for the particular enzyme being studied. In the case of kinases, a phosphate group is added to the peptide's recognition site by the enzyme. The addition of the phosphate group changes both the peptide mass and charge. Such changes can be detected by multiple techniques including mass spectrometry and electromigration techniques. A simpler family of enzymes to study are the proteases. These enzymes cleave specific peptide sequences at the recognition site. A common example of a protease is the enzyme Trypsin. Trypsin is a serine protease that cleaves a peptide mainly at the carboxyl side of the amino acids lysine or arginine, except when either is followed by proline.

Proteases are the most common enzyme to study with nanobiosensors due to the ability to detect the cleavage via Förster Energy Transfer (FRET) studies as well as mass spectrometry and electromigration techniques.^{40, 41}

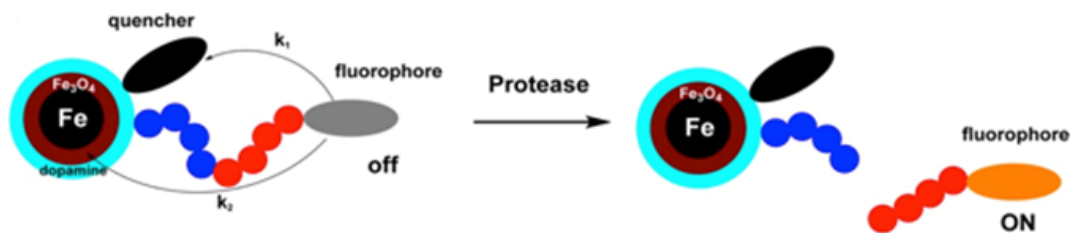


Figure 2.1: Mechanistic scheme of the “light switch effect” upon proteolytic cleavage: the fluorophore is switched on due to the increase in distance between the Fe/Fe₃O₄ core/shell nanoparticle, leading to decreased Förster Energy Transfer (FRET), k_1 , and dipole-surface energy transfer (SET), k_2 . Reproduced from Ref 41 with permission of The Royal Society of Chemistry.⁴¹

Figure 2.1 shows the scheme for the use of FRET to detect protease activity with nanobiosensors. The nanopatform consists of dopamine-covered, iron-iron oxide core-shell nanoparticles to which one fluorescent dye (TCPP, tetrakis-carboxyphenyl porphyrin) is tethered via a consensus peptide sequence. A second dye (Cyanine 5.5) is permanently linked to the dopamine coating and when the peptide sequence is cleaved by the protease and released from the nanoparticle the fluorophore is no longer quenched and can then be detected with a plate reader for quantitative evaluation. Most of the protease assay microfluidic devices, however, use single⁴²⁻⁴⁴ or multiple FRET-based fluorophores⁴⁵⁻⁴⁷ that limit the number of enzymes that can be monitored simultaneously in a single sample. To achieve multiplexed detection in these kinds of devices either complex and expensive optical schemes are required, or some type of sample preparation and separation are required.

An alternative option for nanobiosensors that are amenable to separation and multiplexed detection are composed of five specific components including: a superparamagnetic Fe-Fe₃O₄

nanoparticle, a disulfide bridge, a protease specific peptide substrate, a fluorophore and 1 or 2 pI tags (Figure 2.2).

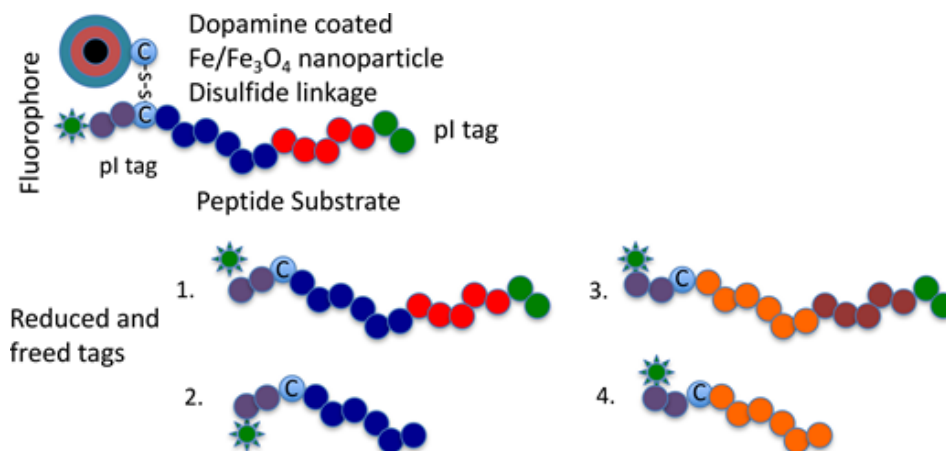


Figure 2.2: Schematic for the design of peptide substrates for protease activity studies.

The variable component of the nanobiosensor is the protease specific peptide substrate and the amino acids added on either end to adjust the pI of the substrate and cleaved substrate for separation by isoelectric focusing. Between one of the pI tags and the enzyme substrate is the amino acid cysteine which can be linked to another cysteine on a superparamagnetic Fe-Fe₃O₄ nanoparticle through a disulfide bridge. The N-terminus of the pI tag nearest the disulfide linkage will also be labeled with a fluorophore for laser induced fluorescence detection of the intact and cleaved peptide substrate. The magnetic nanoparticle provides a means to transport the nanobiosensor out of a sample solution via the translation of a magnet. The ability to remove the biosensor from the matrix, reduces matrix effects and thus noise and background in the final optical readout. There are multiple peptide substrates per nanoparticle and thus a separation of the two components needs to occur. Also, the nanoparticles can also hinder many types of separation due to their charge and size dispersion⁴⁸ and thus the need to be separated from the peptide substrates. The disulfide bridge allows the peptide substrates, both uncleaved and cleaved to be delinked from the nanoparticle by exposing the nanobiosensor to a reducing

solution before the separation is performed. Tris(3-hydroxypropyl) phosphine (THPP) is an air stable and water soluble reducing agent that can be used to reduce small molecule disulfide bonds.⁴⁹

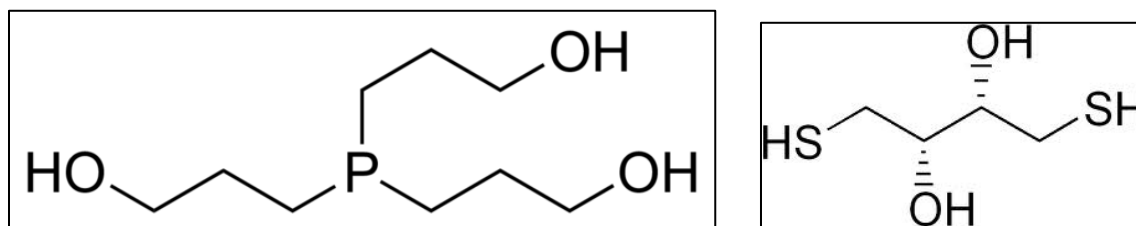


Figure 2.3: Diagram of the reducing agents (Left) Tris(3-hydroxypropyl) phosphine and (Right) Dithiothreitol.

This reducing agent was chosen over the traditional reagent dithiothreitol (DTT) as aqueous solutions of DTT show limited stability, particularly at biological pH and slightly above (pH 7.5–8.5). To reduce the peptide substrate from the nanoparticle and into the IEF separation channel, the nanobiosensors will be incubated in the IEF carrier ampholyte-THPP solution to complete the reduction of the disulfide linkage between the nanoparticle and the peptide substrate and release the substrate for IEF separation.

Recent research has found that these types of nanobiosensors can be used to detect multiple types of cancer. This is possible because proteases are dysfunctional (over or under expressed) in solid tumors which can be detected in liquid biopsies such as blood. Matrix metalloproteinases (MMPs), serine proteases and cysteine proteases have well-documented roles in malignant progression of tumors and immune dysregulation in cancer.⁵⁰ Udukala et al. and Kalubowilage et al. have shown that these expression differences can be detected via nanobiosensors for breast and pancreatic cancers.^{51, 52}

The typical method for using these nanobiosensors is to mix the sensors with the biological sample and incubate for one hour then a plate reader is used for detection of the released fluorescent peptides. The main disadvantage with this method is that there is no separation, and

therefore, only one enzyme can be studied in at a time. To overcome this issue a separation needs to be included in the process. Plate readers are very expensive and not amenable to point of care testing which would be ideal for this type of cancer detection.

The main issue to overcome is that these enzymes are present at very low concentrations in a liquid biopsy. There are minor differences between normal activity levels and abnormal ones.

That means that any separation and detection method that is used must have a very low LOD or the ability to concentrate the analytes of interest above the detector LOD.

Liquid biopsies are typically whole blood samples that have undergone no sample preparation and thus consist of multiple unneeded sample components. The part of the sample that does not contain the analyte of interest is called the matrix and can cause many difficulties when using the sample in a separation and detection device. Most commonly, in the case of blood, the cells clog microfluidic devices due to their large size. However, due the magnetic nature of the nanobiosensors these matrix affects can be eliminated by mixing the sensor with the liquid biopsy and then moving the sensor to another solvent, thus only moving the reacted peptide substrate into another portion of the channel to detect the results and leaving behind the matrix.

The small size of the nanobiosensors and the capability of moving them with an external magnetic field makes these sensors an ideal choice for use in microfluidic devices. A simple microfluidic device would allow for the mixing of the nanoparticles with a small volume of approximately 1 mL biological sample and then the automated motion of the sensors into a detection channel (see Figure 2.5). This combination of nanobiosensors and microfluidics could easily be adapted into a point of care device for the detection of cancer through enzyme monitoring.

Point of Care Devices

A point of care device is an instrument that moves patient sample testing from an external laboratory to the bedside or the place of patient care.⁵³ Current examples of these types of devices are blood glucose testing⁵⁴, blood gas and electrolytes analysis⁵⁵, rapid coagulation testing⁵⁶, rapid cardiac markers diagnostics⁵⁷, drugs of abuse screening⁵⁸, urine strips testing⁵⁹, pregnancy and neonatal testing⁶⁰, fecal occult blood analysis⁶¹, food pathogens screening^{62, 63}, hemoglobin diagnostics⁶⁴, infectious disease testing⁶⁵ and cholesterol screening.^{66, 67}

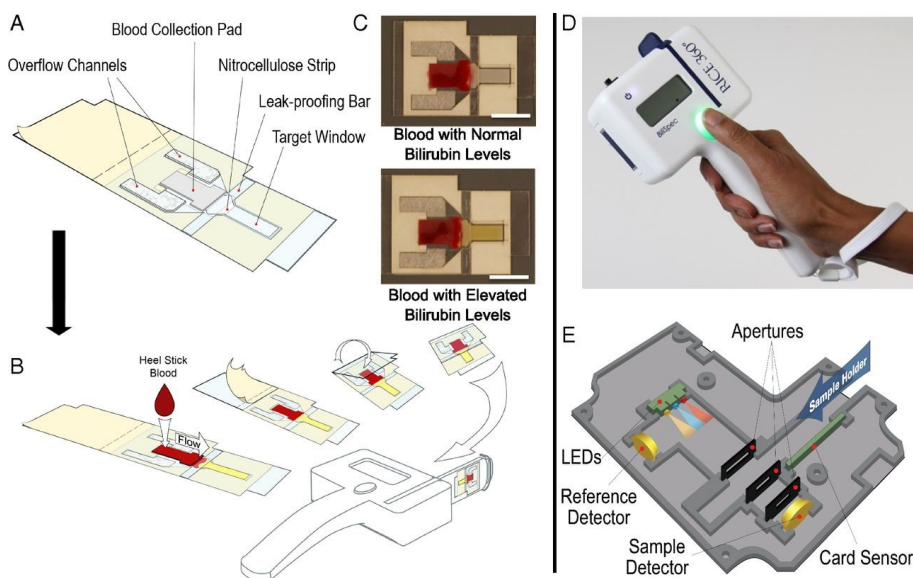


Figure 2.4: A point of care device to diagnose and monitor neonatal jaundice in low-resource settings. Copyright 2017 National Academy of Sciences. ⁶⁰

To create a point of care device for detecting cancer there are a few goals that must be achieved.

The patient sample required should be noninvasive or at least minimally invasive (peripheral blood, saliva, mucus etc.) to allow for more routine use of the system to monitor the onset or reoccurrence of cancer. The device also must be fast, robust, relatively inexpensive per sample, versatile, ultrasensitive, and highly automated.

An option for a point-of-care device to use the nanobiosensors explained above is to use a three-region microfluidic chip as pictured in Figure 2.5. The first region is a 1 mL sample incubation

well for the mixing of the nanobiosensors with the liquid biopsy (Figure 2.5-A). After the incubation time the proteases present in the liquid biopsy will have cleaved the peptide substrates at the recognition site and there will be a ratio metric difference between the cleaved and uncleaved peptides which correlates to the amount of that protease present. The nanobiosensor will then be moved via an external magnet into a rinsing chamber to remove the matrix affects (Figure 2.5-B). The final region of the device is for the release of the peptides (Figure 2.5-C) from the nanoparticle and the external magnet will then move the nanoparticle out of this region and leave behind the peptides. The final step is the isoelectric focusing and detection of the cleaved and uncleaved peptides (Figure 2.5-D).

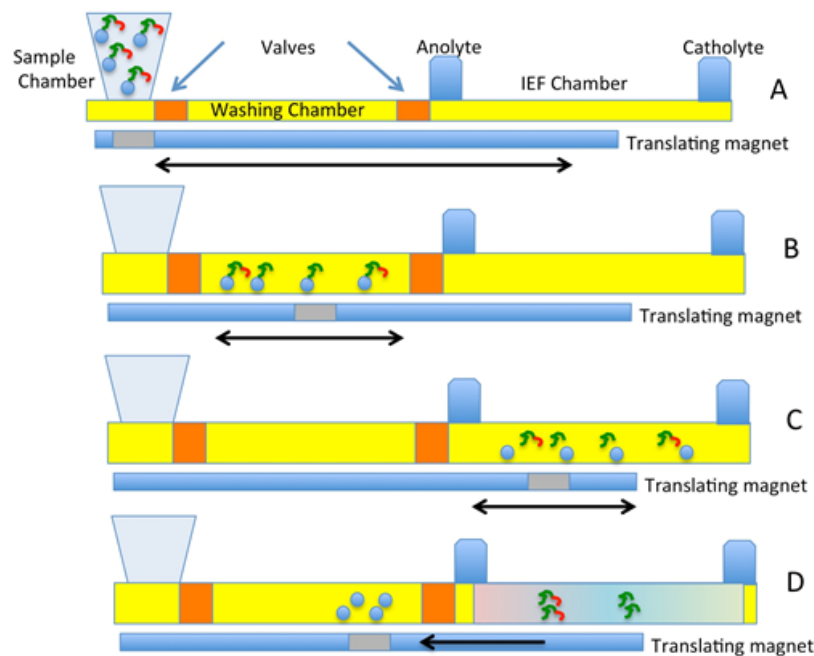


Figure 2.5: (A) Sample and nanobiosensors are mixed and incubated; (B) Magnet moved nanobiosensors to the washing chamber; (C) Magnet moved to IEF chamber and disulfide linkage is reduced; (D) Magnet moved out of IEF chamber and IEF separation and detection is performed.

Sample Preparation and Handling

The first obstacle to overcome is the sample preparation and handling. The ideal method involves no sample preparation by the operator and uses the direct liquid biopsy. One method to meet this goal is to use a method of sampling that can overcome matrix effects. To do this magnetic nanobiosensors can be used that can be mixed with the sample to incubate the peptide substrate with the patient sample using a rotating magnet. The magnetic nanobiosensors could also move via a translating magnet from one region of the device to another without transferring the matrix.

Separation

The type of separation to choose was also a challenge to determine. To be a point of care device, traditional laboratory separation methods such as HPLC-MS or gel electrophoresis cannot be chosen even though they could work for peptide detection. Therefore, the smaller platform for microfluidic separations was looked at for inspiration. Electrophoresis would be an option due to its ability to separate out peptides however, it is not easily compatible with nanoparticle sample preparation when it comes to sample injection. Also, to form a complete picture of health multiplexed detection is required due to low statistical differences between normal and cancerous samples for early cancer detection. There would be a limit of approximately 10 analytes when it comes to microfluidic electrophoresis, which is not sufficient.⁶⁸ Also, microchip electrophoresis is not compatible with nanobiosensor sample injection. Another form of electrophoretic separation that does fulfill most of the requirements is microfluidic isoelectric focusing the theory of which is discussed in Chapter 1. The method is compatible with the sample preparation with magnetic particles as IEF does not require injection of the analyte into a portion of the channel. The sample will focus from any portion of the channel at its isoelectric point. Thus,

peptide release in the channel from the THPP reduction of the cysteine bond that binds nanobiosensor is amenable with the IEF separation.

Microfluidic IEF also has a high peak capacity with a resolution of 0.2 pH units a gradient from 3-10 could contain 40 analytes and thus 20 different peptides with intact and fragmented fractions. Another advantage of IEF is that it is a static concentrating method that is described in Chapter 3 and has the capability of concentrating the signal from this nanobiosensor $\sim 10^6$ fold.

Detection

With the choice of isoelectric focusing for the peptide detection there are only a few options for the detection. The main two are absorbance at 205 nm to detect the amino acid backbone or fluorescence to detect a fluorescent label that must be added to the substrate. In traditional protein analysis by IEF fluorescent labeling adds increased complexity to the procedure as the protein must be purified and the time must be taken to allow the labeling reaction to proceed before the sample analysis. However, in the case of using peptide substrates for enzyme activity measurements, the peptides must be synthesized via solid phase synthesis and during the process fluorescent labeling possible without further complex reactions.

One of the main difficulties with IEF as a separation method is that it is typically done via chemical or pressure induced mobilization to move the analytes past a single detection spot. This point of care device however, will include a motorized holder to move the microfluidic chip over the detection spot. This would remove the band broadening that occurs due to the movement of the focused bands as the chip could be scanned while the voltage is applied.

Automation

A point of care device needs to be highly automated to allow for non-expert use by clinicians.

The system that was proposed in the previous sections is highly amenable to automation. The use

of magnets for sample transfer and mixing can be easily controlled using a DC motor for spinning the magnet for sample mixing and using a stepper motor to move a magnet for transfer of the nanoparticles into other sections of the microfluidic chip. The isoelectric focusing is also compatible with automation as the voltage that is applied to induce the separation can be controlled and monitored programmatically. The scanning detector requires automation for the control of the chip holder via a stepper motor and data collection and saving. Without automation there would be too much variability in the motion of the scanning and this would cause a loss a resolution. Therefore, automation of the system is one of the most important components for the development of a point of care device.

Conclusion

The overall point of care device will consist of a translating and rotating magnet to aid in nanobiosensor mixing and handling. The peptide substrates will be reduced from the nanoparticle with THPP and then separated with isoelectric focusing. This system will have voltage control via software to increase the resolution and the focused peptides will be detected with scanning laser induced fluorescence. The development of the device for microfluidic IEF with scanning laser induced fluorescence will be discussed in Chapter 3. The testing and development of the nanobiosensor sample preparation and miniaturized LIF optics are outside the scope of this dissertation and are concurrently being developed by Shu Jia in the Culbertson lab.

Chapter 3: A whole channel scanning fluorescence microfluidic isoelectric focusing

Introduction

In this chapter the fabrication, testing and optimization of a scanning microfluidic IEF platform with LIF detection of labeled peptide substrates for proteases will be discussed. This system will be incorporated into the point of care nanobiosensor device described in Chapter 2 in the future, for the automatic analysis and detection of proteases on the microfluidic platform.

Isoelectric focusing is a method that requires very small sample volumes and concentrations which are also some of the main advantages of the microfluidic platform. Thus, the two methods are amenable. The main concern with integrating IEF with microfluidics is that typically, microfluidics is performed under flow conditions while IEF is a static method. There have been reports of microfluidic free flow IEF, but it is relatively difficult to perform as the electrode materials perpendicular to the separation channel must completely seal to the substrate to prevent leaking and to maintain a uniform electric field across the width of the channel.^{69, 70} The other main concern with free flow IEF is that a much larger sample is used compared to static conditions which is detrimental to sample limited studies. Also, a shorter pH gradient is available which limits the determination of a wide range of pI's in one experiment.

One obstacle with incorporating static IEF with microfluidics is the very low limits of detection (LOD) that are required for most biological applications. To achieve this needed low LOD, the best choice for detection is laser induced fluorescence (LIF). LIF has advantages over absorbance based detection as it is very selective and thus the background can be very low for the separation.

However, most LIF setups involve the flow of the analyte of interest in the channel past a single point for excitation and detection. To traditionally use this type of detection with IEF, the focused bands of analyte must be moved over the detection spot via chemical or pressure mobilization.^{11, 12, 18, 24, 71} These mobilization methods can perturb the separation and cause a loss of resolution due to band broadening which leads to a higher detection limit. This makes LIF less sensitive in the case of IEF and makes the combination not a viable choice for low concentration studies with the traditional methods of detection.

Takahashi et al. has studied cIEF and developed a scanning capillary detector for LIF to overcome the single point detection issue.¹⁵ In this system an electric field was applied across the capillary to focus the analytes into bands, then the capillary was moved via a commercial positioning system to pull the length of the capillary over the detection spot. One of the main difficulties with this method is that the capillaries that are used are typically >12cm in length and this length leads to difficulty in maintaining alignment of the center point of the capillary along the complete scan of the separation. The length also leads to increased noise as it is difficult to move a long and thin glass tube in a stable and consistent manner for optical detection.

Beale and Sudmeier developed a scanning capillary system where the LOD for fluorescein isothiocyanate (FITC)-labeled myoglobin was in the nanomolar range.⁷² They also performed studies regarding the signal to noise ratio (S/N) and found that the capillary ID/OD ratio had a measurable effect due to inconsistencies in manufacturing. Olazábal et al. constructed a scanning LIF detector that used the separation capillary as an optical guide for a fiber optic-based excitation laser source that scanned the length of the channel.⁷³ However, the noisy data required complicated mathematical functions to reconstruct the signal.

To overcome many of these challenges a scanning LIF detector for microfluidic IEF has been developed. The main advantages to this system are the ease of alignment, low cost, automation, low sample volume requirements, and low limit of detection.

Materials

The following chemicals were obtained from commercial sources: Methyl Cellulose and SinuLyte Ampholyte high resolution, pH 3.0-10.0, were purchased from Sigma Aldrich (St. Louis, Mo). Servalyte Ampholyte high resolution, pH 3.0-10.0, was purchased from Biophoretics (Sparks, NV). Thermo Scientific™ Pierce™ MS Grade Trypsin Protease, Tetramethylrhodamine-5-Iodoacetamide Dihydroiodide (5-TMRIA), single isomer, Acetonitrile (HPLC Grade), Trifluoroacetic Acid, Glacial Acetic Acid, Calcium Chloride, Phosphoric Acid, Sodium Hydroxide, Iminodiacetic acid, and Brij 35 (Enzymatic Grade), were purchased from Fisher Scientific (Waltham, MA). 1.5M Tris-HCl, pH 8 was purchased from BioRad (Hercules, CA). DL Arginine was purchased from Acros Organics (Geel, Belgium).

Methods

Linear Scanning Detection System

The overall system is composed of three main parts. This includes the motion system to hold and move the microfluidic chip over the detection point, the high voltage power supply to apply the electric field and the LIF system for detection.

The motion system is composed of a stepper motor that turns a lead axis screw that drives the motion of a linear ball bearing slide. A holder for the microfluidic chip attaches to the linear slide and is made with 3D printing from PLA on a MakerGear Rev 2 (Figure 3.1). The entire system, including the slide translation, is controlled by LabView via a National Instruments USB 6002 interface.

A CZE 1000R by Spellman is used for voltage application of 0.3-4 kV that is controlled programmatically via LabView.

A Collimated Laser Diode Module, 532 nm, 4.5 mW is the excitation source for the system. To reduce the amount of excitation light that reaches the detector, a 533 nm Notch Filter from Thor Labs was placed in front of the PMT. The emission light was also passed through a 565 nm Long pass filter and a 565-637 nm Bandpass filter from Edmund Optical to reduce any background fluorescence and remove noise from scattered light. A Hamamatsu Photonics R-928 Photomultiplier Tube is used for detection and whose output was input into a SR 570 Preamplifier with the following settings: 12dB Lowpass Filter at 300 Hz, and Low Noise Gain, 10 μ A/V-500 nA/V Sensitivity (Stanford Research Systems, Sunnyvale Ca).

Fabrication of PDMS Microfluidic Isoelectric Focusing Device

Soft photolithography was used to create the desired channel pattern, by using a positive photoresist on a Si-wafer substrate. PDMS prepolymer and curing agent (Sylgard 184, Dow Corning Inc., Midland, MI) were uniformly mixed at a ratio of 10:1, respectively, and degassed for 30 min under vacuum. The PDMS was poured into the mold on the Si-wafer that contained the channel pattern. The PDMS was cured in an 80°C oven for 90 min. At the end of the curing process, the PDMS was carefully peeled from the glass substrate to become the bottom layer of the microchip. The reservoirs were created with a 3 mm biopsy punch and then the channel layer was sealed to a glass slide. The microchannel was 3 cm in long, 300 μ m wide, and 16 μ m deep in a rectangular shape.¹⁷ The full procedure is located in Appendix B.

Fabrication of Glass Microfluidic Isoelectric Focusing Device

Briefly 25 by 75 mm glass microscope slides were patterned with AZ P4620 with the photoresist covering the areas that did not require etching. Then buffered hydrofluoric acid etchant was used

to etch the channels into the glass and the progress was monitored using a stylus-based surface profiler.⁷⁴ The full procedure is located in Appendix B.

Peptide Substrate and pI Markers Synthesis

The peptides were synthesized using a solid phase with standard Fmoc chemistry.^{75, 76} They were fluorescently labeled with Rhodamine B while still on the resin through amide bond formation. This bond is more stable than the isothiocyanate and succinimidyl ester bonds normally used to link fluorophores to peptides.⁷⁷ This may be especially important for IEF as some of the peptide substrates will be exposed to pH extremes during focusing. For the peptides containing the amino acid cysteine, the solvents were distilled to remove any water and degassed with argon to remove any oxygen. This was done to prevent the early loss of the cysteine protecting group to maintain its activity at the end of the synthesis.

Table 3.1: Peptide sequences and pI's for IEF		
Sequence	Calculated pI	Observed pI ¹⁴
GCEE	3.82	3.99
GCEEH	4.54	4.5
GCEHH	6.42	6.86
GCYYYKK	9.36	9.56
GCYYKK	9.52	9.70
GCYKK	9.76	9.94
EGEKEEAG	4.5	
HRDEVGKHG	6.0	

This table contains the pI markers for use in monitoring the stability of the pH gradient

pI Marker Fluorescence Labeling

Dye purification and labeling was done via previously published methods.¹⁴ Briefly Tetramethylrhodamine 5-iodoacetamide from the supplier was further purified by preparative reversed-phase chromatography with a C18 column and 12 mL/min flow rate at 50%

Acetonitrile, 0.1%TFA. The fraction from 6.5-8 min was saved and tested via analytical HPLC. The concentration of dye was determined by measurement of the absorbance at 549 nm in 20% methanol (v/v) based on an extinction coefficient of 87,000. The purified dye was freeze dried by evaporation in 50 nmol aliquots. The purified dye (50 nmol) was dissolved in 200 μ L of acetonitrile and mixed with 800 μ L of 0.1 M sodium phosphate buffer (pH 7.5) containing 5 mM EDTA. A 10- μ L portion of a peptide solution (50 mM) was added to the dye solution and allowed to react at room temperature overnight in the dark. The reaction mixture was acidified by the addition of 150 μ L of 1 M HCl. The concentration of dye labeled peptide was determined by measurement of the absorbance at 549 nm in 20% methanol (v/v) based on an extinction coefficient of 87,000.

Trypsin Digestion

50mM Tris-HCl (pH 7.8), 1 mM CaCl₂, 0.005 mg/mL Trypsin, and 0.1 mg/mL Trypsin Substrate(RhB-EGEKEEAG) were mixed and then incubated at 37°C with samples taken for analysis at 0 hr, then at hours 1-8, and 24 hr. The digestion was stopped by adding acetic acid to adjust the pH below 4 which is outside of the activity range of trypsin. The full procedure can be found in Appendix A.

HPLC Testing

The progress of the trypsin digestion of the peptide substrate was monitored via separation of the cleaved/uncleaved peptides on HPLC and detected using absorbance. The digestions were tested on a Thermo Fisher Ultimate 3000 with a Variable Wavelength Detector and an Acclaim 300 C18 column. The parameters were 0.3 mL/min flow rate, with a gradient of 5% acetonitrile to 80% over a 15 min time period and a 5 min hold at 80%. The resultant chromatographic data was analyzed with Igor Pro (WaveMetrics Inc., Lake Oswego, OR).

Isoelectric Focusing

The progress of the trypsin digestion of the peptide substrate was also tested using reported microfluidic IEF device. The channel was cleaned with 50% 1 M NaOH and 50% methanol for 10 min. Then the channel was pretreated with 0.4% methyl cellulose for 20 min to develop a dynamic coating. The IEF sample consisted of: 50 mM arginine (high pI sacrificial ampholyte), 0.11% Brij 35 (surfactant), 500 fM to 10 nM rhodamine B tagged peptide (sample), 1% SinuLyte® and 1% Servalyte® carrier ampholytes, and 0.4% methyl cellulose (EOF Suppressor). The sample was loaded into the channel via suction and then the reservoirs were filled with the anolyte (20 mM iminodiacetic acid with 2% methyl cellulose) and catholyte (300 mM sodium hydroxide with 2% methyl cellulose) respectively. The microfluidic chip was then aligned on the motion system and the initial voltage was applied (300 V/cm). The voltage increased every scan (35 sec) by 600 V until the maximum voltage of 3 kV was reached. While this process was occurring, the channel was automatically scanned at 8.57 mm per second over the detection point and the fluorescence was collected using a μ PMT (Hamamatsu Photonics, Japan). LabView (National Instruments, Austin, TX) programming was used to automatically control all motion, voltage, data collection, and saving. Data was analyzed using Igor Pro with a procedure that is used to load the files and code to rescale and create and label the appropriate graphs. The full procedure as well as the LabView and Igor programs are located in Appendix A.

Results

Scanning Detector

The initial prototype scanning system was created with parts from other projects and required minimal purchases. An image of the device is shown in Figure 3.1

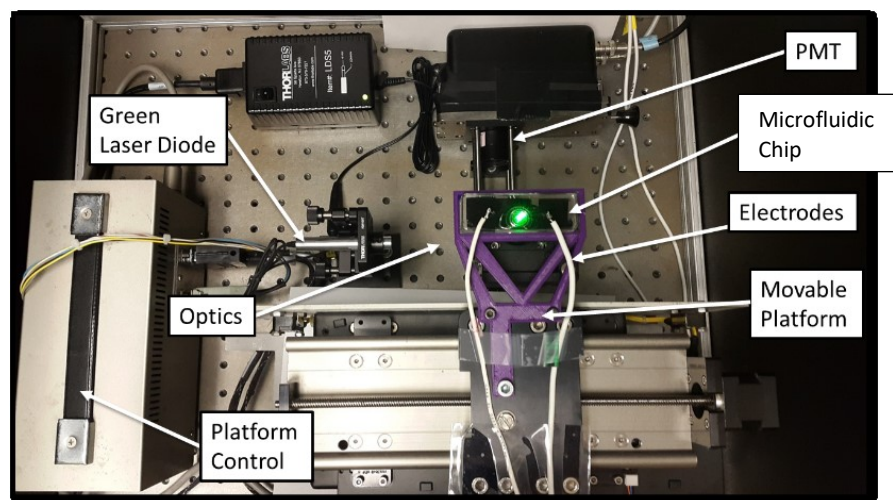


Figure 3.1: The prototypes IEF device with LabView control and automation for the detection of fluorescent peptides.

Version two was created with approximately \$260 of supplies. The main components consisted of a 4-inch travel linear bearing slide from Edmund Optics (37-365), an 8 mm lead screw set, a Nema 17 stepper motor and driver from Amazon, and a 3D printed microscope slide adaptor to act as a platform for the whole device and hold the microfluidic chip. The simple and inexpensive setup could scan a microfluidic IEF separation with minimal additional noise or scattering vs a stationary data collection of the filled channel as shown in Table 3.2.

Table 3.2: Analysis of background and noise of the detection system					
Trial Number	PMT Detector	Motion	Chip	Average Background	Noise
1	Closed	Off	Yes	0.0012	±0.0004
2	Closed	On	Yes	0.0018	±0.0005
3	Open	Off	Yes	0.02	±0.01
4	Open	On	Yes	0.08	±0.02
5	Open	Off	No	0.0015	±0.0006
6	Open	On	No	0.002	±0.001
7	Open	Off	No	0.002	±0.001
8	Open	Off	Yes	0.08	±0.02

The chip was filled with 0.4% methyl cellulose, 4% carrier ampholyte, 1.7mM IDA, and 40mM Arg and data was collected for 35 secs with the amplifier set at 50uA/V. For each set of data one parameter was changed and then the average background and the standard deviation of the background(noise) was then calculated.

Trials 1 and 2 Table 3.2 show that the vibration of the motion system has negligible effect on the background signal or noise of the system. In these trials the PMT(detector) was closed with a shutter which allowed no light to pass. Thus, only the noise arising from the electrical system and the environmental noise was measured in this case. With the system in full operational mode as it is for typical IEF data collection, the background increases 4x and the noise increases 2x when the motion system is turned on as seen with trial 3 and 4. A large part of the background increase arises from light scattering from the presence of the microfluidic chip. This is seen with trials 4, 6, 7 and 8 which show a 40x increase in background and a 20x increase in noise when the microfluidic chip is present as opposed to absent. To reduce this effect, additional filters can be used to reduce the incident light of the system that reaches the detector. However, these filters will also reduce the fluorescence signal that reaches the detector and thus reduce the LOD more than the scattering increases the background.

Chip Material

The material composition of the microfluidic channel is highly important when considering scanning fluorescence detection. If the microfluidic chip is made via PDMS-based soft lithography, the channels are recessed in the flexible polymer PDMS and the base of the channels are formed with a glass slide. However, the PDMS molded channels are inherently rough and that arises when peeling the PDMS from the mold. This roughness can cause increased scattering of the incident light as well as difficulty in filling the channels with the viscous methylcellulose. Also, these devices can be very difficult to create for linear scanning detection as any slight warping of the PDMS channel along its length leads to a channel that is not fully linear. This distortion of the channel causes many problems with the alignment of the detection system and leads to high background noise and incomplete fluorescence collection of the focused peptides thus leading to a loss in signal intensity (Table 3.3).

Channel Type	Background	Noise	Signal	S/N
PDMS	0.059	±0.008	5.754	688
SU-8	0.016	±0.002	0.244	160
Glass	0.021	±0.001	3.306	2637

The sample composition was 74 nM Trypsin Substrate, 1%CA, 50 mM Arg, 0.4%MC, 0.05%AA, and 0.11% Brij 35 with 2.5% MC in 200 mM H₃PO₄ anolyte, and 2.5%MC in 300 mM NaOH catholyte.

An alternative method for the fabrication of microfluidic channels is the use of the SU-8 negative tone photoresist as the channel side wall material on a glass slide(channel bottom) with a blank PDMS top to form the four sides. This chip was easy to align and thus had lower noise overall, however, the material is not as compatible with fluorescence detection as the signal was very low due to absorption of the light by the channel material as seen in Table 3.3. This may arise from incomplete removal of the SU-8 from the base of the channel which could cause signal reduction.

The traditional method for creating microfluidic chips is using glass etching with buffered hydrofluoric acid etchant followed by the bonding of a flat glass slide with the etched slide to form an enclosed channel which is then thermally annealed. However, glass bonding is a somewhat complicated process and cleaning an irreversibly sealed chip for reuse can be difficult when using a dynamic coating with high viscosity. Therefore, a hybrid device was created with channels etched into the glass and a smooth PDMS top with reservoirs punched using a 3D printed alignment tool as seen in use in Figure 3.2.

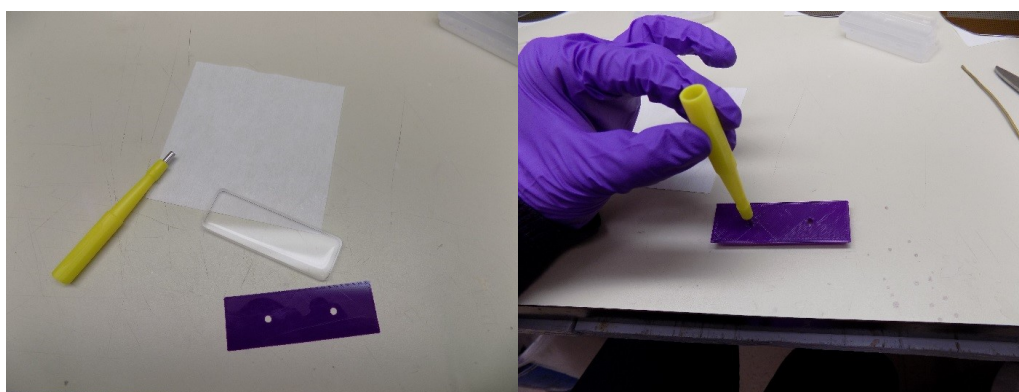


Figure 3.2: 3D printed PDMS blank hole punching with alignment tool

The main advantage of the glass channels is that they have very smooth sides therefore the channels are easily filled with the viscous methylcellulose. Also, the channel is linear as the glass is not flexible, and therefore, the alignment is very easy and there is much less background noise as seen in Table 3.3.

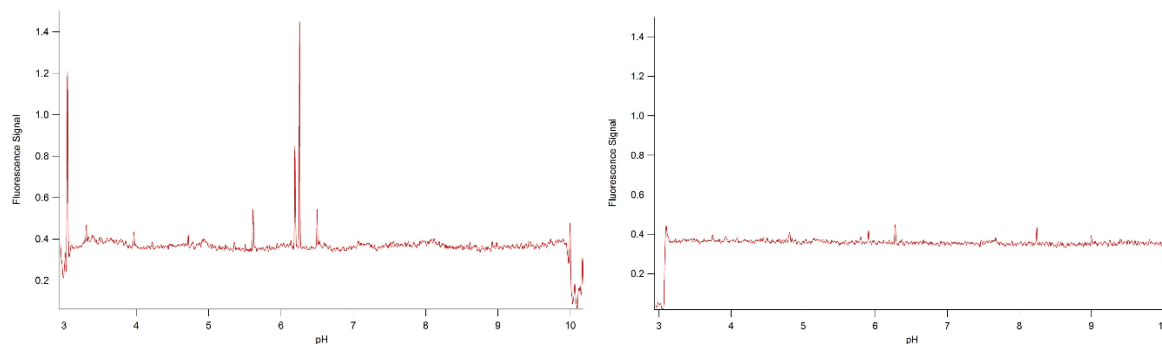


Figure 3.3: Scans of microfluidic chips made of PDMS channels (left) and glass channels (right)

The background peak-to-peak noise of the methyl cellulose filled PDMS chip was 0.05 which was 5x the noise of the glass chip at 0.01 (Figure 3.3). This difference is thought to arise from the misalignment of the flexible PDMS which allows for easy warping of the channel which makes alignment nearly impossible without extensive time and effort.

As seen in Table 3.3 all of the advantages from the transparent material, ease of alignment and surface smoothness lead to a high S/N ratio for the glass channels in comparison to the other materials tested.

pH Gradient Stability

The main concern with microfluidic isoelectric focusing in a microfluidic chip is gradient mobilization and compression. As the channel is much shorter than in capillary IEF, these factors are of greater concern as their affect is much more easily observed. One of the main sources of gradient mobilization is EOF.

To reduce and remove EOF a coating is often applied to the channel wall to remove charge effects. Commonly, polyacrylamide coatings are used as in glass capillaries, but they can often be unstable over the whole pH range of 3-10.^{11, 12, 14} They are also difficult to apply, and their loss leads to the need for a new capillary and thus added expense and time.

Another option is to use a dynamic coating that is applied before the experiment and then removed as needed and reapplied. Methyl cellulose is an ideal dynamic coating as it also increases the viscosity of the sample, which also helps reduce EOF due to the reduced mobility of the charged species. When a dynamic coating is used the surface chemistry of the initial channel material is less important which leads to the ability to use multiple materials such as the PDMS and glass channels without the need to optimize the sample composition in each case.

The other main source of pH gradient distortion in microfluidic IEF is the isotachophoretic motion of the low and high carrier ampholytes into the anolyte and catholyte reservoirs. This leads to loss of resolution on either end of the gradient. The basis for this loss is if the mobility of the negative ion of the anolyte or the positive ion of the catholyte are higher than the mobility of the most acidic or basic carrier ampholyte then an ITP train will form and drag the carrier ampholyte into the anolyte or catholyte.

Reservoir Compositions	Average pH drift per 35sec scan	Standard deviation of the average drift	Calculated pI	Observed pI	Peak width	Signal to Noise ratio
200mM H ₃ PO ₄ *, 300mM NaOH*	0.06	±0.07	6.86	6.08	0.42	484
250mM H ₃ PO ₄ *, 300mM NaOH*	0.04	±0.03	6.86	7.58	0.46	1114
500mM H ₃ PO ₄ *, 300mM NaOH*	0.06	±0.02	6.86	6.26	0.38	1288
1M H ₃ PO ₄ *, 300mM NaOH*	0.05	±0.04	6.86	7.45	0.49	346
250mM H ₃ PO ₄ *, 1M NaOH*	0.03	±0.04	6.86	7.90	0.37	261
600mM H ₃ PO ₄ *, 500mM NaOH*	0.05	±0.03	6.86	7.69	0.48	290
40mM Asp*, 300mM NaOH*	0.03	±0.09	6.86	8.98	0.76	1024
20mM IDA*, 40mM NaOH*	0.08	±0.07	6.86	6.52	0.62	358
20mM IDA*, 100mM Ca(OH) ₂ *	0.08	±0.03	6.86	5.19	0.85	334
20mM IDA*, 300mM NaOH*	0.01	±0.03	6.86	7.00	0.77	347

The sample composition was: 50 nM pI 3.99, 150 nM pI 6.86 (analyzed for data), 150 nM pI 9.7, 1%CA, 0.05%AA, 40 mM Arg, 0.4%MC, and 0.11% Brij 35. * also includes 2.5% Methyl cellulose in each reservoir solution.

To reduce this affect, the mobility of the negative ion of the anolyte or the positive ion of the catholyte must be chosen to be as low as possible. To achieve this goal large ions are preferable to small. However, the pH of the anolyte and catholyte need to be more acidic and more basic than the pH range of the carrier ampholytes. These factors imply that for microfluidic IEF the best anolyte choice would not be phosphoric acid as is typical with capillary and gel IEF. This can be seen, in Table 3.4 where the drift was 6 times greater when using phosphoric acid as the anolyte than when using IDA. Also, there is much less acidic gradient loss with the use of IDA as anolyte rather than a pH spacer as it is often used as in capillary IEF.

Another variable of great concern is the balance in the concentrations of the anolyte and catholyte. If there is too much of one or the other, then the gradient will compress and start midway across the channel rather than directly next to the reservoir. This can be observed by the difference in observed pI in Table 3.4. For example the sample with 40 mM Arg as the anolyte focused at approximately pH 9 for a pI 6.8 marker. This indicates that the entire gradient is compressed into the cathodic side of the channel.

Also, when considerable amounts of methyl cellulose (i.e. 2.5%) were added to the anolyte and catholyte to increase the viscosity and thus decrease the mobility of the ions, the ITP effect was further reduced. The data is not shown from the experiments of the methyl cellulose concentration as the drifting of the pI markers was so extreme in the case of lower concentrations of methyl cellulose that the pH drift was not able to be calculated with any reliability. The higher percentages of methyl cellulose were either too difficult to create as a consistent viscosity stock solution or never degassed from mixing in order to use as the anolyte and catholyte.

Automated Voltage Control

The microfluidic IEF with scanning LIF system controlled the voltage applied for the separation and monitored the current decay so that the separation could be monitored while it was running. This dynamic high voltage control was necessary because if high voltage was applied at the beginning of the experiment then the current would be very high which causes excess Joule heating and experiment failure. However, if low a voltage was applied throughout the experiment there was decreased resolution of the separation. To overcome this issue the voltage was controlled programmatically with the same program that collected and saved the data. The ideal separation was started at 300 V for the 3 cm channel and then increased every 35 sec by 600 V to a maximum of 3300 V. When still higher voltages were used up to (e.g. 5000 V) there was a loss of resolution most likely from Joule heating.

pI Markers

pI markers are required as even if the gradient distortions are minimized, there is still some run to run variability of the gradient. If peptides of known pI are added to each sample then the gradient conditions can be validated (mapped, calculated), and the pH scale can be used as the x axis for the separation. This also allows for the identification of peptide substrates via their calculated pI. For the identity of these pI markers Shimura et al. published a paper in which they synthesized short peptides that were labeled via the amino acid cysteine for pI markers in capillary IEF.¹⁴ These pI markers are helpful to visualize the conditions of the low and high ends of the pH gradient, however, there is great run-to-run variability in the focusing location of the peptides. Even when the pI markers at the acidic and basic end of the gradient are focused in the expected location, intermediate pI markers may focus at slightly lower or higher pI than calculated as seen with Figure 3.4.

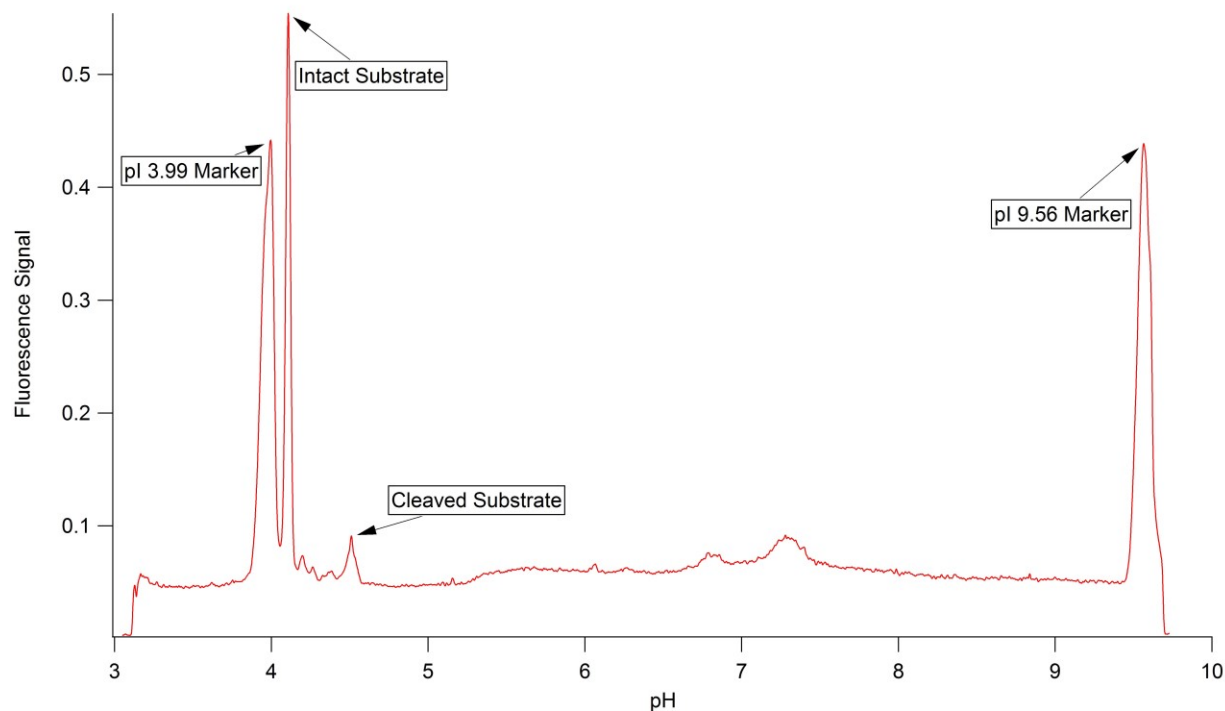


Figure 3.4: Focused pI markers 3.99, 4.5, 6.86, and 9.5 in a glass chip at 5 nM concentration each. Sample (20 mM Arg, 0.11% Brij 35, 1% Servalyte Carrier Ampholyte, 0.4% Methyl Cellulose), $V_{\min}=300, V_{\max}=3300, V_{+}=600$, 10 $\mu\text{A}/\text{V}$ sensitivity, 100 Hz.

This variability in the focusing location leads to imprecise determination of an unknown peptide or proteins pI. Despite this issue, this method is still highly valuable for the motoring of protease activity as the observed pI of the peptide substrate does not matter as long as the peptide and cleaved substrate are fully resolved. For the determination of the protease activity the peak area is used to calculate the percent of substrate present in each form and since the peptides always focus in the same order, even if the pI is shifted, the identity of the cleaved and uncleaved substrates can still be determined.

To monitor the IEF separation over time the data collection was automated and before the voltage was applied, two scans were obtained to visualize the filling of the channel. If these scans were of even height then the fluorescent material fully filled the entire channel, if not then the channel was cleaned and refilled. After these two scans the voltage was applied and a scan

was completed of the channel every 35 sec. In Figure 3.5 each 35 sec scan is a different color with scan one at the bottom and scan 50 at the top of the graph. The intensity of the signal is offset by the preceding scans. This graph is useful to monitor the effects of EOF and gradient drift on either end of the channel. It is not useful to determine the peak intensity of the separation as there is no time axis present.

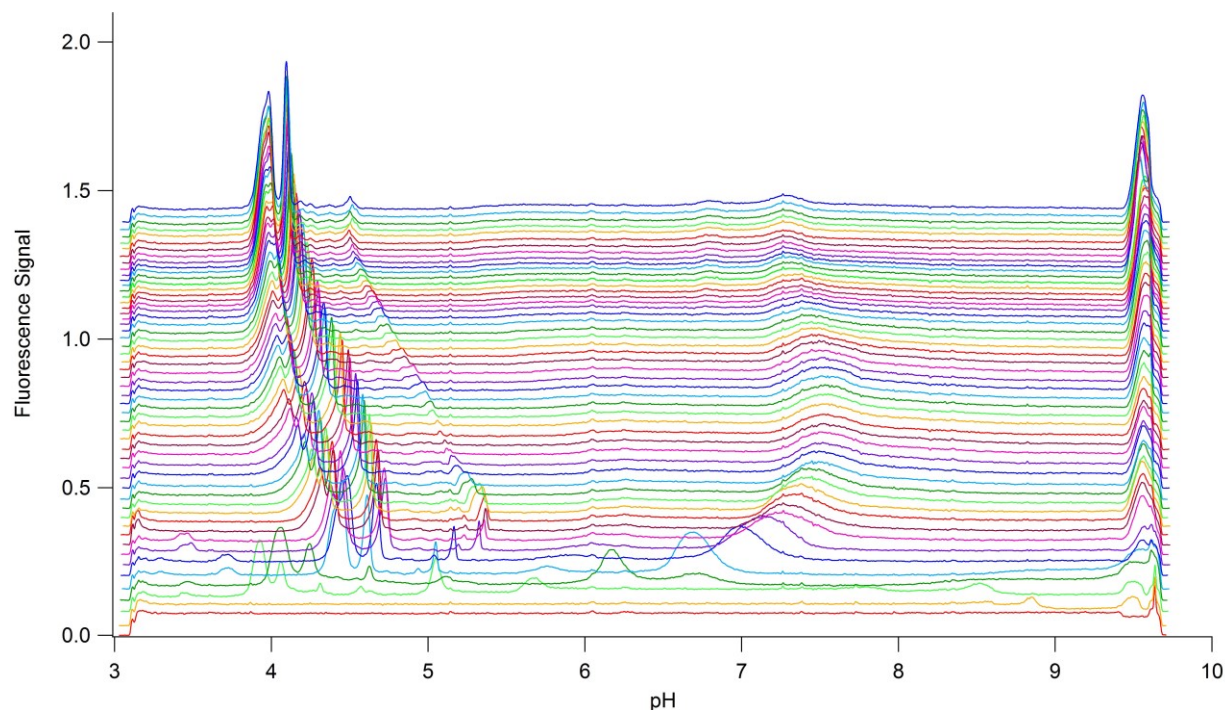


Figure 3.5: A graph of pI markers 3.99, 4.5, 6.86, and 9.5 in a glass chip at 5 nM concentration each. Sample (20 mM Arg, 0.11% Brij 35, 1% Servalyte Carrier Ampholyte, 0.4% Methyl Cellulose) to study the drift of the focused peaks over time.

As seen in Figure 3.5 at early timepoints in the separation the peaks are present, but often sharpen over time as the experiment proceeds. This type of graph is particularly helpful when working with low concentrations as very small peaks can be identified by following the focusing over time to identify stationary noise over true analyte peaks.

Figure 3.6 is a 3D graph of the scans of the same separation as seen in Figure 3.5 with time as the z-axis.

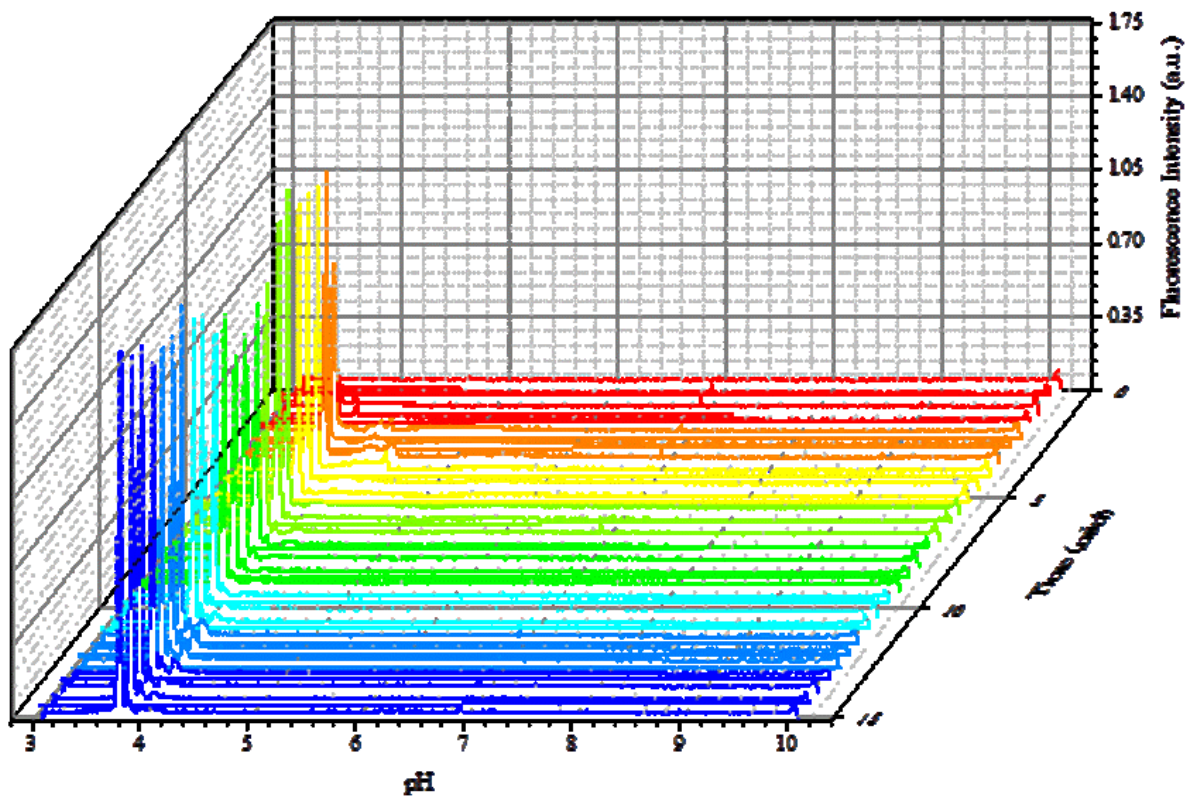


Figure 3.6: 3D graph of pI markers 3.99, 4.5, 6.86, and 9.5 in a glass chip at 5 nM concentration each. Sample (20 mM Arg, 0.11% Brij 35, 1% Servalyte Carrier Ampholyte, 0.4% Methyl Cellulose), $V_{\min}=300, V_{\max}=3300, V_{+}=600$, 10 $\mu\text{A/V}$ sensitivity, 100 Hz.

Figure 3.6 is useful to monitor the fluorescence intensity over time to determine the max focusing of the pI markers for the separation.

Another use for the pI markers was to calculate the limit of detection for the overall system. This is possible as the concentration of the labeled pI markers was determined via absorbance measurements using the molar absorptivity. To complete this study, samples were tested with decreasing concentrations of the pI markers until the resultant peaks could no longer be discerned from the noise. The limit of detection was determined using the pI 9.5 marker as approximately 500 fM as seen in Figure 3.7.

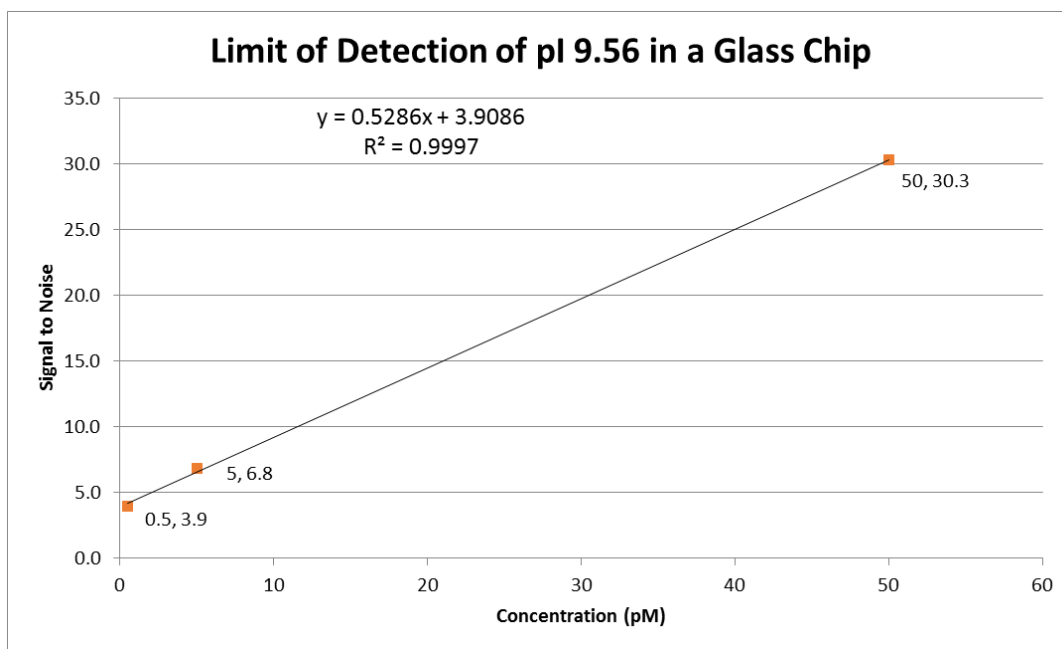


Figure 3.7: Graph of the LOD of pI 9.5 marker

For the experiments represented in Figure 3.7 the single channel glass chip was used with a new PDMS top for each sample to eliminate possible background increase from rhodamine B staining.

Trypsin Digestion

As a proof of concept for the monitoring of enzyme activity the standard enzyme trypsin was used to validate the use of IEF as the separation method. A peptide substrate with the sequence EGEKKEEAG was labeled with rhodamine B on the N-terminus of the peptide through an amide bond. Therefore, the uncleaved peptide had a pI of approximately 4.09 and the cleaved sequence EGEK which was labeled with the rhodamine B had a pI of 4.53. The ratio between the peak area of the cleaved and uncleaved was used to determine the activity of the enzyme. This was confirmed with HPLC injections and detection at 532 nm. As seen in Figure 3.8 and Figure 3.9 the relative areas of the digestions were comparable with HPLC and IEF results.

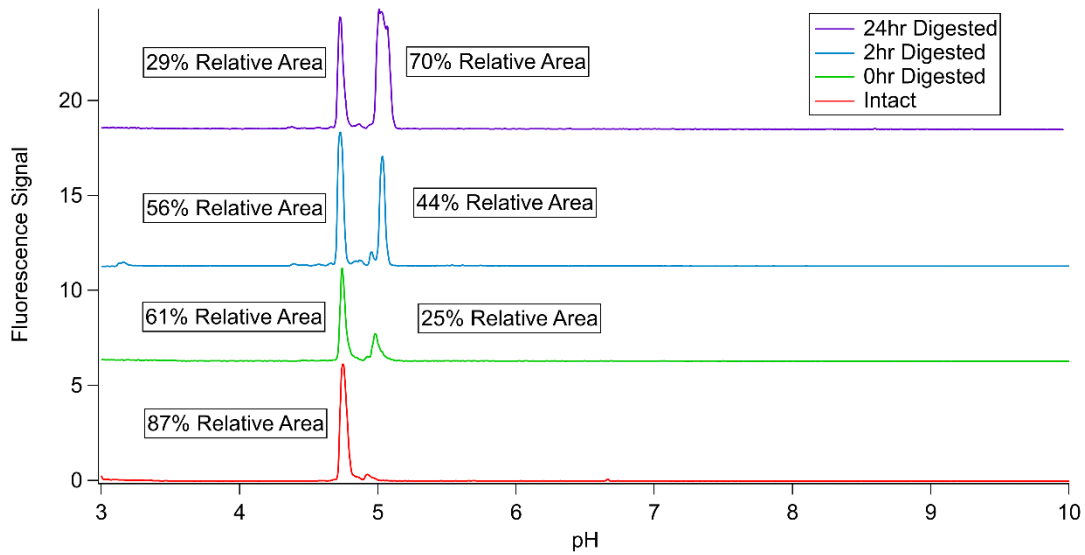


Figure 3.8: Trypsin 4hr digestion results with pI markers 3.99 and 9.5 in a glass chip at 5 nM concentration each. Sample (20 mM Arg, 0.11% Brij 35, 1% Servalyte Carrier Ampholyte, 0.4% Methyl Cellulose)

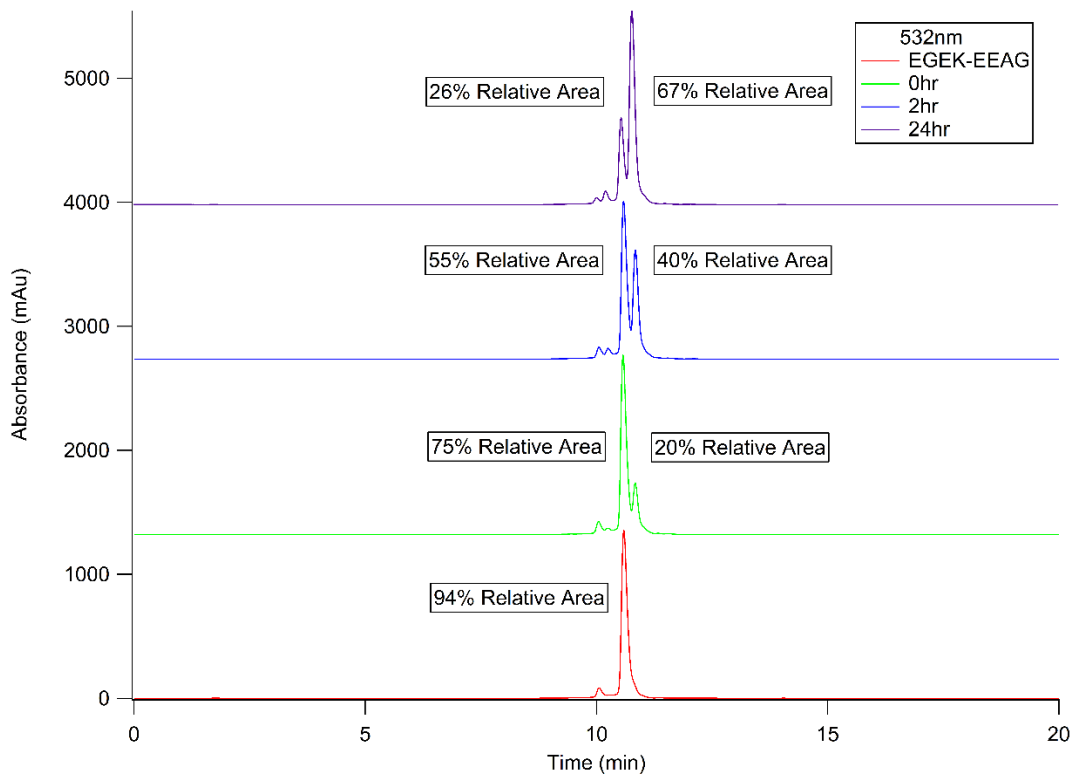


Figure 3.9: HPLC results of Trypsin Digestion samples

Conclusion

An automated detection system was created for microfluidic isoelectric focusing. This detector had minimal noise that arose from the motion component of the system and when a glass channel device was used and had LOD down to 500 fM for fluorescently labeled peptide pI markers. The system was optimized by stabilizing the pH gradient through the use of a dynamic coating of methyl cellulose and low mobility anolyte and catholyte with high viscosity additives. The detection system was used to monitor the digestion of a labeled peptide substrate by trypsin which was confirmed by HPLC with detection at 532 nm. This method of detection and separation should be an ideal component of many microfluidic devices that require low LOD and need to avoid flow. The lack of the requirement of flow can make much simpler devices than are currently used.

Chapter 4: Innate immune response studies on *Anopheles gambiae* via immunoaffinity chromatography and mass spectrometry

Introduction

Biological systems often must be observed outside of the physiological environment. These in-vitro studies frequently begin with researchers seeking to observe a singular interaction and due to this small scope of observation the results yielded are often of little use beyond the extent of the specific study. An alternative approach is to study the system in the physiological environment by looking at interactions that have already taken place in the system. This type of in-vivo experiment is often used in large model organisms due to the large volume of samples that can be obtained. When studying smaller organisms (e.g. insects) often only in-vitro experiments using samples collected and pooled from several organisms are feasible due to the smaller sample volume obtained from each organism. An example of such a problem can be seen when studying the mosquito *Anopheles gambiae*.

The components of the protein complexes that regulate the melanization cascades in the *Anopheles gambiae* mosquito have not been fully identified but are critical because they are involved in the regulation of the mosquitos' immune system. This connection can have implications in the control of the malaria parasite *Plasmodium* as the mosquito *Anopheles gambiae* is its main vector. A better understanding of the immune system of the mosquito may lead to novel methods to control the disease.

Some known components of the innate immune system are serine protease inhibitors (Serpins). Serpin 2 has been shown to be involved in melanization cascade regulation but the identity of the protease(s) that it binds to are not completely known. The total Serpin complex concentration involved in the melanization cascades are ≈ 0.1 ng/nL in mosquito hemolymph and while the

protein concentrations are relatively high, the sample volume, (i.e. the volume of hemolymph in a mosquito) is only $\approx 0.01 \mu\text{L}$. These small volumes are difficult to handle analytically without significant dilution due to the relatively large injection volumes of traditional column separations.

One novel way of approaching this challenge is to move the separation from the macro scale to the micro-scale by reducing the column dimensions. This can be done for immunoextraction (the purification and separation of proteins from complex mixtures by antibodies) because the resolution of the column depends on the elution step and not the column size. In immunoaffinity chromatography an antibody is attached to a substrate which can capture an antigen from substantial amounts of sample and then elute into a smaller volume thus increasing the concentration. There are also many advantages to reducing the size of the column including reducing solvent consumption, reducing sample volume, and the decreased amount of costly purified antibody required for the column preparation.

Large scale column chromatography has many pitfalls including the time required for analysis due to the slow mass transfer properties of traditional column supports such as agarose and cellulose.⁷⁸ A good column support must have low non-specific binding of non-target molecules, large total surface area, and fast mass transfer kinetics for the separation.

One substrate of interest is magnetic beads in the 1-2.8 μm diameter range. These beads have large relative surface area due to their small size. They also do not require the use of frits as they can be retained by an external magnetic field, thus reducing flow disruptions. This project demonstrates the use of Serpin 2 antibody functionalized beads for the separation, purification and identification of Serpin complexes. Multiple proteins including CLIP B4 and CLIP B5 were identified as seen in Appendix C.

Background

Malaria

Anopheles gambiae is the main vector of *Plasmodium falciparum* otherwise known as the malaria parasite. Malaria is responsible for the death of hundreds of thousands of people in the world each year, mostly in African countries.⁷⁹ This causes a devastating socioeconomic burden on countries where the disease is endemic. These are generally also developing countries.⁸⁰ There are many possible methods to prevent malaria, however, most of these focus on vector control including the use of bed nets and insecticides.⁸¹ The use of insect pesticides, in particular can be problematic, as insecticide resistance can arise.

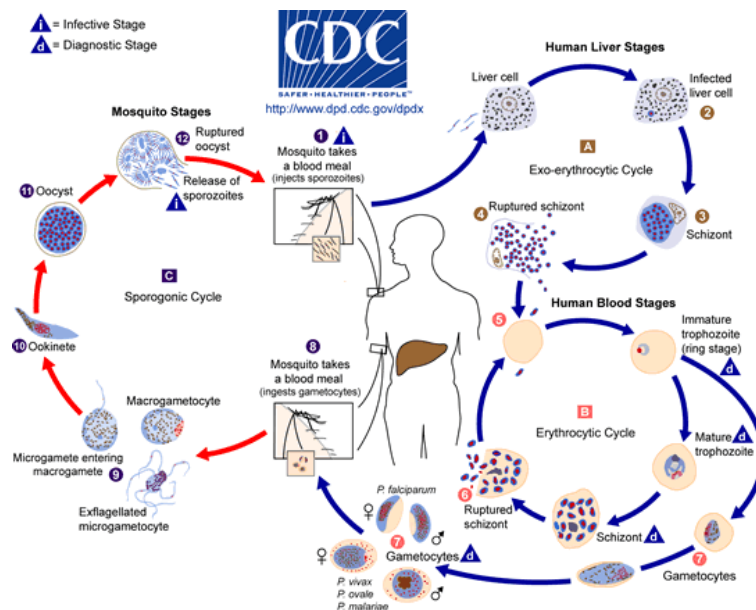


Figure 4.1: A diagram of the transmission and lifecycle of the malaria parasite. Center of Disease Control. (2016). Global Health- Division of Parasitic Diseases and Malaria. About Malaria. Retrieved May 3, 2018, from <https://www.cdc.gov/malaria/about/biology/> ⁷⁹

One possible solution to prevent malaria transmission is late-life acting insecticides. These insecticides would kill infective females late in their reproductive cycle, therefore minimizing insecticide resistance.⁸² However, identifying targets for these late-life acting insecticides is lengthy due to the biological methods used to determine late life death.⁸² However, one possible

source of late-life acting pesticides could arise from studying the immune system of the mosquito and exploiting a known component in the system to cause premature mosquito death.

Immune Response

Insects' immune systems are not composed of the typical adaptive immune system that involves antibodies, but only the innate immune system. The innate immune system is composed of systemic cellular and humoral responses.⁸³ The main steps of the innate response are: recognition of infectious non-self which often involves thioester-containing proteins (TEP), signal modulation and amplification pathways of which include clip domain serine proteases (CLIPs) and serine protease inhibitors (Serpins), signal transduction pathways including the Toll pathway, and effector response systems which include prophenoloxidasases (PPOs) which upon activation by CLIPs promote melanotic encapsulation of pathogens.⁸³

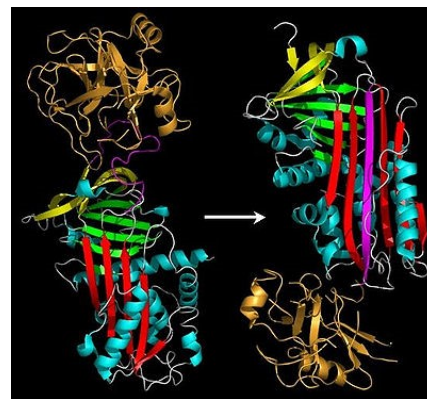
Melanization is used as an immune response to encapsulate foreign microorganisms and is also a basic part of the hardening of an insects' cuticle. If the cascades that control melanization are not tightly regulated, then melanin can be overproduced which eventually leads to insect death. One known and studied regulating molecule in the *Anopheles gambiae* mosquito is Serpin 2.

Serpin Inhibition

There are over 1000 serpins that have been identified that control an array of biological processes. These processes include coagulation and inflammation in many organisms including animals, plants, fungi, bacteria, and archaea and even some viruses.⁸⁴⁻⁸⁸

There are diverse types of inhibition involved in an immune system response, but the most straightforward type to study is known as the suicide inhibitor. This type of inhibitory protein can only inactivate its substrate once and then becomes inactive. In the case of serine protease inhibitors (Serpins) the suicide inhibitor forms a covalent bond to its substrate (a Serine Protease). This covalent bond is formed from a conformational change that the serpin undergoes upon binding with one of its substrates where the reactive center loop is inserted into the beta sheets.⁸⁹

Figure 4.2: X-ray crystal structure of the covalent complex serpin and a protease. The serpin is rendered in orange and protease in red with the reactive center loop in blue. Reprinted with permission from Gettins, P. G. W., Serpin structure, mechanism, and function. Chemical Reviews (Washington, DC, United States), 102 (12), 4751-4803. Copyright 2002 American Chemical Society.⁸⁹



In the *Anopheles gambiae* mosquito, Serpin 2 depletion results in continuous activation of PO and the formation of large melanotic pseudotumors and increased mortality rates. These results were initially discovered through the use of phenotypic studies of knockdown mosquitoes. Therefore Serpin 2 is the main control for the triggering of the melanization cascades involved in the immune system and also regulates the spread of the activated signal.⁹⁰ The generalized sequence of the PPO cascade is as follows: the protease cascades are triggered by pathogens or aberrant cells by soluble receptor molecules. This leads to the activation of a modular serine proteinase (MSP). MSP in turn activates a CLIPC that then activates the terminal CLIPB proteinase in this cascade, also called PPO activating proteinase (PAP). Active PAP then cleaves PPO to PO (see Figure 4.3).

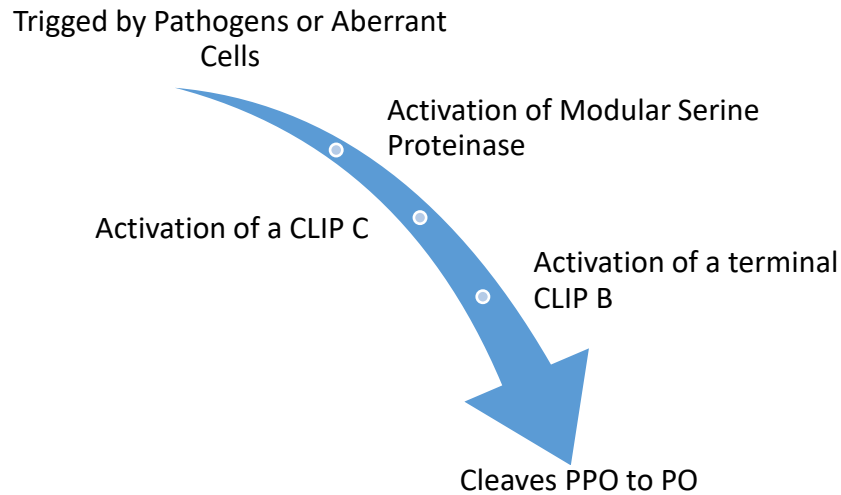


Figure 4.3: Flowchart of general steps of the mosquito melanization cascade.

In addition, the formation of the final active phenoloxidase complex on the foreign surface is mediated by one or more proteolytically inactive CLIPAs.^{91, 92} There are many different CLIP A, B and C proteases, however the identity of particular inhibition binding partners is not well known. Due to the covalent bond the identity of these binding partners (complex) may possibly be identified by separating one part of the complex and pulling the other binding partner(s) along. One method for this type of separation would be affinity chromatography.

Affinity Chromatography

Affinity chromatography is one of the most sensitive and selective of all of the chromatographic techniques.⁹³ It is based on the binding affinity of a particular analyte or class of analytes to a certain molecule. This binding interaction can be between an enzyme and substrate, receptor and ligand, or antibody and antigen. These typically reversible interactions can be used to purify or deplete molecules from a complex mixture or matrix with many contaminants.⁵ An important step in affinity chromatography is the optimization of the purification protocol to achieve efficient capture and maximum recovery of the target analyte.^{93, 94}

Immunoaffinity Chromatography

Immunoaffinity Chromatography is a subset of affinity chromatography where antigen-antibody binding is exploited as the basis of the separation.⁹⁵ In the most common form of immunoaffinity chromatography, the antibody is bound to a solid substrate i.e. solid phase support in a column and a complex mixture that contains the antigen is passed through the column.⁷⁸ The paratope of the antibody reversibly binds the epitope of the antigen through four forces: hydrogen bonding, coulombic attraction (NH_3^+ , COO^-), van Der Waals forces, and hydrophobic interactions. The unbound mixture can be washed away. Some high concentration components will non-specifically bind to the substrate and, therefore, the composition of the wash solution must be carefully controlled and chosen to minimize such reactions. The antigen can then be released by disrupting the reversible interactions between the antigen and antibody by changing ionic strength or pH and thus a pure fraction of the antigen can be obtained. This interaction can be modeled using Equation 30 where K_{eq} is the strength of the binding interaction, $[\text{Ab}]$ is concentration of the antibody and $[\text{Ag}]$ is concentration of the antigen.⁶

$$\text{Equation 30: } K_{eq} = \frac{[\text{Ab-Ag}]}{[\text{Ab}][\text{Ag}]} = 10^6\text{-}10^{12} \text{ L mol}^{-1}$$

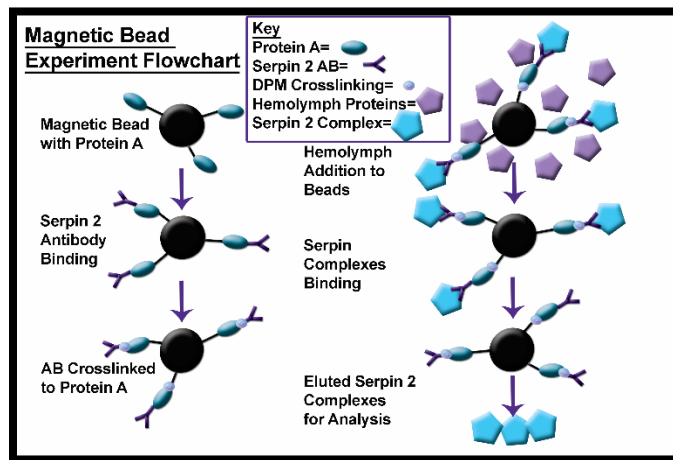


Figure 4.4: The standard immunoaffinity protocol with Serpin complexes as the antigen.

Co-immunoprecipitation

Co-immunoprecipitation (Co-IP) is a technique that is used to identify protein-protein interactions. It builds upon immunoprecipitation (IP) in that antibodies bound to a solid substrate are used to pull down an antigen. The difference is that the antigen is not a single protein, but a protein complex in which one member's identity is known and the antibody indirectly is able to capture and purify the other member of the complex. Through this technique binding partners, binding affinities, the kinetics of binding and the function of the target protein can be studied. Co-IP is a method that only works when the complex forms a stable, non-transient, high affinity relationship. In the case of identifying Serpin 2 binding partners in the PPO cascade an antibody to Serpin 2 can be used to separate out the Serpin 2 and its binding partners from the complex hemolymph for later identification by mass spectrometry. IP is required as the hemolymph sample is too complex for identification of proteins and the volume is 0.01 uL/mosquito which makes most chromatographic separations highly difficult. For enrichment and purification of the Serpin 2 complex the buffers and elution solutions must be tested and optimized so the non-specific binding is reduced, and the conditions are optimum for the identification.⁹⁶

Magnetic Bead Chromatography

In traditional chromatography the solid substrate (i.e. stationary phase support) is typically agarose, resins, or silica.⁹⁷⁻¹⁰⁷ These substrates have the advantage of stability and can have high porosity and thus have a large reactive surface area.¹⁰⁸ As well as being relatively inexpensive they are also very commonly chosen as support materials and thus most labs possess the proper equipment that is needed for their use. However, for very large proteins or protein complexes much of the surface area may not be available if the antigen is larger than the pore size of the support. This makes the support less amenable for the use of separating large protein complexes.

Also, to create a standard column, a frit must be used to contain the particles. Frits lead to many problems including cross contamination, flow disruptions, and bubble formation.

An emerging alternative is the use of magnetic beads as a substrate for chromatographic separations.¹⁰⁹⁻¹¹⁴ The conventional size for these spherical particles is 1-2.8 μm in diameter however, they are available to purchase in sizes ranging from 1-100 μm . These particles are smaller than the traditional substrates used in immunoaffinity chromatography; therefore, they have similar surface area even with the lack of pores.

The magnetic beads consist of super paramagnetic materials that exhibit magnetic properties in the presence of a magnetic field but retain no magnetism once the field is removed. When this property is exploited, the magnetic beads can be mixed with a solution to create a dispersion and allow for quick mass transfer of the reactants, and then an external magnet can be used to separate the beads from the solution. This leaves behind a substrate free solution without the need of centrifugation. Without centrifugation more fragile protein complexes can be studied that have not been purified previously.

By using these magnetic properties columns can be formed without the use of frits and their associated problems by using the magnetic properties to retain the column. Additional advantages are the resistance of the column to air bubble disruption as well as reduced reagent use due to the smaller sizes of columns that can be utilized.

The beads themselves are a polymer encapsulated shell with a magnetic compound, usually iron oxide, inside. The polymer surface coating allows biological substances to be bound and the beads then can be functionalized similarly to traditional substrates.

Mass Spectrometry

Mass spectrometry (MS) is the separation and detection of ions based on their mass to charge ratio (m/z). This technique can be used to determine the molecular composition of an unknown analyte.⁵

The analyte of interest must be an ion in the gas phase for this type of detection therefore this detector is often coupled to an ionization source. The three main components of MS are the ion source, mass analyzer, and detector.¹ The most common ion sources used in biological studies are electrospray ionization (ESI) and matrix assisted laser desorption ionization (MALDI) which are both considered soft ionization sources in that there is little fragmentation of the analyte molecule.

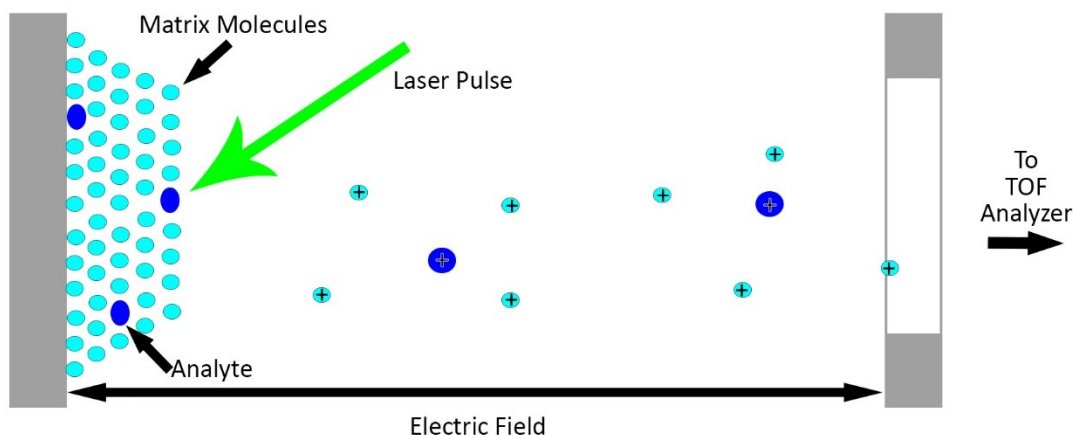


Figure 4.5: Schematic of MALDI desorption

MALDI is different than the other sources of ionization as it can transfer large biomolecules greater than 100 kDa into gas phase without fragmentation. Thus, it is known as a soft ionization source. MALDI is performed through the co-crystallization of 1000-10000 times excess of a matrix (such as cinnamic acid) with the analyte. The matrix consists of small, UV absorbing molecules that when a laser pulse at the molecules excitation wavelength reaches the co-crystal,

the matrix is transferred into the gas phase along with the non-absorbing analyte. The gaseous ions are then typically transferred into a time of flight (TOF) mass analyzer (Figure 4.5).⁵

The mass analyzer is the component that has the most effect on the sensitivity and mass accuracy of the instrument. The most common mass analyzers are quadrupole, TOF and sector field. This component only allows ions of a particular mass to charge ratio to reach the detector at any point of time or space. The mass analyzer scans hundreds of values a second to create the spectrum. This spectrum can be considered an analyte's fingerprint and can be used to identify unknown compounds manually or through the use of database searching software.¹

One crucial factor when comparing the different mass analyzers is the mass resolution. The most sensitive mass analyzer used in this research is the sector field instrument known as the Orbitrap which has a resolving power of 100,000.¹¹⁵ This instrument introduces ion packets tangentially into an electric field. The electric field is then ramped up until the ions are in a dispersed elliptical trajectory. The axial motion is harmonic and common among all ions, but the rotational frequency is dependent on the m/z (Equation 31).

Equation 31: $\omega = \sqrt{\frac{k}{m/z}}$ where k is the force constant of the potential

Thus, ions of the same m/z will spread into rings which can then be released into the detector.

Low concentration ions have a higher probability of identification as multiple packets of ions can be introduced into the trap before detection.¹¹⁶

Another type of mass analyzer is the TOF which has a typical resolving power of 10,000.¹¹⁵ The TOF analyzer separates the gaseous ions by accelerating them with an electric field. The ions separate based of their drift mobility and the m/z ratio can be determined through measurement of the drift time with Equation 32

Equation 32: $\frac{m}{z} = \frac{2eV}{L^2} t^2$ where e is the elementary charge, V is the voltage of the applied electric field, L is the length of the field free drift tube, and t is the drift time of the ion.⁵

After the ions are separated, the detector records either the charge induced or the current produced when an ion passes by or hits a surface. Normally, some type of electron multiplier is used since the number of ions leaving the mass analyzer at an instant is often quite small, therefore, considerable amplification is needed.

Mass spectrometry is commonly linked to other analytical techniques such as liquid or gas chromatography due to the need for slowly introduced and separated compounds for sensitive detection. Liquid chromatography (LC) is most commonly used for protein studies due to the thermal degradation of most physiological compounds as well as their aqueous nature being incompatible with gas chromatography.¹¹⁷

Trypsin Digestion

When trying to identify unknown molecules the instrument chosen is the mass spectrometer.

There are two different approaches that can be taken when identifying proteins. They are top down or bottom up. The top down approach is to ionize complete proteins into the mass spectrometer and then detect their mass to charge ratio and deconvolute the mass spectra. This is common with small proteins and small molecules. However, when the protein is large or part of a complex it becomes very difficult to deconvolute the spectra due to multiple charged states.

Therefore, for large proteins the bottom up approach is often taken in which the protein is digested by a specific enzyme into small peptides that can be detected and analyzed much easier.

Trypsin is the most commonly used enzyme for this purpose since it has a well-defined specificity; it hydrolyzes only the peptide bonds in which the carbonyl group is followed either by an arginine (Arg) or lysine (Lys) residue due to the presence of a negative residue in the

catalytic pocket.⁵ Due to the specificity of the enzyme the fragmentation of the peptide can be predicted and used to deconvolute the resultant mass spectra of the digested protein. This can be done using peptide prediction algorithms and protein databases that are built into mass spectrometry analysis software. The search requirements can be set by the user to define the required number of unique peptides and other statistical variables that must be reached to identify a protein.

One of the usual challenges faced when performing a trypsin digestion is that the sample is often collected from an excised spot of an electrophoresis gel. This is often done as a sample preparation step to purify the protein of interest. However, the cutting of the band of the protein of interest can lead to a loss of resolution as it can be difficult to excise the spot reproducibly.

Another option is to perform more extensive sample preparation using affinity chromatography and then digest the proteins in-tube. This purifies the protein to the level required for mass spectral identification without the need of electrophoresis of the MS sample. However, a small sample can still be tested by gel electrophoresis to test the purity of the separated protein.

Standard Biochemical Techniques

The Western blot is a common biochemical assay that is frequently used when trying to detect specific proteins in a complex mixture. The process involves loading an electrophoresis SDS-PAGE precast gel with the protein sample and then running the gel to separate proteins based on size. The proteins are then transferred to a nitrocellulose membrane by applying the electric field perpendicular to the gel and allowing the proteins to migrate into the membrane. After the transfer is complete a color reagent or fluorescence conjugated antibody is used to detect and visualize the proteins and protein complexes of interest. All other proteins remain unlabeled. The

results can be made semi-quantitative by using the open source software NIH Image J if standard proteins are used to make a calibration plot.

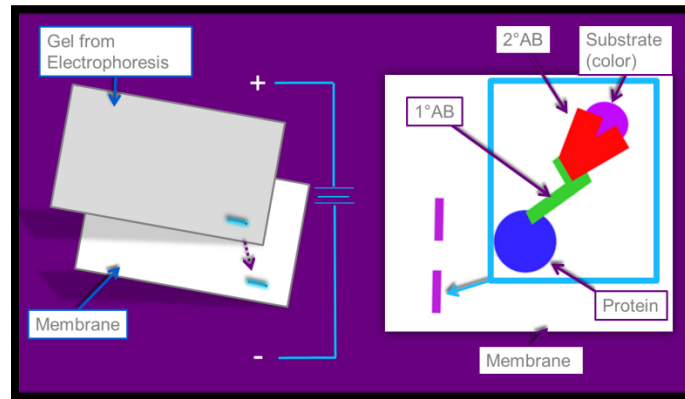


Figure 4.6: A diagram of the Western blot procedure.

Another common biochemical assay is a silver stain where all proteins in a sample are visualized. Coomassie brilliant blue staining can usually detect a 50 ng protein band; silver staining increases the sensitivity typically 50 times.¹¹⁸ This is done using an electrophoresis gel that is then stained with a silver nitrate solution.¹¹⁹ This can be performed in conjunction with a Western blot in that the silver stain shows all proteins whereas a Western blot only detects the protein to which the antibody used to develop the membrane has an affinity.

Methods

Insect rearing

The *An. gambiae* G3 strain was reared at 27°C and 80% humidity using a 12:12 light: dark cycle. After hatching, larvae were fed baker's yeast (Active Dry Yeast, Red Star) for 48 h and subsequently fish food (TetraMin® Tropical Flakes, Tetra) and baker's yeast. Adult mosquitoes were provided sugar solution (8% fructose supplemented with 2.5 mM PABA; SIGMA) ad libitum. Heparinized horse blood (PlasVac) was used as a blood meal source and provided via an artificial glass feeder system (KSU, Chemistry Department) using stretched parafilm as the membrane.

Hemolymph Sample Collection

Adult female G3 mosquitoes within 48 h of eclosion were anesthetized (approximately 25 insects at a time) with carbon dioxide and then injected with approximately 7 nL of a bacterial challenge to the mosquito via a Nanoject II system. The mosquitoes were fed sugar solution *ad libitum* throughout the experiment and were incubated for 17-19 hours. After this time, the insects were again anesthetized with carbon dioxide and placed on ice. In batches of 15 insects on an ice dish, the proboscis of the mosquito was clipped and the hemolymph (appx. 0.01 μ L/insect) was collected by squeezing the abdomen and collecting the drop of hemolymph in 1 μ L 1x Roche Protease Inhibitor in PBS per insect. The samples were then frozen immediately in liquid nitrogen and stored at -80 °C to preserve the *in-vivo* protein complexes and to prevent the formation of new complexes.



Figure 4.7: Left is the magnified side of a mosquito with the injection point labeled and right is the hemolymph collection after incubation into 1x Roche protease inhibitor

Purification of Serpin 2 Antisera

The Serpin 2-KSU-238 rabbit antisera (bleed 2) was custom produced from Cocalico Biologicals and was purified using recombinant Serpin 2 protein and then dialyzed into PBS. The final concentration was determined via Nanodrop® analysis to be 1.56 μ g/ μ L.

Procedure for In-tube Immunocapture and Separation

To remove protein interferants that may non-specifically bind to the beads during IAC, the hemolymph was first mixed with magnetic beads precoated with Protein A. Any potential interferants could then non-specifically bind to the particles so that they could be removed from the sample prior to analysis. For this process 1.2 mg of Protein A Coated Magnetic Dynabeads were prepared by rinsing three times with a buffer containing 1x PBS and 0.7% w/v n-Octyl-B-D- Glucopyranoside (PBSOg). They were then rinsed once with 0.1 M Glycine for two minutes. The previously frozen hemolymph was then allowed to thaw on ice and incubated with the prepared beads for 1.5 hr with on-axis rotation using an in-house mixing device to keep the beads in solution without excessive agitation (Figure 4.8). This mixing of the sample with the unlabeled substrate is called preclearing the sample and allows for better binding efficiency to the antibody coated beads.

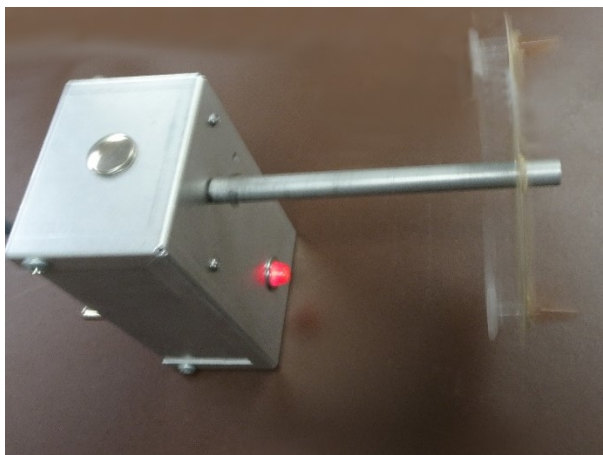


Figure 4.8: In-house mixing device for axis rotation

An aliquot of 78 μg of the purified antibody was bound to 1.2 mg Protein A Coated Magnetic Dynabeads with a 30 min incubation. The beads were then rinsed two times with PBSOg and one time with triethanolamine. The antibody was then irreversibly cross-linked to the Protein A using dimethyl pimelimidate (DMP) and letting the solution incubate for 30 min. DMP is an imidoester

that reacts with primary amines to form amidine bonds. The reaction was performed in triethanolamine which is a tertiary amine and a weak base which is required to maximize the efficiency of the DPM reaction. To quench the reaction and prevent the DMP from crosslinking non-specific proteins later in the procedure, 50 mM Tris was added. Tris, as a primary amine, reacts with all residual DMP to prevent further crosslinking once the hemolymph sample is added to the magnetic beads.

The beads were then rinsed three times with PBSOg. To increase the density of antibody bound to the beads, an additional 78 µg of the antibody was applied a second time so that a total of 156 µg was theoretically bound. A 0.1M Glycine rinse for two min was used to remove all unbound antibody. Then the precleared hemolymph from the antibody free beads was removed and added to the antibody coated beads for 1.5 hr with on axis rotation. The beads were then rinsed 2 times with PBSOg and 4 times with water before being eluted into a small volume of 0.1%TFA.

Mass Spectrometric Analysis

The sample was then shipped on ice to University of Nevada, Reno Proteomics Department for analysis via LC-Orbitrap-MS. They used a GE 2D clean up kit to separate proteins from detergents, salts, lipids, phenolics or nucleic acids that remained in the solution. An in-tube trypsin digestion was then preformed, and the resultant peptides were run through a Michrom Paradigm Microdialysis Liquid Chromatography (MD/LC) and Michrom CaptiveSpray coupled to a Thermo LTQ Orbitrap XL with Electron-transfer dissociation (ETD).

Database Searching-- All MS/MS samples were analyzed using Sequest (XCORR Only) (Thermo Fisher Scientific, San Jose, CA, USA; version 2.1.0.81). Sequest (XCORR Only) was set up to search Anoga_NCBI_20150226.fasta assuming the digestion enzyme trypsin. Sequest (XCORR Only) was searched with a fragment ion mass tolerance of 0.60 Da and a parent ion tolerance of

10.0 PPM. Carbamidomethyl of cysteine was specified in Sequest (XCorr Only) as a fixed modification. Oxidation of methionine and acetyl of the n-terminus were specified in Sequest (XCorr Only) as variable modifications.

Criteria for Protein Identification-- Scaffold (version Scaffold_4.6.1, Proteome Software Inc., Portland, OR) was used to validate MS/MS based peptide and protein identifications. Peptide identifications were accepted if they could be established at greater than 95.0% probability by the Peptide Prophet algorithm (Keller, A et al Anal. Chem. 2002;74(20):5383-92) with Scaffold delta-mass correction. Protein identifications were accepted if they could be established at greater than 99.0% probability and contained at least 2 identified peptides. Protein probabilities were assigned by the Protein Prophet algorithm (Nesvizhskii, Al et al Anal. Chem. 2003;75(17):4646-58). Proteins that contained similar peptides and could not be differentiated based on MS/MS analysis alone were grouped to satisfy the principles of parsimony.

Online Immunocapture and Separation Device

The rotor device for magnetic bead mixing and immunocapture on column was created with a NEMS 23 stepper motor attached to a plexiglass spinning rotor that contained 15 pairs of neodymium magnets in machined and press fit holes in a circular pattern. A plexiglass capillary holder was machined to the correct dimensions to hold the capillary directly above the rotor where the north-south intersections of the magnets meet to allow for the highest electric field. The rotor height was adjusted with set screws to allow for a distance of separation of one sheet of paper or (0.1 mm). The capillary holder was held in place with 3M packaging tape and the excess space around the capillary was filled with gelatin to allow for increased visibility of the capillary. The monitoring of the capillary was achieved with a Samsung Galaxy S5 cell phone with a 10X clip on lens.



Figure 4.9: Left magnetic rotor for the mixing of magnetic beads and right diagram of the magnetic bead mixing device.

Procedure for Rotor Immunocapture and Separation

To test the rotor the procedure above was followed until the removal of the hemolymph. Half of the beads were used to follow the in-tube elution procedure and the other half of the beads were loaded into the capillary at 25 $\mu\text{L}/\text{min}$ using reverse flow. The beads were then rinsed with PBS for 5 min at 5 $\mu\text{L}/\text{min}$ with a rotor speed of 50 Hz (24RPM) and then with water for 2 min with the same conditions. The sample was then eluted with 0.1%TFA for 10 min at the same conditions with sample collection in two-minute blocks (10 μL samples). The elution's were then tested with a Western blot to determine elution efficiency compared to in-tube elution.

Results

Hemolymph Sample Collection

The first step of the study was to optimize the sample collection and to test the collected samples for Serpin 2 complexes via the Western blot procedure with serpin 2 antibodies and anti-rabbit AP conjugate for visualization. To optimize the sample collection procedure, three immune system challenges were tested for maximum complex formation and minimal insect death. The immune systems challenges tested were *Micrococcus luteus* at OD = 0.55, *Enterococcus faecalis* at 5000 and 50,000 CFU, and *Escherichia coli* at OD = 0.05.

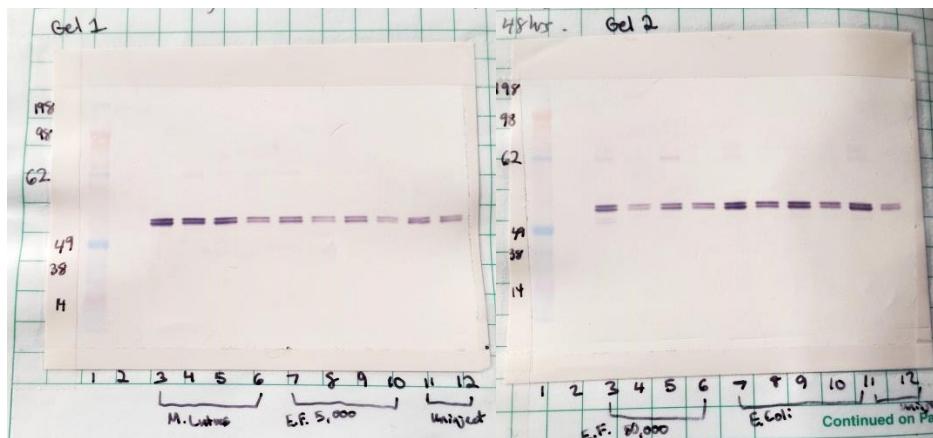


Figure 4.10: A picture of the Western Blots used to determine which immune system challenge gave optimum complex formation.

We discovered that *Micrococcus luteus* at OD = 0.55 and EF at 50,000 CFU produced the highest complex formation, while *Enterococcus faecalis* killed 30%-85% of the injected population depending on the time of incubation. Therefore, *Micrococcus luteus* was chosen for the bacterial challenge to induce complex formation. In successive sample testing and collection, the injection and bleeding procedure was optimized by changing the number of the mosquitos injected in each cage from 25 to 50. Also changed was the time between injection and bleeding, from 24 hours to 17-18 hours, as the incubation after injection time was found to produce a higher complex amount if it occurred mostly overnight rather than during the day. This agrees

with findings from Rund et al that stated CLIPB8, PPO, CTLMA2, CLIPA7 were found to have a diel rhythm. Additionally, they also found that at least 15.8% of the genome is under diel and/or circadian control. The research suggests time-of-day specific effects should be considered when developing new biopesticide-based interventions. ¹²⁰

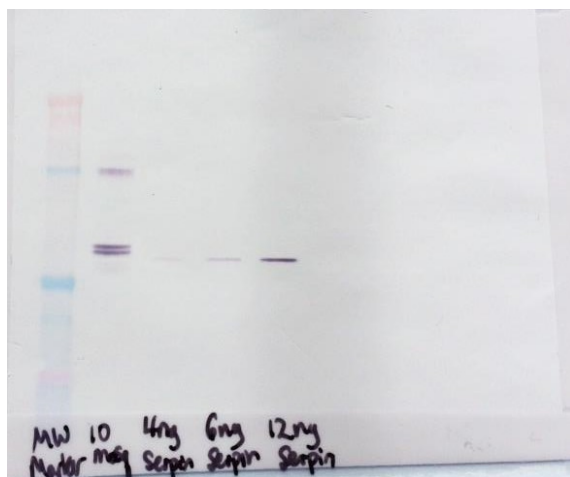


Figure 4.11: A picture of a Western Blot of a sample that was collected with the optimized sample collection procedure. Using Image J, it was determined that each mosquito contained 1ng Serpin complex and 2.5ng Serpin 2.

Detergent effects on Non-Specific Binding

The main affinity chromatography experiment was first completed in a batch in-tube method to optimize the buffer detergent. The detergent needs to be optimized to balance the reduction of non-specific binding and the loss of the serpin-protease complex in the washes. The stronger the detergent the purer the final sample, but the lower the concentration of the analytes. As an additional factor to consider, some detergents can suppress the ionization of the molecules when performing Mass Spectrometry which is vitally important with low concentration and sample limited studies.

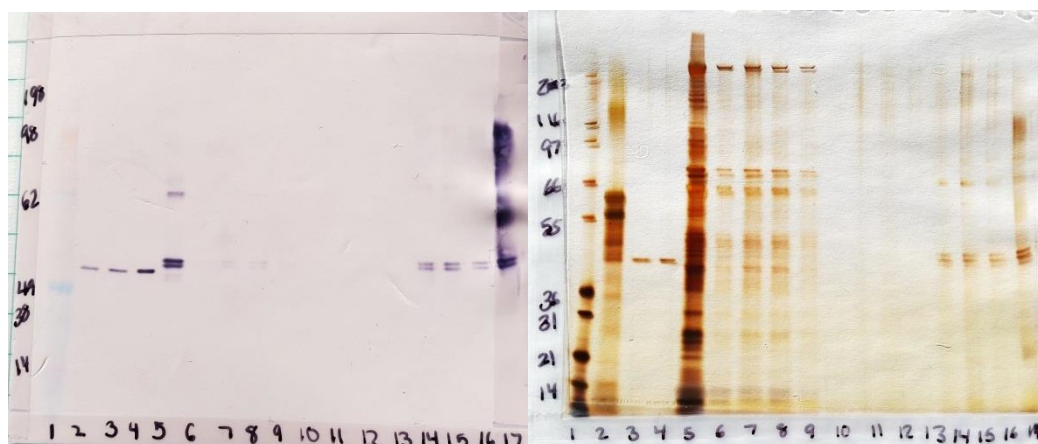


Figure 4.12: A Western Blot and Silver Stain of the detergent washes and elution of the immunoaffinity protocol with four different methods of detergent washes. The methods were PBS, PBS + n-octyl- β -D-Glucopyranoside (Og) 0.7%, PBS + Og 0.35%, and PBS + TWEEN-20(PBST).

Lane Number	Contents	Lane Number	Contents
1	MW Marker	10	Water Wash PBS
2	5 ng Serpin 2 Standard	11	Water Wash PBS-Og 0.7%
3	10 ng Serpin 2 Standard	12	Water Wash PBS-Og 0.35%
4	15 ng Serpin 2 Standard	13	Water Wash PBS-TWEEN 20
5	Hemolymph Supernatant	14	Elution PBS
6	Wash 1 PBS	15	Elution PBS-Og 0.7%
7	Wash 1 PBS-Og 0.7%	16	Elution PBS-Og 0.35%
8	Wash 1 PBS-Og 0.35%	17	Elution PBS-TWEEN 20
9	Wash 1 PBS-TWEEN 20		

Multiple wash buffer compositions were tested including removing the detergent from the PBS as well as the non-ionic surfactant TWEEN-20. TWEEN-20 is a common non-ionic detergent and is used in various biological experiments, including protein IP and Western blotting.¹²¹

However, TWEEN-20 can cause significant signal suppression and high polymer background in addition to the formation of adducts with the proteins when the sample is introduced into MS.

The detergent n-octyl- β -D-Glucopyranoside (Og) was tested as it has a relatively high critical micelle concentration and thus can be easily removed by dialysis which makes it MS friendly. Og is also a low-molecular weight, non-ionic detergent that is optically clear with low absorbance at 280nm. It was also shown to increase the selectivity and sensitivity of immunopurification.¹²¹ This can be attributed to its ability to occupy the binding sites of substrate surface or inhibit the interaction between substrate and peptides.

Ionic surfactants such as SDS, despite being the strongest surfactants, are unfortunately not compatible with MS analyses since they can inhibit enzymatic digestion and severely suppress the ionization of proteins and peptides.

The optimum buffer detergent system was determined to be 1x PBS + 0.7% Og for all antibody binding steps and PBS with no detergent for the rinses after Serpin binding to the antibody. This was sufficient to reduce the non-specific binding while maintaining the concentration of the Serpin complexes high enough for mass spectrometry detection.

MALDI-TOF Contamination Testing

The initial orbitrap MS results contained very low amounts of expected peptides when compared to the western blot results. (See Appendix C.) Because of this, the undigested samples were tested on a Bruker UltraFlex III MALDI-TOF Mass Spectrometer. Through this testing it was determined that there was a contaminant that came from the dialysis of the serpin 2 antibody that was overwhelming the detector. The antibody contained a great deal of 1300-1600 Da polyethylene glycol from the use of a syringe from the dialysis cassette. This was removed by spin filtering the antibody before use with a 30,000 Da Amicon Ultra 0.5mL Spin Filter for later experiments. This change allowed for more *Anopheles* protein identifications from the MS results and a higher probability of the protein identifications.

Immunoaffinity Western Blot Results

One of the easiest methods for testing the efficacy of the separation is to use a western blot. This testing can be completed in a day and can detect very low amounts of protein down to approximately 1ng. One of the best reasons to use a western blot for this experiment is to test the enrichment of the serpin and complex compared to the initial hemolymph. This is shown in Figure 4.13 when lane 5 is compared to lane 7, as lane 7 has much more intensity in color for the serpin at the lower purple band and the complex at the faint higher molecular weight band.

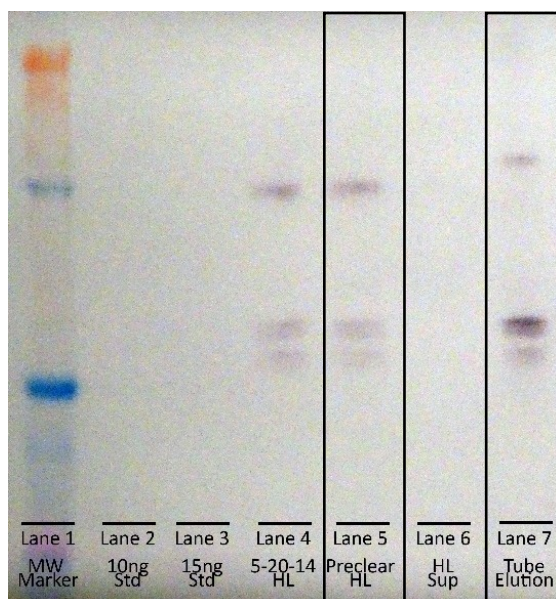


Figure 4.13: Western blot showing enrichment of serpin and complex from lane 5 and 7.

Mass Spectrometry Results

If the Western blot showed enrichment in the initial stages and the silver stain was relatively clear of contaminants the samples were shipped to University of Nevada, Reno for testing on their Thermo LTQ Orbitrap XL. The mass spectrometry results (see Appendix C) from hemolymph pooled from 200-400 mosquitoes, were used to tentatively identify nine possible Serpin 2 complex binding partners via the mass spectrometry search methods described in the method section. There were more than 6 samples tested with this method over the course of 3

years and as the process was optimized more relevant identifications were made. Initially only Serpin 2 was identified in the samples before the optimization of the rinsing and elution buffers to the most MS friendly options. As more components were optimized, more biologically relevant compounds were identified as seen when comparing the sample from 2/25/13 which had few Anopheles proteins identified to the sample from 1/14/15 which had many. This includes other molecules that were expected, based on the known PPO pathway. Additional MS identification tables are located in Appendix C.

These identifications would need to be confirmed via supplemental techniques such as mixing recombinant proteins of the identified partners together and testing them for complex formation. This could be done by testing the western blot with the antibody for the identified proteins and looking to see if the complex is visualized as well as further MS analysis.

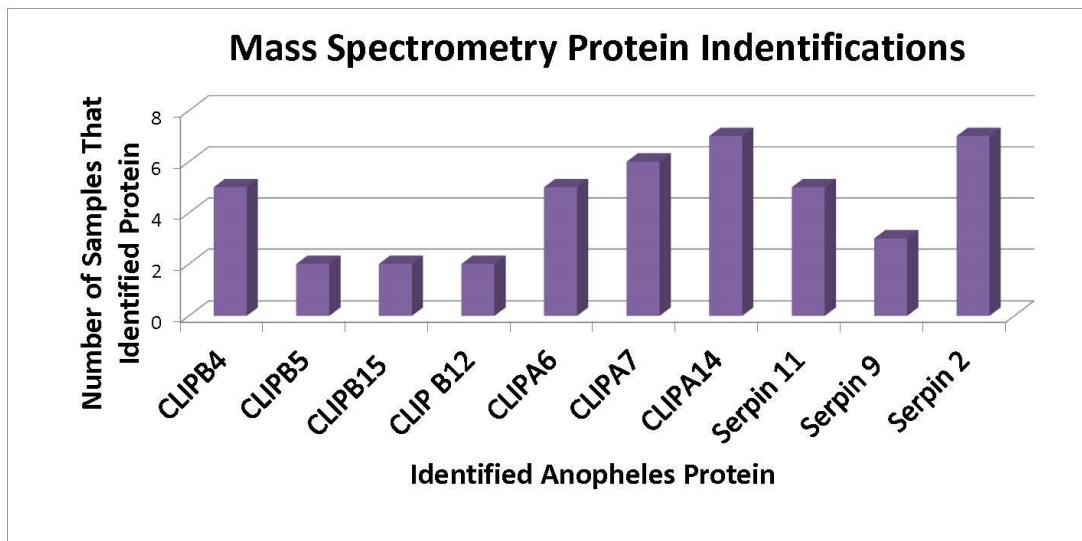


Figure 4.14: This graph shows the consistency of the mass spectrometry results with the new sample collection and detergent washes.

Initial Magnetic Bead Column Formation

To automate the process of serpin complex isolation and to reduce the elution volume of the isolated compounds the immunoaffinity column was moved from an in-tube batch format to a column formed in a capillary tube.

There were two main options for possible configurations of using magnetic beads to create a small volume capillary column. The simplest was to position two large disk magnets in an attractive position with a small ID glass capillary tube in a gap between the magnets (Figure 4.15). When the functionalized magnetic beads of 1-2.8 μm diameter are introduced to the capillary column the attractive magnetic field contains the beads and causes the formation of a small column that is stable against pressures from the mobile phase from a syringe pump.

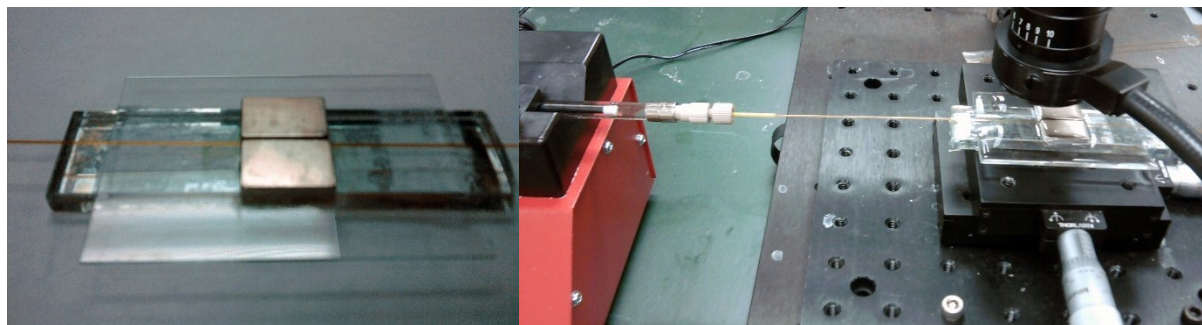


Figure 4.15: Left the initial magnetic bead column creation. Right the initial setup for the simple magnetic bead column

The advantage of this type of column design is its simplicity and the ease of fabrication. It also does not require any external electronics other than a syringe pump. The main disadvantage is that there is no mixing of the beads with the sample while the analyte is flowing through the column. This causes a need to increase the residence time of the analyte with the substrate. To do this the flow would need to be stopped which greatly increases the amount of time required for the procedure. The stopping and starting of the flow lead to issues with retaining the beads and was thus abandoned for the second method.

Magnetic Bead Rotary Column

An alternative method was to create a rotary device to allow for the formation of many small magnetic bead columns as well as the agitation of the beads to allow for continuous flow and mixing. This bead trap device was modeled after a prototype from Anderson et al. that was used

to contain and agitate 2.8 μ m diameter magnetic beads for SISCAPA ¹²²Pepptide Enrichment. The prototype consisted of a low speed (2rpm) reversible synchronous motor that rotated an aluminum rotor on which eight pairs of ¼ inch disk magnets were countersunk evenly spaced on the perimeter in an attractive position. Using four threaded rods with springs for resistance and finger nuts for adjustments, an acrylic plate with the capillary taped in place was lowered into the magnetic field (Figure 4.16). A small volume of magnetic beads was then introduced to the capillary via a syringe pump with the magnet rotor in parallel of the flow. Once the beads were loaded into a magnetic region, the rotor direction was reversed and with the flow balanced to oppose the magnetic field, the beads were mixed with the mobile phase. The flow ranged from 1-50 μ L/min in the device. Only one set of magnets was used to create the column. The other seven sets were used to promote mixing and to reduce the chance of magnets leaving the capillary and into the downstream detection where it could interfere. The paper reports better capture efficiency than batch mode.

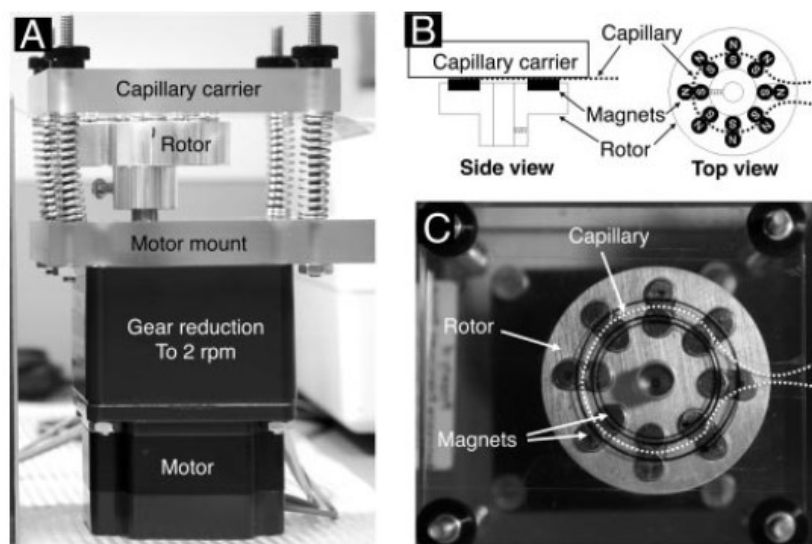


Figure 4.16: The bead trap device used in for SISCAPA Peptide Enrichment. A) side view; B) schematic diagram; C) top view. This figure was originally published in Molecular & Cellular Proteomics. N. Leigh Anderson, Angela Jackson, Derek Smith, Darryl Hardie, Christoph Borchers and Terry W. Pearson. SISCAPA Peptide Enrichment on Magnetic

Beads Using an In-line Bead Trap Device. Mol Cell Proteomics. 2009; Vol: 995–1005. © the American Society for Biochemistry and Molecular Biology.¹²²

To improve this device and make it more suitable for use with the Serpin 2 complex application many modifications were made. The largest change came from the fact that for the immunoaffinity part of the project, magnetic bead sample volume is much larger than the 5 μL reported in the paper. This was due to the need for more functionalized ligands to bind the Serpin 2 antibody and thus retain enough Serpin 2 complex to elute in identifiable amounts for MS. To allow for this larger number of magnetic beads, the capillary diameter was increased from 150 μm ID to 300 μm ID. The rotor diameter was also increased from 2 inches to 3 inches. This allowed for more pairs of magnets to be used to contain beads and thus a larger column in total. There are fifteen pairs of magnets which allowed the beads to spread out along the perimeter of the rotor and achieve greater mixing (Figure 4.17).

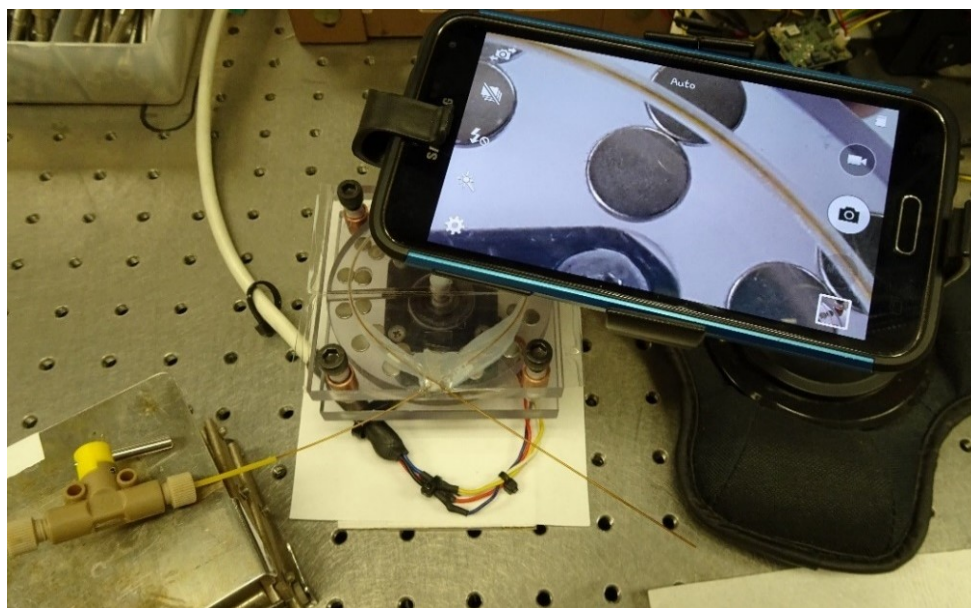


Figure 4.17: The setup of the mixing device with the camera in place with a 10x magnification lenses for visualization.

Another change was to change the type of motor used to control the rotor speed. A stepper motor was used as it turns based off of how many electrical pluses the motor receives. This type of

motor can be controlled very easily to different speeds by interfacing it with a computer or Arduino type device. In this case the motor was interfaced with the software LabVIEW and a custom program was written to control the motor speed to retain the beads in the column with maximum agitation and mixing.

Once the device was built and tested one of the fundamental issues was that once the magnetic beads were loaded into the column there were a substantial number of things that caused the beads to be lost through the waste. Some of these factors were surges in flow when the two-way valve was used to switch between solvents, unbalanced flow vs rotor speed and loss of sizable portions of the column (i.e. retained beads) to the waste when large bubbles occurred. These parameters led to decreased amounts of peptide in the elution fraction even if the fraction was smaller and theoretically more concentrated than in the tube method of elution. This can be seen in Figure 4.18 where lane 7 had strong bands and lanes 8-11 show no evidence of Serpin 2 peptide or complex.

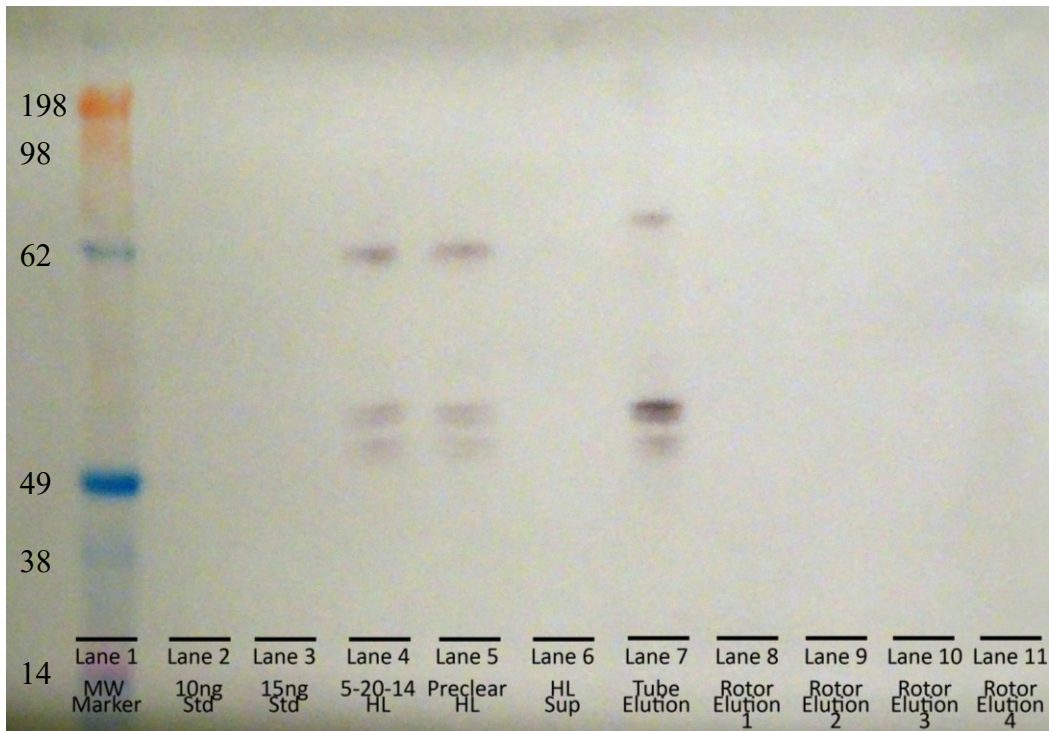


Figure 4.18: Western blot of the comparison of the in-tube elution to the rotor elution.

Due to these issues, mostly the loss of the retained magnetic beads, this method was abandoned as it was not robust enough for multiple uses.

Conclusion

Multiple possible serpin 2 binding partners were identified by mass spectrometry using an in-tube method with optimized buffers for rinsing and elution to increase the ionization of low concentration compounds for sensitive detection.

The rotational mixing column device was tested and found to not be a robust method for reducing the elution volume of the beads and thus did not concentrate the analytes of interest.

The main issue was the loss of the beads during rinsing steps as well as during the elution which caused less complex in the elution.

Funding

The project described was supported by R01AI095842 from the National Institute of Allergy and Infectious Diseases to Dr. Kristin Michel, Biology Department, Kansas State University. Its contents are solely the responsibility of the authors and do not necessarily represent the official views of the NIH. *The project was also supported by a grant from the National Institute of General Medical Sciences (P20GM103440) and supported by DGE-0841414, PI Ferguson from the KSU NSF GK-12 Program.*

References

1. Skoog, D. A., *Principles of instrumental analysis*. 6th edition.. ed.; Belmont, CA : Thomson Brooks/Cole: Belmont, CA, 2007.
2. Miller, J. M., *Chromatography : concepts and contrasts*. 2nd edition.. ed.; Hoboken, N.J. : Wiley: Hoboken, N.J., 2005.
3. Buszewski, B.; Dziubakiewicz, E.; Szumski, M., *Electromigration techniques : theory and practice*. Heidelberg Germany ; New York : Springer: Heidelberg Germany] ; New York, 2013.
4. Martin, A. J.; Synge, R. L., Some applications of periodic acid to the study of the hydroxyamino-acids of protein hydrolysates: The liberation of acetaldehyde and higher aldehydes by periodic acid. 2. Detection and isolation of formaldehyde liberated by periodic acid. 3. Ammonia split from hydroxyamino-acids by periodic acid. 4. The hydroxyamino-acid fraction of wool. 5. ;Hydroxylysine' With an Appendix by Florence O. Bell Textile Physics Laboratory, University of Leeds. *The Biochemical journal* **1941**, 35 (3), 294.
5. Manz, A., *Bioanalytical chemistry*. London : Imperial College Press ; River Edge, NJ : Distributed by World Scientific Pub: London : River Edge, NJ, 2004.
6. Katz, E., *Handbook of HPLC*. New York : M. Dekker: New York, 1998.
7. Garfin, D. E.; Ahuja, S., *Handbook of isoelectric focusing and proteomics*. 1st edition.. ed.; Amsterdam ; Boston : Elsevier Academic Press: Amsterdam ; Boston, 2005.
8. Choi, H., Sequential phosphorylation analysis using dye- tethered peptides and microfluidic isoelectric focusing electrophoresis. *Biosensors & bioelectronics*. **2015**, 73, 93-99-93-99.
9. Pharmacia Fine Chemicals, A. B., *Isoelectric focusing : principles & methods*. Uppsala, Sweden : Pharmacia Fine Chemicals AB: Uppsala, Sweden, 1982.
10. Kang, J., Dynamic coating for resolving rhodamine B adsorption to poly(dimethylsiloxane)/glass hybrid chip with laser-induced fluorescence detection. *Talanta*. **2005**, 66 (4), 1018-1024-1018-1024.
11. Mack, S., A systematic study in CIEF: Defining and optimizing experimental parameters critical to method reproducibility and robustness. *Electrophoresis*. **2009**, 30 (23), 4049-4058-4049-4058.
12. Ramsay, L. M., Femtomolar concentration detection limit and zeptomole mass detection limit for protein separation by capillary isoelectric focusing and laser- induced fluorescence detection.(Accelerated Articles)(Author abstract)(Report). *Analytical chemistry*. **2009**, 81 (5), 1741.

13. Sommer, G., Microscale Isoelectric Fractionation Using Photopolymerized Membranes. *Analytical chemistry*. **2011**, 83 (8), 3120-3125-3120-3125.
14. Shimura, K., Fluorescence- labeled peptides as isoelectric point (pI) markers in capillary isoelectric focusing with fluorescence detection. *Electrophoresis*. **1995**, 16 (8), 1479.
15. Takahashi, K., A capillary holder for scanning detection of capillary isoelectric focusing with laser- induced fluorescence. *Journal of separation science*. **2009**, 32 (3), 394-398-394-398.
16. Shimura, K., Isoelectric Focusing in a Microfluidically Defined Electrophoresis Channel. *Analytical chemistry*. **2008**, 80 (10), 3818.
17. Cui, H., Isoelectric focusing in a poly(dimethylsiloxane) microfluidic chip. *Analytical chemistry*. **2005**, 77 (5), 1303-1309-1303-1309.
18. Mazzeo, J. R., Improvements in the method developed for performing isoelectric focusing in uncoated capillaries. *Journal of chromatography*. **1992**, 606 (2), 291-296-291-296.
19. Maciążek-Jurczyk, M., The automatic use of capillary isoelectric focusing with whole column imaging detection for carbamazepine binding to human serum albumin. *Journal of pharmaceutical and biomedical analysis*. **2016**, 127, 9-17-9-17.
20. Cui, H. C., Multi-stage isoelectric focusing in a polymeric microfluidic chip. *Abstracts Of Papers Of The American Chemical Society%3B Abstr.Pap.Am.Chem.Soc*. **2005**, 229, 245.
21. Ou, J., Fabrication of a hybrid PDMS/SU-8/quartz microfluidic chip for enhancing UV absorption whole-channel imaging detection sensitivity and application for isoelectric focusing of proteins. *Lab on a chip*. **2009**, 9 (13), 1926-1932-1926-1932.
22. Shameli, S. M., Fully integrated PDMS/ SU- 8/ quartz microfluidic chip with a novel macroporous poly dimethylsiloxane (PDMS) membrane for isoelectric focusing of proteins using whole- channel imaging detection. *Electrophoresis*. **2011**, 32 (3-4), 333.
23. Ou, J., Integration of dialysis membranes into a poly(dimethylsiloxane) microfluidic chip for isoelectric focusing of proteins using whole-channel imaging detection. *ISRN analytical chemistry*. **2008**, 80 (19), 7401.
24. Poitevin, M., Use of quasi- isoelectric buffers as anolyte and catholyte to improve capillary isoelectric focusing performances. *Electrophoresis*. **2008**, 29 (8), 1687-1693-1687-1693.
25. Roman, G.; Chen, Y.; Viberg, P.; Culbertson, A.; Culbertson, C., Single- cell manipulation and analysis using microfluidic devices. *Analytical and Bioanalytical Chemistry* **2007**, 387 (1), 9-12.

26. Jo, K.; Heien, M. L.; Thompson, L. B.; Zhong, M.; Nuzzo, R. G.; Sweedler, J. V., Mass spectrometric imaging of peptide release from neuronal cells within microfluidic devices. *Lab on a Chip* **2007**, 7 (11), 1454-1460.
27. Dydek, E. V.; Jensen, K. F.; Petersen, M. V.; Nocera, D. G., Electrode placement and fluid flow rates in microfluidic electrochemical devices. *Journal of the Electrochemical Society* **2012**, 159 (11), H853-H856.
28. Resto, P. J.; Berthier, E.; Beebe, D. J.; Williams, J. C., An inertia enhanced passive pumping mechanism for fluid flow in microfluidic devices. *Lab Chip* **2012**, 12 (12), 2221-2228.
29. Van Midwoud, P. M.; Verpoorte, E.; Groothuis, G. M. M., Microfluidic devices for in vitro studies on liver drug metabolism and toxicity. In *Integr. Biol.*, 2011; Vol. 3, pp 509-521.
30. Dong, L.; Jankele, R.; Cornaglia, M.; Lehnert, T.; Gönczy, P.; Gijs, M. A. M., Integrated Microfluidic Device for Drug Studies of Early C. Elegans Embryogenesis. *Advanced Science* **2018**, <xocs:firstpage xmlns:xocs=""/>.
31. Kudr, J.; Zitka, O.; Klimanek, M.; Vrba, R.; Adam, V., Microfluidic electrochemical devices for pollution analysis—A review. *Sensors & Actuators: B. Chemical* **2017**, 246, 578-590.
32. Stanley, C. E.; Grossmann, G.; I Solvas, X. C.; Demello, A. J., Soil-on-a-Chip: microfluidic platforms for environmental organismal studies. *Lab on a chip* **2016**, 16 (2), 228.
33. Bahadorimehr, A.; Majlis, B., Fabrication of Glass-based Microfluidic Devices with Photoresist as Mask. *Elektron. Elektrotech.* **2011**, 116 (10), 45-48.
34. Minteer, S. D., *Microfluidic techniques : reviews and protocols*. Totowa, N.J. : Humana Press: Totowa, N.J., 2006.
35. Liu, J.; Sun, X.; Lee, M., Surface-Reactive Acrylic Copolymer for Fabrication of Microfluidic Devices. *Analytical Chemistry* **2005**, 77 (19), 6280-6287.
36. Johnson, A. S.; Anderson, K. B.; Halpin, S. T.; Kirkpatrick, D. C.; Spence, D. M.; Martin, R. S., Integration of multiple components in polystyrene-based microfluidic devices part I: fabrication and characterization. *Analyst* **2012**, 138 (1), 129-136.
37. Kaneda, S.; Fujii, T.; Ono, K.; Fukuba, T.; Nojima, T.; Yamamoto, T., Modification of the glass surface property in PDMS- glass hybrid microfluidic devices. *Analytical Sciences* **2012**, 28 (1), 39-44.
38. Tas; Workshop, *Micro total analysis systems : proceedings of the [Mu] TAS '94 Workshop, held at MESA Research Institute, University of Twente, The Netherlands, 21-*

22 November 1994. Dordrecht ; Boston : Kluwer Academic Publishers: Dordrecht ; Boston, 1995.

39. Cohen, J. D.; Li, L.; Wang, Y.; Thoburn, C.; Afsari, B.; Danilova, L.; Douville, C.; Javed, A. A.; Wong, F.; Mattox, A.; Hruban, R. H.; Wolfgang, C. L.; Goggins, M. G.; Dal Molin, M.; Wang, T.-L.; Roden, R.; Klein, A. P.; Ptak, J.; Dobbryn, L.; Schaefer, J.; Silliman, N.; Popoli, M.; Vogelstein, J. T.; Browne, J. D.; Schoen, R. E.; Brand, R. E.; Tie, J.; Gibbs, P.; Wong, H.-L.; Mansfield, A. S.; Jen, J.; Hanash, S. M.; Falconi, M.; Allen, P. J.; Zhou, S.; Bettegowda, C.; Diaz, L. A.; Tomasetti, C.; Kinzler, K. W.; Vogelstein, B.; Lennon, A. M.; Papadopoulos, N., Detection and localization of surgically resectable cancers with a multi- analyte blood test. *Science (New York, N.Y.)* **2018**, 359 (6378), 926.
40. Paul, R. S., The renaissance of fluorescence resonance energy transfer. *Nature Structural Biology* **2000**, 7 (9), 730.
41. Wang, H.; Udukala, D. N.; Samarakoon, T. N.; Basel, M. T.; Kalita, M.; Abayaweera, G.; Manawadu, H.; Malalasekera, A.; Robinson, C.; Villanueva, D.; Maynez, P.; Bossmann, L.; Riedy, E.; Barriga, J.; Wang, N.; Li, P.; Higgins, D. A.; Zhu, G.; Troyer, D. L.; Bossmann, S. H., Nanoplatfoms for highly sensitive fluorescence detection of cancer- related proteases. *Photochem. Photobiol. Sci.* **2014**, 13 (2), 231-240.
42. Chia-Hung, C.; Miller, M. A.; Sarkar, A.; Beste, M. T.; Isaacson, K. B.; Lauffenburger, D. A.; Griffith, L. G.; Han, J., Multiplexed protease activity assay for low- volume clinical samples using droplet- based microfluidics and its application to endometriosis.(Report). *Journal of the American Chemical Society* **2013**, 135 (5), 1645-1648.
43. Ng, E. X.; Miller, M. A.; Jing, T.; Chen, C.-H., Single cell multiplexed assay for proteolytic activity using droplet microfluidics. *Biosensors and Bioelectronics* **2016**, 81, 408-414.
44. Ng, E. X.; Miller, M. A.; Jing, T.; Lauffenburger, D. A.; Chen, C.-H., Low- volume multiplexed proteolytic activity assay and inhibitor analysis through a pico- injector array. *Lab Chip* **2015**, 15 (4), 1153-1159.
45. Kim, J. H.; Shin, H. J.; Cho, H.; Kwak, S. M.; Cho, H.; Kim, T. S.; Kang, J. Y.; Yang, E. G., A microfluidic protease activity assay based on the detection of fluorescence polarization. *Analytica Chimica Acta* **2006**, 577 (2), 171-177.
46. Chen, W.; Jun, O.; Yun-Yi, W.; De-Kai, Y.; Xing-Hua, X., Sensitive assay of protease activity on a micro/ nanofluidics preconcentrator fused with the fluorescence resonance energy transfer detection technique.(Report). *Analytical Chemistry* **2014**, 86 (6), 3216.
47. Sueyoshi, K.; Nogawa, Y.; Sugawara, K.; Endo, T.; Hisamoto, H., Highly Sensitive and Multiple Enzyme Activity Assay Using Reagent-release Capillary- Isoelectric Focusing with Rhodamine 110- based Substrates. *Analytical sciences : the international journal of the Japan Society for Analytical Chemistry* **2015**, 31 (11), 1155.

48. Arnaud, I.; Abid, J.-P.; Roussel, C.; Girault, H. H., Size- selective separation of gold nanoparticles using isoelectric focusing electrophoresis (IEF). *Chemical communications (Cambridge, England)* **2005**, (6), 787.
49. McNulty, J.; Krishnamoorthy, V.; Amoroso, D.; Moser, M., Tris(3- hydroxypropyl) phosphine (THPP): A mild, air- stable reagent for the rapid, reductive cleavage of small- molecule disulfides. *Bioorganic & Medicinal Chemistry Letters* **2015**, 25 (19), 4114-4117.
50. Mason, S. D.; Joyce, J. A., Proteolytic networks in cancer. *Trends in Cell Biology* **2011**, 21 (4), 228-237.
51. Udukala, D. N.; Wang, H. W.; Wendel, S. O.; Malalasekera, A. P.; Samarakoon, T. N.; Yapa, A. S.; Abayaweera, G.; Basel, M. T.; Maynez, P.; Li, P.; Higgins, D. A.; Gadbury, G.; Troyer, D. L.; Bossmann, S. H., Early breast cancer screening using iron/iron oxide-based nanoplatfoms with sub-femtomolar limits of detection. *pli; higgins; gadbury; troyer; sbossmann*, Eds. 2016.
52. Kalubowilage, M., Liquid Biopsies of Solid Tumors: Non-Small-Cell Lung and Pancreatic Cancer. *Bossmann, S. H.; Culbertson, C.; Higgins, D.; Troyer, D.*, Eds. ProQuest Dissertations Publishing: 2017.
53. Kost, G. J., The hybrid laboratory: shifting the focus to the point of care. (Special Supplement: Point-of- Care Testing). *Medical Laboratory Observer* **1992**, 24 (9), S17.
54. Ng, R.; Feldman, B.; McGarraugh, G.; Guerrero, Z.; Le, P.; Sharp, C.; Krishnan, R., Advance in technology: Coulometry for point-of- care blood glucose monitoring. *Clin. Chem.* **2005**, 51, A204-A204.
55. Ardiaca, M.; Bonvehí, C.; Montesinos, A., Point-of- Care Blood Gas and Electrolyte Analysis in Rabbits. *Veterinary Clinics of North America: Exotic Animal Practice* **2013**.
56. Herbstreit, F.; Winter, E. M.; Peters, J.; Hartmann, M., Monitoring of haemostasis in liver transplantation: comparison of laboratory based and point of care tests. *Anaesthesia* **2010**, 65 (1), 44-49.
57. Audet, G.; Quinn, C.; Leon, L., Point-of- care cardiac troponin test accurately predicts heat stroke severity in rats. *American Journal of Physiology* **2015**, 309 (10), R1264.
58. Li, Y.; Uddayasankar, U.; He, B.; Wang, P.; Qin, L., Fast, Sensitive, and Quantitative Point-of- Care Platform for the Assessment of Drugs of Abuse in Urine, Serum, and Whole Blood. *Analytical chemistry* **2017**, 89 (16), 8273.
59. Ochodo, E. A.; Gopalakrishna, G.; Spek, B.; Reitsma, J. B.; van Lieshout, L.; Polman, K.; Lambertson, P.; Bossuyt, P. M.; Leeflang, M. M., Circulating antigen tests and urine reagent strips for diagnosis of active schistosomiasis in endemic areas. *The Cochrane Database of Systematic Reviews* **2015**, (3), 1-292.

60. Keahey, P. A.; Simeral, M. L.; Schroder, K. J.; Bond, M. M.; Mtenthaonnga, P. J.; Miros, R. H.; Dube, Q.; Richards-Kortum, R. R., Point-of- care device to diagnose and monitor neonatal jaundice in low-resource settings. *Proceedings of the National Academy of Sciences of the United States of America* **2017**, *114* (51), E10965.
61. Bustinduy, A. L.; Sousa-Figueiredo, J. C.; Adriko, M.; Betson, M.; Fenwick, A.; Kabatereine, N.; Stothard, J. R., Fecal Occult Blood and Fecal Calprotectin as Point-of-Care Markers of Intestinal Morbidity in Ugandan Children with *Schistosoma mansoni* Infection (Intestinal Schistosomiasis Point-of- Care Markers). **2013**, *7* (11), e2542.
62. Walczak, R.; Dziuban, J. A.; Koszur, J.; Bang, D. D.; Ruano-Lopez, J., Miniaturized real-time PCR system: Toward smart diagnostic device for point-of- care food pathogens DNA analyze. 2008; pp 633-636.
63. Primiceri, E.; Chiriac, M. S.; De Feo, F.; Santovito, E.; Fusco, V.; Maruccio, G., A multipurpose biochip for food pathogen detection. *Anal. Methods* **2016**, *8* (15), 3055-3060.
64. Gayat, E.; Aulagnier, J.; Matthieu, E.; Boisson, M.; Fischler, M., Non-Invasive Measurement of Hemoglobin: Assessment of Two Different Point-of- Care Technologies (Non-Invasive Measurement of Hemoglobin). *PLoS ONE* **2012**, *7* (1), e30065.
65. Park, S.; Zhang, Y.; Lin, S.; Wang, T.-H.; Yang, S., Advances in microfluidic PCR for point-of- care infectious disease diagnostics. *Biotechnology Advances* **2011**, *29* (6), 830-839.
66. Kaur, G.; Tomar, M.; Gupta, V., A Simple Paper Based Microfluidic Electrochemical Biosensor for Point-of- Care Cholesterol Diagnostics. *physica status solidi (a)* **2017**, *214* (12), n/a-n/a.
67. Point of Care Diagnostic Testing World Markets. 2016.
68. Roman, G. T.; Carroll, S.; McDaniel, K.; Culbertson, C. T., Micellar electrokinetic chromatography of fluorescently labeled proteins on poly(dimethylsiloxane)-based microchips. *ELECTROPHORESIS* **2006**, *27* (14), 2933-2939.
69. Poehler, E., Label- free microfluidic free- flow isoelectric focusing, pH gradient sensing and near real- time isoelectric point determination of biomolecules and blood plasma fractions. *The Analyst*. **2015**, *140* (22), 7496-7502-7496-7502.
70. Yang, K. S., Free- flow isoelectric focusing microfluidic device with glass coating by sol- gel methods. *Current applied physics*. **2009**, *9* (2), 66-70-66-70.
71. Mazzeo, J. R., Capillary Isoelectric Focusing of Proteins in Uncoated Fused- Silica Capillaries Using Polymeric Additives. *Analytical chemistry*. **1991**, *63* (24), 2852-2857-2852-2857.

72. Beale, S. C., Spatial- scanning laser fluorescence detection for capillary electrophoresis. *Analytical chemistry*. **1995**, 67 (18), 3367.
73. Olazábal, V., A Full Scanning System and a New Processing Method for Capillary Electrophoresis. *JALA*. **2003**, 8 (5), 35-41-35-41.
74. Culbertson, C. T.; Jacobson, S. C.; Ramsey, J. M., Microchip devices for high-efficiency separations. *Analytical chemistry* **2000**, 72 (23), 5814.
75. Stewart, J. M., *Solid phase peptide synthesis*. 2nd edition.. ed.; Rockford, Ill. : Pierce Chemical Co.: Rockford, Ill., 1984.
76. Jensen, K. J.; Shelton, P. T.; Pedersen, S. L.; Tofteng Shelton, P., *Peptide synthesis and applications*. Second edition.. ed.; Totowa, New Jersey : Humana Press: 2013.
77. Walker, J. M., *The Protein Protocols Handbook*. 3rd ed.. ed.; Totowa, NJ : Humana Press : Imprint: Humana Press: 2009.
78. Moser, A. C., Immunoaffinity chromatography: an introduction to applications and recent developments. *Bioanalysis* **2010**, 2 (4), 769-790.
79. Center for Disease, C., About Malaria- Biology. 2012; Vol. 2014.
80. Chong, W.-C.; Basir, R.; Fei, Y. M., Eradication of malaria through genetic engineering: the current situation. *Asian Pacific journal of tropical medicine* **2013**, 6 (2), 85-94.
81. Ndiath, M. O.; Mazonot, C.; Sokhna, C.; Trape, J.-F., How the malaria vector *Anopheles gambiae* adapts to the use of insecticide-treated nets by African populations. *PLoS One* **2014**, 9 (6), e97700/9, 9 pp.
82. An, C.; Budd, A.; Kanost, M. R.; Michel, K., Characterization of a regulatory unit that controls melanization and affects longevity of mosquitoes. *Cellular and Molecular Life Sciences* **2011**, 68 (11), 1929-1939.
83. Christophides, G. K.; Zdobnov, E.; Barillas-Mury, C.; Birney, E.; Blandin, S.; Blass, C.; Brey, P. T.; Collins, F. H.; Danielli, A.; Dimopoulos, G.; Hetru, C.; Hoa, N. T.; Hoffmann, J. A.; Kanzok, S. M.; Letunic, I.; Levashina, E. A.; Loukeris, T. G.; Lycett, G.; Meister, S.; Michel, K.; Moita, L. F.; Mueller, H.-M.; Osta, M. A.; Paskewitz, S. M.; Reichhart, J.-M.; Rzhetsky, A.; Troxler, L.; Vernick, K. D.; Vlachou, D.; Volz, J.; von Mering, C.; Xu, J.; Zheng, L.; Bork, P.; Kafatos, F. C., Immunity-Related Genes and Gene Families in *Anopheles gambiae*. *Science (Washington, DC, United States)* **2002**, 298 (5591), 159-165.
84. Penelope, E. S.; Robin, W. C., What do dysfunctional serpins tell us about molecular mobility and disease? *Nature Structural Biology* **1995**, 2 (2), 96.

85. Irving, J. A.; Pike, R. N.; Lesk, A. M.; Whisstock, J. C., Phylogeny of the serpin superfamily: implications of patterns of amino acid conservation for structure and function. *Genome research* **2000**, *10* (12), 1845.
86. Irving, J. A.; Steenbakkens, P. J. M.; Lesk, A. M.; Op Den Camp, H. J. M.; Pike, R. N.; Whisstock, J. C., Serpins in prokaryotes. *Molecular biology and evolution* **2002**, *19* (11), 1881.
87. Steenbakkens, P. J. M.; Irving, J. A.; Harhangi, H. R.; Swinkels, W. J. C.; Akhmanova, A.; Dijkerman, R.; Jetten, M. S. M.; van Der Drift, C.; Whisstock, J. C.; Op Den Camp, H. J. M., A serpin in the cellulosome of the anaerobic fungus *Piromyces* sp. strain E2. *Mycological Research* **2008**, *112* (8), 999-1006.
88. Geiger, M.; Wahlmüller, F.; Furtmüller, M., *The serpin family proteins with multiple functions in health and disease*. Cham : Springer: 2015.
89. Gettins, P. G. W., Serpin structure, mechanism, and function. *Chemical Reviews (Washington, DC, United States)* **2002**, *102* (12), 4751-4803.
90. An, C.; Lovell, S.; Kanost, M. R.; Battaile, K. P.; Michel, K., Crystal structure of native *Anopheles gambiae* serpin-2, a negative regulator of melanization in mosquitoes. *Proteins: Structure, Function, and Bioinformatics* **2011**, *79* (6), 1999-2003.
91. An, C.; Kanost, M. R., *Manduca sexta* serpin- 5 regulates prophenoloxidase activation and the Toll signaling pathway by inhibiting hemolymph proteinase HP6. *Insect Biochemistry and Molecular Biology* **2010**, *40* (9), 683-689.
92. Kanost, M. R.; Jiang, H., Clip- domain serine proteases as immune factors in insect hemolymph. *Current Opinion in Insect Science* **2015**, *11*, 47-55.
93. Zachariou, M., *Affinity chromatography : methods and protocols*. 2nd edition.. ed.; Totowa, NJ : Humana Press: Totowa, NJ, 2008.
94. Twyman, R. M., *Principles of proteomics*. New York : BIOS Scientific Publishers: New York, 2004.
95. Hennion, M. C.; Pichon, V., Immuno-based sample preparation for trace analysis. *Journal of Chromatography A* **2003**, *1000* (1-2), 29-52.
96. G Protein-Coupled Receptor-Protein Interactions.(ANATOMY, PHYSIOLOGY)(Brief Article)(Book Review). *SciTech Book News* **2005**, *29* (2), 62.
97. Cingöz, A.; Hugon-Chapuis, F.; Pichon, V., Total on-line analysis of a target protein from plasma by immunoextraction, digestion and liquid chromatography–mass spectrometry. *Journal of Chromatography B* **2010**, *878* (2), 213-221.
98. Pfaunmiller, E.; Anguizola, J.; Milanuk, M.; Papastavros, E.; Carter, N.; Matsuda, R.; Zheng, X.; Hage, D., Development of microcolumn-based one-site immunometric assays

- for protein biomarkers. *Journal Of Chromatography A; J.Chromatogr.A* **2014**, 1366, 92-100.
99. Zheng, X.; Li, Z.; Beeram, S.; Podariu, M.; Matsuda, R.; Pfaunmiller, E. L.; White, C. J., II; Carter, N.; Hage, D. S., Analysis of biomolecular interactions using affinity microcolumns: A review. *Journal of Chromatography B: Analytical Technologies in the Biomedical and Life Sciences* **2014**, 968, 49-63.
 100. Anguizola, J.; Joseph, K. S.; Barnaby, O. S.; Matsuda, R.; Alvarado, G.; Clarke, W.; Cerny, R. L.; Hage, D. S., Development of Affinity Microcolumns for Drug-Protein Binding Studies in Personalized Medicine: Interactions of Sulfonylurea Drugs with in vivo Glycated Human Serum Albumin. *Analytical Chemistry (Washington, DC, United States)* **2013**, 85 (9), 4453-4460.
 101. Queiroz, M. E. C.; Oliveira, E. B.; Breton, F.; Pawliszyn, J., Immunoaffinity in-tube solid phase microextraction coupled with liquid chromatography–mass spectrometry for analysis of fluoxetine in serum samples. *Journal of Chromatography A* **2007**, 1174 (1), 72-77.
 102. Schiel, J. E.; Tong, Z.; Sakulthaew, C.; Hage, D. S., Development of a flow-based ultrafast immunoextraction and reverse displacement immunoassay: analysis of free drug fractions. *Analytical chemistry* **2011**, 83 (24), 9384.
 103. Jackson, A. J.; Karle, E. M.; Hage, D. S., Preparation of high-capacity supports containing protein G immobilized to porous silica. *Analytical Biochemistry* **2010**, 406 (2), 235-237.
 104. Neubert, H.; Muirhead, D.; Kabir, M.; Grace, C.; Cleton, A.; Arends, R., Sequential protein and peptide immunoaffinity capture for mass spectrometry-based quantification of total human β -nerve growth factor. *Analytical chemistry* **2013**, 85 (3), 1719.
 105. Schiel, J.; Joseph, K. S.; Hage, D., Biointeraction Affinity Chromatography: General Principles and Recent Developments. In *Adv. Chromatogr.*, 2010; Vol. 48, pp 145-193.
 106. Peoples, M. C.; Phillips, T. M.; Karnes, H. T., A capillary- based microfluidic instrument suitable for immunoaffinity chromatography. *Journal of Chromatography B* **2007**, 848 (2), 200-207.
 107. Zheng, X.; Li, Z.; Podariu, M.; Hage, D., Determination of Rate Constants and Equilibrium Constants for Solution-Phase Drug-Protein Interactions by Ultrafast Affinity Extraction. *Analytical Chemistry* **2014**, 86 (13), 6454.
 108. Peoples, M. C.; Karnes, H. T., Microfluidic immunoaffinity separations for bioanalysis. *Journal of Chromatography B* **2008**, 866 (1), 14-25.
 109. Gasilova, N.; Gassner, A. L.; Girault, H. H., Analysis of major milk whey proteins by immunoaffinity capillary electrophoresis coupled with MALDI-MS. *ELECTROPHORESIS* **2012**, 33 (15), 2390-2398.

110. Gassner, A.-L.; Proczek, G.; Girault, H. H., Bubble cell for magnetic bead trapping in capillary electrophoresis. *Analytical and Bioanalytical Chemistry* **2011**, *401* (10), 3239-3248.
111. Condina, M. R.; Guthridge, M. A.; McColl, S. R.; Hoffmann, P., A sensitive magnetic bead method for the detection and identification of tyrosine phosphorylation in proteins by MALDI-TOF/TOF MS. *PROTEOMICS* **2009**, *9* (11), 3047-3057.
112. Chen, H.-X.; Busnel, J.-M.; Peltre, G.; Zhang, X.-X.; Girault, H. H., Magnetic beads based immunoaffinity capillary electrophoresis of total serum IgE with laser-induced fluorescence detection. *Analytical chemistry* **2008**, *80* (24), 9583.
113. Bland, C.; Bellanger, L.; Armengaud, J., Magnetic immunoaffinity enrichment for selective capture and MS/MS analysis of N-terminal-TMPP-labeled peptides. *Journal of proteome research* **2014**, *13* (2), 668.
114. Tekin, H. C.; Cornaglia, M.; Gijs, M. A. M., Attomolar protein detection using a magnetic bead surface coverage assay. *Lab on a Chip* **2013**, *13* (6), 1053-1059.
115. Kind, T.; Fiehn, O., Advances in structure elucidation of small molecules using mass spectrometry. *Bioanalytical Reviews* **2010**, *2* (1), 23-60.
116. Zubarev, R. A.; Makarov, A., Orbitrap Mass Spectrometry. *Analytical Chemistry (Washington, DC, United States)* **2013**, *85* (11), 5288-5296.
117. Takahashi, N., *Proteomic biology using LC-MS : large scale analysis of cellular dynamics and function*. Hoboken, N.J. : Wiley-Interscience: Hoboken, N.J., 2008.
118. Switzer, R. C.; Merrill, C. R.; Shifrin, S., A highly sensitive silver stain for detecting proteins and peptides in polyacrylamide gels. *Analytical Biochemistry* **1979**, *98* (1), 231-237.
119. Mireille, C.; Sylvie, L.; Thierry, R., Silver staining of proteins in polyacrylamide gels. *Nature Protocols* **2006**, *1* (4), 1852.
120. Rund, S. S. C.; Hou, T. Y.; Ward, S. M.; Collins, F. H.; Duffield, G. E., Genome- wide profiling of diel and circadian gene expression in the malaria vector *Anopheles gambiae*. *Proceedings of the National Academy of Sciences of the United States of America* **2011**, *108* (32), E421.
121. Zhang, G.; Neubert, T. A., Use of detergents to increase selectivity of immunoprecipitation of tyrosine phosphorylated peptides prior to identification by MALDI quadrupole- TOF MS. *PROTEOMICS* **2006**, *6* (2), 571-578.
122. Anderson, N. L.; Jackson, A.; Smith, D.; Hardie, D.; Borchers, C.; Pearson, T. W., SISCAPA Peptide Enrichment on Magnetic Beads Using an In-line Bead Trap Device. *Molecular & Cellular Proteomics* **2009**, *8* (5), 995-1005.

Appendix A: IEF Protocols and Programs

IEF on Chip Procedure

1. Turn on the Vacuum Pump, PMT power supply, preamplifier, laser, and motor system.
2. Clean the channel with 50% 1 M NaOH+ 50% Methanol, let flow under vacuum for 10 min
3. Pretreat the channel with the 0.4% methyl cellulose (Make sure the channel is bubble free).
 - Fill both reservoirs with 0.4% methyl cellulose and let the chip sit filled for ≥ 20 min.
 - Can complete steps 4-11 during this time
4. Place the chip on the motor system and use the lamp to align the entire length of the channel with the detection spot on the PMT. (Only need to do if a new chip or if the motor was moved)
5. Align the laser to the inside edge of the left reservoir (the laser should be blocked)
6. Check the preamplifier and program settings and make sure they are set as needed for the run.
7. Turn off the light and open the PMT shutter.
8. Make sure the toggle is on blank and click the check mark to start (It will take two scans and stop)
9. Get out all solutions (Carrier Ampholyte, Anolyte, Catholyte, Surfactant, Sacrificial Ampholytes, Sample, EOF Suppressor)
10. Mix the loading sample immediately before use
 - Water
 - 50 mM Arginine (*High pI Sacrificial Ampholyte*)
 - 0.11% Brij 35 (*Surfactant*)
 - ~10 pM-100nM each peptide
 - 1% Carrier ampholytes
 - 0.4% Methyl cellulose (*EOF Suppressor*)
11. Immediately put carrier ampholyte back into fridge
12. Fill the chip with the loading sample
 - Pull a small amount of MC out of channel then add sample and pull all through to make sure the small bubble you made disappears
 - Remove all bubbles and make sure it has been on the vacuum for at least 2min
13. Add the anolyte and catholyte to their respective reservoirs
 - Anolyte [20 mM IDA+ 2.5% Methyl Cellulose] (HV, Left), Catholyte [300 mM NaOH+ 2.5% Methyl Cellulose] (Ground, Right, Blue Sharpie)
14. Turn on the HV power supply and make sure the voltage reads zero
15. Align the laser to the inside edge of the left reservoir (the laser should be blocked by the tape)
16. Wearing gloves, add the HV and ground electrodes to their respective reservoirs
17. Turn off the light and open the PMT shutter.
18. Set the toggle to sample and check the number of scans and the amplifier settings as well as the voltage programing

19. Click the check mark to start
20. When complete turn off the power supply
21. Move all the files to a folder labeled with the date inside a folder of the name of the sample
22. Take the chip to the ultrapure water station and pull it apart
23. Clean the PDMS topper with Alcanox and rub with a clean glove, make sure the reservoirs are well rinsed out with water
24. Clean the glass slide with Alcanox and rub with cleanroom swab then rinse with water
25. Dry off with compressed N₂ gas and put chip back together. If doing another experiment, go to step 2.
26. Clean the vacuum tubing with water and then empty the trap in the sink and leave apart to dry
27. Turn off PMT, Amplifier, Laser, Motion System, and Pump if no one is using it
28. Put away any solutions back into the fridge and samples into the freezer

Trypsin Digestion of Peptides

1. Mix the sample containing: 50mM Tris-HCl (pH 7.8), 1mM CaCl₂, 0.005mg/mL Trypsin, 0.1mg/mL Trypsin Substrate.
 - 0.18mg CaCl₂ + 7.6mg Tris + 447.5uL Water + 2.5uL Trypsin 1mg/mL + 50uL 1mg/mL Trypsin Substrate
2. Incubate at 37°C for 24hrs.
3. Remove 100µL at 0hr, 1hr, 2hr, 3hr, 4hr, 5hr, 6hr, 7hr, 8hr and 24hr for testing.
4. The trypsin digestion can be stopped by freezing or by lowering the pH of the reaction below pH 4 by adding acetic acid (trypsin will regain activity when the pH is raised above pH 4). Digested samples can be stored at -20°C.

Igor IEF Data Analysis Procedure

1. Copy the IEF Data Files into Your Folder on the Computer
2. Open Igor
3. File-Open File-Procedure
 - a. Choose Loader from the Desktop
 - b. Click Compile
 - c. Minimize the procedure window
4. In the command prompt on the bottom type: loader()
 - a. Enter
 - b. Click Browse then choose the folder that contains the data then click OK
5. Analysis-Smooth
 - a. Shift Click to choose all the scans
 - b. Type in 10 to choose a 10-point Binomial Smooth
 - c. Click Do it
6. Open IEF Analysis Code Word Document from the Desktop

- a. Copy the Display..... until the last scan that is contained in your data
 - b. Paste into the command prompt, Enter
 - c. Repeat
 - d. Copy the Label...
 - e. Paste into the command prompt, Enter
 - f. Click on the other graph
 - g. Paste into the command prompt, Enter
 - h. Copy the Modify Data..... until the last scan that is contained in your data
 - i. Paste into the command prompt, Enter
7. Data-Change Wave Scaling
- a. Select everything but the data for the current
 - b. Set the X properties
 - i. Start= 2.9
 - ii. Delta= 0.00205
 - c. Click Do It
 - d. Look at how the start and end line up with the 3 and 10. If they don't then repeat and change the numbers as suggested below until they match
 - i. If the data needs to be shifted to the left the decrease the Start value
 - ii. If the data needs to be shifted to the right the increase the Start value
 - iii. If the end of the data needs to be shifted to the right increase the Delta value
 - iv. If the end of the data needs to be shifted to the left left the Delta value
 - e. If the scale on the bottom does not show the numbers 3-10
 - i. Right click and choose axis properties
 - ii. Choose Bottom Axis on the top left
 - iii. Pick the Auto/Man Ticks window
 - iv. For Auto Ticks Approximately: 7
 - v. Click Do It
8. Maximize Graph 1
9. Choose the tallest / most focused peak and double click on it to see the scan name and change the color to a Bright Blue then click Do It
10. Right Click on the blue scan and Bring to Front
11. Restore Down Graph 1
12. Windows-New Graph
- a. Choose the scan that was the most focused for the Y-Wave and Calculated for X-Wave
 - b. Click Do It
13. Maximize Graph 3
14. Right Click, Add Annotation
- a. In the Text Box Type:
 - i. What is Different About this Scan(If Anything)
 - ii. The Sample and its Concentration
 - iii. The Sequence of the Sample if Known

- iv. The Voltage, Amplification, Sampling Frequency, Scan Duration (All of this is found on the LabView Page or Amplifier)
 - v. Click Do It
- 15. Right Click, Add Annotation
 - a. Type in the Date with – in between each number
 - b. Click Do It
- 16. Drag the date to the upper left corner and the Label to the Upper Middle (Do not put over data)
- 17. Restore Down Graph 3
- 18. Click on Graph 0
- 19. Copy the TextBox lines on code from the bottom and then paste them in the command line
 - a. Press enter
- 20. Click on Graph 1
- 21. Paste again in the command line
 - a. Press enter
- 22. Click on Graph 2
- 23. Paste again in the command line
 - a. Press enter
- 24. Right Click on Graph 3, Add Annotation
 - a. Change the Annotation Type to Legend on the upper Left
 - b. Erase the _smth and ‘ ’ on the right half of the text
 - c. Leave everything in () alone
 - d. Click Do It
- 25. Right Click on Graph 3, Add Annotation
 - a. Change the Annotation Type to Legend on the upper Left
 - b. Scroll down to the bottom and then erase everything but the most focused peak label
 - c. Erase the _smth and ‘ ’ on the right half of the text
 - d. Leave everything in () alone
 - e. Click Do It
- 26. Drag the date to the upper left corner and the Label to the Upper Middle (Do not put over data) on all graphs
- 27. Maximize Graph 0
 - a. Click and Hold then drag up each of the scans to create a rainbow graph
- 28. File-Save Experiment
 - a. Save with the Date-Sample-What is Different
- 29. File-Save Graphics
 - a. If you are saving for a poster change the Size to custom and the size you need in inches
 - b. It should be a JPEG at 300 DPI with Color
 - c. Click Do It
 - d. Then save the Rainbow graph as (Date-Sample-What is Different)

30. Restore Down Graph 0
31. Maximize Graph 1
32. File-Save Graphics
 - a. If you are saving for a poster change the Size to custom and the size you need in inches
 - b. It should be a JPEG at 300 DPI with Color
 - c. Click Do It
 - d. Then save the graph 1 as (Date-Sample-What is Different-All Scans)
33. Restore Down Graph 1
34. Maximize Graph 2
35. File-Save Graphics
 - a. If you are saving for a poster change the Size to custom and the size you need in inches
 - b. It should be a JPEG at 300 DPI with Color
 - c. Click Do It
 - d. Then save the graph 2 as (Date-Sample-What is Different- Current)
36. Restore Down Graph 2
37. Maximize Graph 3
38. File-Save Graphics
 - a. If you are saving for a poster change the Size to custom and the size you need in inches
 - b. It should be a JPEG at 300 DPI with Color
 - c. Click Do It
 - d. Then save the graph 2 as (Date-Sample-What is Different- Max Height)
39. File-Save Experiment
40. Close Igor
41. Copy the Igor File and all of the Images back onto the Flash Drive in the same folder as the data

Igor Procedure Loader Code

```
#pragma rtGlobals=1           // Use modern global access method.

//This function automatically loads all files in a folder that the user
selects. In this instance, the function
//assumes that each file is a Dionex Chromeleon generated ASCII file, and
that the chromatogram's data
//points were collected at 0.2 sec. intervals. You MUST must make the changes
appropriate to your data
//files on the lines below marked with exclamation points!!!
function loader()
  //initialize loop variable
  variable i=0
  string wname, fname           //wave names and file name, respectively

  //Ask the user to identify a folder on the computer
  getfilefolderinfo/D
```

```

//Store the folder that the user has selected as a new symbolic path
in IGOR called cgms
//!!!!!!!!!!!! if you prefer a different name, change ALL instances of
cgms in the function !!!!!!!!!
newpath/O cgms S_path

//Create a list of all files that are .txt files in the folder. -1
parameter addresses all files.
//!!!!!!!!!!!! if your files have a different extension, change .TXT
below to your extension!!!!!!!!!!!!!!
string filelist= indexedfile(cgms,-1,".TXT")

//Begin processing the list
do
    //store the ith name in the list into wname.
    fname = stringfromlist(i,filelist)

    //strip away ".txt" to get the name of the chromatogram, which
is the file name
    //!!!!!!!!!!!! change the next line if you want a different
name for the waves that are created !!!!!!!!!!!!!!!
    wname = fname[0,strlen(fname)-5]

    //reference a wave with the name of the chromatogram.
    wave w = $wname

    //if the referenced wave does not exist, create it.
    if (!waveexists(w) )

        //The /L parameter tells IGOR to load no headers, and
to load the 3rd column of data (indexed as 2) only
        //!!!!!!!!!!!! You must change this next line to tell
IGOR how to load the data in each file !!!!!!!!!!!!!!!
        LoadWave/G/D/A=wave/P=cgms/O/L={0,0,0,2,0}
stringfromlist(i,filelist)

        //wave created is wave0. It is renamed after the
chromatogram.
        rename wave0 $wname

        //And scaled accordingly.
        //!!!!!!!!!!!! you MUST change or delete the following
line according to your data's scaling or lack thereof. !!!!!!!!!!!!!!!
        setscale/P x,0,0.0033333,$wname
        //Print confirmation of what was just loaded.
        print "Loaded "+fname

    else
        //Otherwise, tell the user that this chromatogram was
previously loaded.
        print fname+" was previously loaded. Its
corresponding wave exists."
        endif
        i += 1 //move to next file
    while(i<itemsinlist(filelist)) //end when all
files are processed.
end

```

Igor IEF Analysis Code

Duplicate/O Blank1,Blank1_smth;DelayUpdate
Duplicate/O Blank2,Blank2_smth;DelayUpdate
Duplicate/O 'IEF 0AC','IEF 0AC_smth';DelayUpdate
Duplicate/O 'IEF 0CA','IEF 0CA_smth';DelayUpdate
Duplicate/O 'IEF 1AC','IEF 1AC_smth';DelayUpdate
Duplicate/O 'IEF 1CA','IEF 1CA_smth';DelayUpdate
Duplicate/O 'IEF 2AC','IEF 2AC_smth';DelayUpdate
Duplicate/O 'IEF 2CA','IEF 2CA_smth';DelayUpdate
Duplicate/O 'IEF 3AC','IEF 3AC_smth';DelayUpdate
Duplicate/O 'IEF 3CA','IEF 3CA_smth';DelayUpdate
Duplicate/O 'IEF 4AC','IEF 4AC_smth';DelayUpdate
Duplicate/O 'IEF 4CA','IEF 4CA_smth';DelayUpdate
Duplicate/O 'IEF 5AC','IEF 5AC_smth';DelayUpdate
Duplicate/O 'IEF 5CA','IEF 5CA_smth';DelayUpdate
Duplicate/O 'IEF 6AC','IEF 6AC_smth';DelayUpdate
Duplicate/O 'IEF 6CA','IEF 6CA_smth';DelayUpdate
Duplicate/O 'IEF 7AC','IEF 7AC_smth';DelayUpdate
Duplicate/O 'IEF 7CA','IEF 7CA_smth';DelayUpdate
Duplicate/O 'IEF 8AC','IEF 8AC_smth';DelayUpdate
Duplicate/O 'IEF 8CA','IEF 8CA_smth';DelayUpdate
Duplicate/O 'IEF 9AC','IEF 9AC_smth';DelayUpdate
Duplicate/O 'IEF 9CA','IEF 9CA_smth';DelayUpdate
Duplicate/O IEF10AC,IEF10AC_smth;DelayUpdate
Duplicate/O IEF10CA,IEF10CA_smth;DelayUpdate
Duplicate/O IEF11AC,IEF11AC_smth;DelayUpdate
Duplicate/O IEF11CA,IEF11CA_smth;DelayUpdate
Duplicate/O IEF12AC,IEF12AC_smth;DelayUpdate
Duplicate/O IEF12CA,IEF12CA_smth;DelayUpdate
Duplicate/O IEF13AC,IEF13AC_smth;DelayUpdate
Duplicate/O IEF13CA,IEF13CA_smth;DelayUpdate
Duplicate/O IEF14AC,IEF14AC_smth;DelayUpdate
Duplicate/O IEF14CA,IEF14CA_smth;DelayUpdate
Duplicate/O IEF15AC,IEF15AC_smth;DelayUpdate
Duplicate/O IEF15CA,IEF15CA_smth;DelayUpdate
Duplicate/O IEF16AC,IEF16AC_smth;DelayUpdate
Duplicate/O IEF16CA,IEF16CA_smth;DelayUpdate
Duplicate/O IEF17AC,IEF17AC_smth;DelayUpdate
Duplicate/O IEF17CA,IEF17CA_smth;DelayUpdate
Duplicate/O IEF18AC,IEF18AC_smth;DelayUpdate
Duplicate/O IEF18CA,IEF18CA_smth;DelayUpdate
Duplicate/O IEF19AC,IEF19AC_smth;DelayUpdate
Duplicate/O IEF19CA,IEF19CA_smth;DelayUpdate
Duplicate/O IEF20AC,IEF20AC_smth;DelayUpdate
Duplicate/O IEF20CA,IEF20CA_smth;DelayUpdate

Duplicate/O IEF21AC,IEF21AC_smth;DelayUpdate
 Duplicate/O IEF21CA,IEF21CA_smth;DelayUpdate
 Duplicate/O IEF22AC,IEF22AC_smth;DelayUpdate
 Duplicate/O IEF22CA,IEF22CA_smth;DelayUpdate
 Duplicate/O IEF23AC,IEF23AC_smth;DelayUpdate
 Duplicate/O IEF22CA,IEF23CA_smth;DelayUpdate
 Duplicate/O IEF22AC,IEF24AC_smth;DelayUpdate
 Duplicate/O IEF22CA,IEF24CA_smth;DelayUpdate
 Duplicate/O IEF22AC,IEF25AC_smth;DelayUpdate
 Duplicate/O IEF22CA,IEF25CA_smth;DelayUpdate
 Smooth 10, Blank1_smth,Blank2_smth,'IEF 0AC_smth','IEF 0CA_smth','IEF
 1AC_smth';DelayUpdate
 Smooth 10, 'IEF 1CA_smth','IEF 2AC_smth','IEF 2CA_smth','IEF 3AC_smth';DelayUpdate
 Smooth 10, 'IEF 3CA_smth','IEF 4AC_smth','IEF 4CA_smth','IEF 5AC_smth';DelayUpdate
 Smooth 10, 'IEF 5CA_smth','IEF 6AC_smth','IEF 6CA_smth','IEF 7AC_smth';DelayUpdate
 Smooth 10, 'IEF 7CA_smth','IEF 8AC_smth','IEF 8CA_smth','IEF 9AC_smth';DelayUpdate
 Smooth 10, 'IEF
 9CA_smth',IEF10AC_smth,IEF10CA_smth,IEF11AC_smth,IEF11CA_smth;DelayUpdate
 Smooth 10,
 IEF12AC_smth,IEF12CA_smth,IEF13AC_smth,IEF13CA_smth,IEF14AC_smth;DelayUpdate
 Smooth 10,
 IEF14CA_smth,IEF15AC_smth,IEF15CA_smth,IEF16AC_smth,IEF16CA_smth;DelayUpdate
 Smooth 10,
 IEF17AC_smth,IEF17CA_smth,IEF18AC_smth,IEF18CA_smth,IEF19AC_smth;DelayUpdate
 Smooth 10,
 IEF19CA_smth,IEF20AC_smth,IEF20CA_smth,IEF21AC_smth,IEF21CA_smth;DelayUpdate
 Smooth 10,
 IEF22AC_smth,IEF22CA_smth,IEF23AC_smth,IEF23CA_smth,IEF24AC_smth;DelayUpdate
 Smooth 10, IEF24CA_smth,IEF25AC_smth, IEF25CA_smth;DelayUpdate
 Display 'IEF 0AC_smth','IEF 1AC_smth','IEF 1CA_smth','IEF 2AC_smth','IEF 2CA_smth','IEF
 3AC_smth','IEF 3CA_smth','IEF 4AC_smth','IEF 4CA_smth','IEF 5AC_smth','IEF
 5CA_smth','IEF 6AC_smth','IEF 6CA_smth','IEF 7AC_smth','IEF 7CA_smth','IEF
 8AC_smth','IEF 8CA_smth','IEF 9AC_smth','IEF
 9CA_smth',IEF10AC_smth,IEF10CA_smth,IEF11AC_smth,IEF11CA_smth,IEF12AC_smth,IE
 F12CA_smth,IEF13AC_smth,IEF13CA_smth,IEF14AC_smth,IEF14CA_smth,IEF15AC_smth,IE
 F15CA_smth,IEF16AC_smth,IEF16CA_smth,IEF17AC_smth,IEF17CA_smth,IEF18AC_smth
 ,IEF18CA_smth,IEF19AC_smth,IEF19CA_smth,IEF20AC_smth,IEF20CA_smth,IEF21AC_sm
 th,IEF21CA_smth,IEF22AC_smth,IEF22CA_smth,IEF23AC_smth,IEF23CA_smth,IEF24AC_s
 mth, IEF24CA_smth,IEF25AC_smth, IEF25CA_smth
 Label left "Fluorescence Signal";DelayUpdate
 Label bottom "pH"
 ModifyGraph rgb('IEF 1AC_smth')=(65280,43520,0);DelayUpdate
 ModifyGraph rgb('IEF 1CA_smth')=(16384,65280,16384);DelayUpdate
 ModifyGraph rgb('IEF 2AC_smth')=(0,39168,0),rgb('IEF
 2CA_smth')=(0,43520,65280);DelayUpdate

ModifyGraph rgb('IEF 3AC_smth')=(0,0,65280),rgb('IEF
 3CA_smth')=(29440,0,58880);DelayUpdate
 ModifyGraph rgb('IEF 4AC_smth')=(65280,0,52224);DelayUpdate
 ModifyGraph rgb('IEF 4CA_smth')=(39168,0,15616);DelayUpdate
 ModifyGraph rgb('IEF 5CA_smth')=(65280,43520,0);DelayUpdate
 ModifyGraph rgb('IEF 6AC_smth')=(16384,65280,16384);DelayUpdate
 ModifyGraph rgb('IEF 6CA_smth')=(0,39168,0),rgb('IEF
 7AC_smth')=(0,43520,65280);DelayUpdate
 ModifyGraph rgb('IEF 7CA_smth')=(0,0,65280),rgb('IEF
 8AC_smth')=(29440,0,58880);DelayUpdate
 ModifyGraph rgb('IEF 8CA_smth')=(65280,0,52224);DelayUpdate
 ModifyGraph rgb('IEF
 9AC_smth')=(39168,0,15616),rgb('IEF10AC_smth')=(65280,43520,0);DelayUpdate
 ModifyGraph
 rgb('IEF10CA_smth')=(16384,65280,16384),rgb('IEF11AC_smth')=(0,39168,0);DelayUpdate
 ModifyGraph
 rgb('IEF11CA_smth')=(0,43520,65280),rgb('IEF12AC_smth')=(0,0,65280);DelayUpdate
 ModifyGraph
 rgb('IEF12CA_smth')=(29440,0,58880),rgb('IEF13AC_smth')=(65280,0,52224);DelayUpdate
 ModifyGraph
 rgb('IEF13CA_smth')=(39168,0,15616),rgb('IEF14CA_smth')=(65280,43520,0);DelayUpdate
 ModifyGraph
 rgb('IEF15AC_smth')=(16384,65280,16384),rgb('IEF15CA_smth')=(0,39168,0);DelayUpdate
 ModifyGraph
 rgb('IEF16AC_smth')=(0,43520,65280),rgb('IEF16CA_smth')=(0,0,65280);DelayUpdate
 ModifyGraph
 rgb('IEF17AC_smth')=(29440,0,58880),rgb('IEF17CA_smth')=(65280,0,52224);DelayUpdate
 ModifyGraph
 rgb('IEF18AC_smth')=(52224,0,20736),rgb('IEF19AC_smth')=(65280,43520,0);DelayUpdate
 ModifyGraph rgb('IEF19CA_smth')=(0,65280,0),rgb('IEF20AC_smth')=(0,39168,0);DelayUpdate
 ModifyGraph
 rgb('IEF20CA_smth')=(0,43520,65280),rgb('IEF21AC_smth')=(0,0,65280);DelayUpdate
 ModifyGraph
 rgb('IEF21CA_smth')=(29440,0,58880),rgb('IEF22AC_smth')=(65280,0,52224);DelayUpdate
 ModifyGraph rgb('IEF22CA_smth')=(39168,0,15616),
 rgb('IEF23CA_smth')=(65280,43520,0);DelayUpdate
 ModifyGraph
 rgb('IEF24AC_smth')=(16384,65280,16384),rgb('IEF24CA_smth')=(0,39168,0);DelayUpdate
 ModifyGraph rgb('IEF25AC_smth')=(0,43520,65280),rgb('IEF25CA_smth')=(0,0,65280)
 Display 'IEF 0AC_smth','IEF 1AC_smth','IEF 1CA_smth','IEF 2AC_smth','IEF 2CA_smth','IEF
 3AC_smth','IEF 3CA_smth','IEF 4AC_smth','IEF 4CA_smth','IEF 5AC_smth','IEF
 5CA_smth','IEF 6AC_smth','IEF 6CA_smth','IEF 7AC_smth','IEF 7CA_smth','IEF
 8AC_smth','IEF 8CA_smth','IEF 9AC_smth','IEF
 9CA_smth','IEF10AC_smth,IEF10CA_smth,IEF11AC_smth,IEF11CA_smth,IEF12AC_smth,IE
 F12CA_smth,IEF13AC_smth,IEF13CA_smth,IEF14AC_smth,IEF14CA_smth,IEF15AC_smth,I
 EF15CA_smth,IEF16AC_smth,IEF16CA_smth,IEF17AC_smth,IEF17CA_smth,IEF18AC_smth

,IEF18CA_smth,IEF19AC_smth,IEF19CA_smth,IEF20AC_smth,IEF20CA_smth,IEF21AC_smth,IEF21CA_smth,IEF22AC_smth,IEF22CA_smth,IEF23AC_smth,IEF23CA_smth,IEF24AC_smth, IEF24CA_smth,IEF25AC_smth, IEF25CA_smth
Label left "Fluorescence Signal";DelayUpdate
Label bottom "pH"
Display Current
Label left "Current(uA)";DelayUpdate
current=current*30
Label bottom "Time(min)"
SetScale/P x 0,0.00016666667,"", Current
SetAxis left 0,60
Display Voltage
Label left "Voltage(V)";DelayUpdate
Voltage=Voltage*3000
Label bottom "Time(min)"
SetScale/P x 0,0.00016666667,"", Voltage
SetAxis left 0,6000

Appendix B: IEF and Microfluidic Protocols

Glass Etching for Microfluidic Devices

Safety Precautions with HF. Hydrofluoric acid is particularly dangerous. It contains fluoride ions that can easily penetrate the skin and cause the destruction of deep tissue layers including bone. Unlike other acids that are easily neutralized, the activity of the F⁻ ion can continue for days. As such, prevention of exposure should be paramount and the appropriate personal protective gear should always be worn. Over 15 years of glass etching we have never experienced an exposure incident; nonetheless should one occur all personnel in the lab should be aware of the proper first aid response and how to clean up any spills.

Materials

1. Major lab Equipment needed
 - a. UV flood exposure system (e.g. OAI (San Jose, CA) or ThermoOriental (Stratford, CT))
 - b. Radiometer/Photometer with detector (e.g. Model IL1400A (Radiometer/Photometer), Model XRL340B (detector); International Light; Newburyport, MA)
 - c. Photoresist spinner (e.g. Model WS-400A-6NPP/LITE; Laurell; North Wales, PA) (NOTE: if coating microscope slides with photoresist)
 - d. Custom chuck for coating glass slides ((e.g. Embedded Vacuum Chuck; Laurell; North Wales, PA) can be ordered special to fit various sizes of glass slide)
 - e. Surface Profiler (KLA-Tencor, Milpitas, CA) (allows one to measure the channel depth)
 - f. Sonicator bath (e.g. 3510 Ultrasonic Cleaner; Branson; Danbury, CT)
 - g. Source for 18 MOhm•cm water (e.g. E-pure system; Barnstead; Dubuque, IA)
 - h. Clean hood (bench) to provide a clean area for bonding ((e.g. Purifier Horizontal Clean Bench; Labconco; Kansas City, MO). NOTE: A clean room could be used but it is significantly more expensive to maintain and operate)
 - i. Dicing saw (if using photomask blanks as a substrate material (e.g. (Model EC-400; MTI Corp.; USA; inexpensive but more than adequate to the task) NOTE: Alternatively, the glass plate can be scored and split using a glass scoring tool.
 - j. Air knife (optional, but makes drying the chips easier (e.g. Standard Air Knife; Exair; Cincinnati, OH)
 - k. Drying oven (e.g. Isotemp Vacuum Oven Model 280A; Fisher Scientific; Pittsburg, PA)
 - l. Programmable high temperature oven (e.g. Copper 120V Small Annealer; Evenheat; Caseville, MI)
 - m. Stirring plates (e.g. Isotemp Stirring Hotplate; Fisher Scientific; Pittsburg, PA)
2. Consumable Materials
 - a. Substrate material (One can use 4" square pre-coated glass photomask blanks or standard microscope slides)
 - i. 4" in x 4" (10.16 cm x 10.16 cm x 0.16 cm) soda-lime (or borosilicate or B-270) photomask blanks coated with chrome and AZ positive tone

- photoresist (e.g. Telic Co.; Santa Monica, CA. (This plate is used to make 8, 2" x 1" chips in parallel)
- ii. 1" x 3" or 2" x 3" glass slides (e.g. Fisher Scientific)
 - b. Clean, inert air source (e.g. cylinder of N₂, He or Ar)
 - c. 2-liter polypropylene containers with lids to hold the etching and developing solutions (e.g. Nalgene Polypropylene Jar; Fisher Scientific; Pittsburg, PA)
 - d. Cleaning detergent (e.g. Versa-Clean Liquid soap solution (Fisher Scientific; Pittsburgh, PA)
 - e. Cleanroom Swabs (e.g. Texwipe Microdenier Swab; Fisher Scientific; Pittsburg, PA)
 - f. Positive Tone Photoresist (for coating slides; e.g. AZ P4620; AZ Electronic Materials; Branchburg, NJ)
 - g. AZ 400K Developer (Shipley Co.; Marlborough, MA)
 - h. Chrome Mask Etchant (Transene, Co.; Danvers, MA)
 - i. Buffered Oxide Etchant (Transene Co.; Danvers, MA)
 - j. Wax
 - k. Concentrated HCl
 - l. 5M H₂SO₄
 - m. Acetone
 - n. Ethanol
 - o. Ammonium hydroxide
 - p. 30% Hydrogen peroxide
 - q. binder clips
 - r. Epoxy (e.g. Epo-tek 353ND; Epoxy Technologies, Inc.; Billerica, MA)

Methods

Solution preparation and glass slide coating.

1. Glass etch solution preparation (stable solution that can be used for several months depending upon the number of slides etched).
 - a. Add 1000 mL of 18 MOhm•cm water to 2 L polypropylene container.
 - b. Add 500 mL of concentrated HCl slowly to the same container to limit the temperature rise.
 - c. Wait 5 min.
 - d. Add slowly 250 mL of buffered oxide etchant (NH₄F/HF, 10:1) to the same container.
 - e. Stir for 10 min before use.
2. Hydrolysis solution preparation (This solution should be prepared immediately prior to use and disposed of properly afterward).
 - a. Prepare fresh each time just prior to use.
 - b. Add 400 mL of water to 1 L beaker.
 - c. Add 200 mL concentrated ammonium hydroxide slowly to same beaker.
 - d. Add 200 mL 30% hydrogen peroxide to the basic solution and use immediately.
3. Coating microscope slides with AZ photoresist. New, clean microscope slides should be coated with photoresist for transferring the pattern from the photomask to the substrate material. NOTE: chrome is not needed underneath the photoresist. The photoresist will hold up in the glass etching solution.

- a. Pour ~3 mL of AZ photoresist into a light tight vial and ensure that bubbles are removed. Let it warm up to room temperature for 1hr before using (do not let it stand at room temperature for more than 3 hours).
- b. Turn on UV Source to warm up.
- c. Preheat hot plate to 65°C. (NOTE: Processing parameters specific for AZ P4620. Refer to datasheet associated with photoresist for these parameters if using a different photoresist.)
- d. Check that the photoresist spin coater is clean (clean with acetone if necessary).
- e. Clean glass slide thoroughly using cleanroom swab and glassware detergent.
- f. Rinse slide with 18 MOhm•cm water and dry with compressed inert air.
- g. Place slide in oven at 100°C for 20 min, then let cool in clean hood.
- h. Turn on vacuum to the spin coater.
- i. Place slide on spin coater in a custom slide chuck and turn on vacuum.
- j. Pour ~1-2 mL of AZ onto the center of slide and close lid.
- k. Spin at 1000 rpm for 17 sec. (this will yield a 17 µm thick film).
- l. Open the lid slowly to prevent dripping.
- m. Soft bake the slide (covered to prevent exposure to light) on the hot plate for 2 min at 65°C and then ramp to 95°C and hold for 2 min then ramp to 120°C and hold for 4 min and let cool covered in clean hood for 20 min.
- n. Begin procedure for patterning immediately (see section 3.2).

Microchip Design and Fabrication

1. Chip designs can be drawn in-house using a CAD drawing program (e.g. AutoCAD LT;Thompson Learning Albany, NY) and electronically sent to photomask fabricators for translation and fabrication (e.g Fineline Imaging; Colorado Springs, CO). Laser photoplotted photomasks at a variety of resolutions (10,000-50,000 DPI) can be obtained from several sources and are much more economical than trying to create such masks in-house. (**Figure 1**) For mask features below 10 µm a more expensive glass photomask needs to be ordered (e.g. Advance Reproductions Corporation, Andover, MA).
2. Patterning microfluidic substrate material.

(Measure flood exposure system output using Photometer/Radiometer with detector to calculate exposure time to achieve proper UV dosage for photoresist used and film thickness. i.e. exposure time (sec) = dosage (mJ/cm²) ÷ output power (mW/cm²))

 - a. Place photomask PRINTED SIDE DOWN and quartz block (to ensure flatness of photomask) onto photoresist covered substrate (i.e. photomask blank or coated glass slide)
 - b. Place assembled substrate, photomask and quartz block into UV flood exposure enclosure and expose for the calculated exposure time (e.g. 25.2 sec for 17 µm thick film of AZ P4620 at a measured output power of 25 mW/cm²).

NOTE: From this point on in the protocol make sure that you have donned the proper personal protective gear to ensure safety including labcoat, safety glasses and the appropriate gloves.
3. Submerge the exposed slide in a stirred solution of Microposit Developer (Shipley Co.; Marlborough, MA) until channels are developed, followed by a thorough rinse with 18 MOhm•cm water.
4. Place the developed slide into a stirred, dilute buffered oxide etchant made up in section 3.1.1 for chemical etching.

5. Periodically measure the channel dimensions during the etching process using a stylus-based surface profiler. The average etch rate for this solution will be $\sim 1.03 \mu\text{m}/\text{min}$ for borosilicate glass. Every 5 min the chips should be turned 90° in order to ensure even etching. (NOTE: Over time the etching solution will get cloudy and the etch rate will decrease. Once the etch rate decreases below 75% of the initial rate, replace it.)
6. Once the channels are the desired depth, remove the remaining photoresist by rinsing the plate with acetone followed by an 18 MOhm \cdot cm water rinse.

Microchip Bonding

1. Thoroughly clean the etched and cover slides by swabbing with acetone followed by rinses with ethanol and 18 MOhm \cdot cm water.
2. Dry the slides under inert gas.
3. Submerge the slides in a stirred 5 M sulfuric acid solution for 5 min, rinse with 18 MOhm \cdot cm water, and then clean by swabbing with acetone followed by rinses with ethanol and 18 MOhm \cdot cm water.
4. Dry the slides under a flow of inert gas.
5. In a laminar flow hood, immerse the slides in a Versa-Clean Liquid soap solution (Fisher Scientific; Pittsburgh, PA), sonicate (3510 ultrasonic cleaner; Branson; Danbury, CT) for 15 min, rinse with 18 MOhm \cdot cm water and dry under inert gas.
6. Sonicate the slides in acetone for 10 min, dry, and place in the previously described dilute buffered oxide etch solution for 10 sec.
7. Immediately rinse the slides with 18 MOhm \cdot cm water and place in a dilute hydrolysis solution (1:1:2 parts NH_4OH , H_2O_2 , H_2O , respectively) for 12 min at 60°C .(9)
8. Rinse the slides with 18 MOhm \cdot cm water and sonicate in flowing 18 MOhm \cdot cm water for 60 sec before joining.
9. Remove the etched slides one at a time from the flowing stream of 18 MOhm \cdot cm water and place on a Cleanroom Wiper (DURX 670; Great Barrington, MA).
10. Remove the drilled cover slides from the flowing water and place on top of the respective etched slide.
11. Fasten binder clips on the perimeter of the chip to ensure contact between the two surfaces.
12. Remove the water from the channels with a vacuum hose.
13. Place the joined chips in the oven at 95°C for 15 min to drive out any remaining water.
NOTE: At this point if you see Newton's rings near or over a channel place the chip in a water bath, separate the 2 pieces and repeat steps 1-13. The rings indicate something is interfering with the bonding and that the chip will be unusable if you continue.
14. Place the chips in the high temperature oven and anneal using the following temperature program.
 - a. Ramp the temperature from room temperature to 530°C at $400^\circ\text{C}/\text{min}$
 - b. Once 530°C is reached, ramp to 560°C at $100^\circ\text{C}/\text{min}$ until the annealing temperature is reached. This can vary slightly depending upon the glass composition. We have found generally that 560°C works well.
 - c. Hold at the annealing temperature for 25 min and then allow to cool to room temperature overnight before removing.
15. Attach cylindrical glass reservoirs ($\sim 140 \mu\text{L}$ capacity) using Epo-tek 353ND Epoxy (Epoxy Technologies, Inc.; Billerica, MA) where the access holes are located.

Appendices

A.1 First-aid measures for hydrofluoric acid exposure

A. Skin contact

1. Remove victim from contaminated area and immediately (within seconds) shower and flush with plenty of water for 5 min.
2. Remove all clothing while in the shower. (Remove goggles last and double-bag contaminated clothes)
3. Take a tube of Calcium gluconate gel from First Aid kit. Use gloves while applying to prevent contact with uncontaminated skin. Massage the gel promptly and repeatedly into burned area until pain is relieved. Even if pain subsides within 20 to 30 minutes get medical help.

B. Breathing vapor

1. Immediately get to fresh air.
2. Keep the victim lying down, quiet and warm.
3. Call or have someone call for medical help.

C. ingestion

1. Drink large amount of water. Do not induce vomit.
2. Drink several glasses of milk or several ounces of magnesia may be given for a soothing effect.
3. Get medical help for the victim.

D. Eye contact

1. Irrigate eyes for at least 15 minutes with large amount of gently flowing water. Keep the eyes apart and away from eyeballs during irrigation.
2. Seek medical attention immediately after flushing the eyes.
3. Apply ice water compresses and if possible, continue irrigating the eyes until medical aid arrives.

Advice to physician:

For large skin area burns (totaling greater than 25 square inches), for ingestion and for significant inhalation exposure, severe systemic effects may occur. Monitor and correct for hypocalcemia, cardiac arrhythmias, hypomagnesemia and hyperkalemia. In some cases, renal dialysis may be indicated. For certain burns, especially of the digits, use of intra-arterial calcium gluconate may be indicated. For inhalation exposures, treat as chemical pneumonia. Monitor for hypocalcemia. 2.5% calcium gluconate in normal saline by nebulizer or by IPPB with 100% oxygen may decrease pulmonary damage, Bronchodilators may also be administered.

A.2 Neutralizing buffered oxide etch.

Use the Acid Spill Emergency Cleanup Kit.

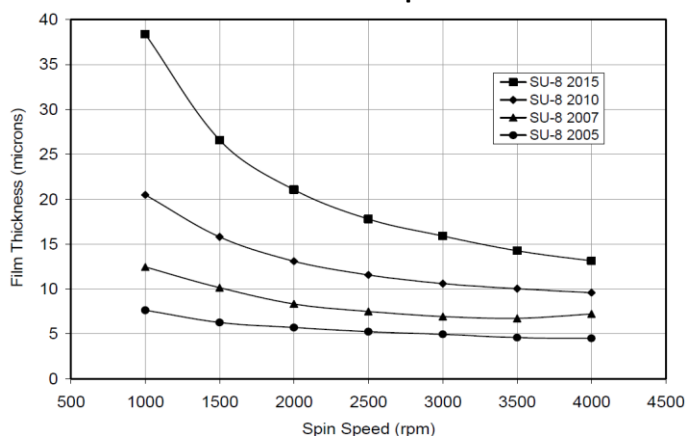
1. Protect yourself. Put on facial covers, gloves and shoes coverings.
2. Contain the spill. Surround the spill with absorbent/neutralizer mixture then fill circle with remaining mixture.
3. Dispose of used mixture and kit contents. After mixture turn blue, put it into waste bag using dust pan and brush. Seal bag tightly and place in kit along with kit contents. Close kit securely and dispose of in the appropriate manner.
4. Call the Department of Environmental Health and Safety for waste pickup.

Photolithography Procedure

SU-8 2010, Square Channels (Mostly Black Photomask = Negative Photoresist = Keep UV Exposed)

1. Clean Si wafer with piranha solution (70:30) ($\text{H}_2\text{SO}_4:\text{H}_2\text{O}_2$) for 20 min
2. Turn on UV Source to warm up
3. Preheat hot plates to 65°C and 95°C
4. Check that spin coater is clean (If not clean with acetone)
5. Rinse Si wafer with Ultrapure water and dry with compressed N_2
6. Place wafer in oven at 100°C for 20 min then let cool in clean hood
7. Turn on vacuum pump and verify it is on with the spin coater (should read >18)
8. Pour SU-8 into vial to remove bubbles (or use pre-poured located under spin coater)
9. Place Si wafer on spin coater and press Vac and then open N_2 cylinder (side small valve)
10. Pour ~3-4mL of SU-8 onto center of wafer and close lid
11. Set the spin coater to program M, then Press F1 to change the method and use the arrows to move through the method then press step to move to part two of the method and change then press F1 again to enter it
 - a. Spin at 700 rpm for 10sec at 300 RPM/sec
 - b. Spin at ___ rpm (use spin graph, 2nd line from top to determine) for 30sec at 300 RPM/sec
12. Soft bake the wafer covered on the hot plate for 2 min at 65°C and then 4 min at 95°C and let cool in clean hood
13. Determine the current power of the lamp by exposing the meter for 10sec
14. Use the table below to determine the dosage then divide by the power (from the meter) to get the time in sec for exposure
15. Clean off photomask with N_2 gas and clean quartz block with tape
16. Align mask on the wafer then place quartz block on top
17. Expose the mask for ___ sec (Turn away to reduce exposure of your eyes to UV light)
18. Post Exposure bake the wafer on the hot plate for 2 min at 65°C and then 4 min at 95°C, let cool in clean hood
19. Develop in 2(1-methoxy) propylacetate (reusable- store in fume hood in vial, labeled) and verify with isopropyl alcohol once complete (Should not turn cloudy if complete)
20. Dry with N_2 gas <50kPa
21. Hard Bake at 145°C for 5min then turn off hotplate and let cool with wafer

SU8 Data Graphs



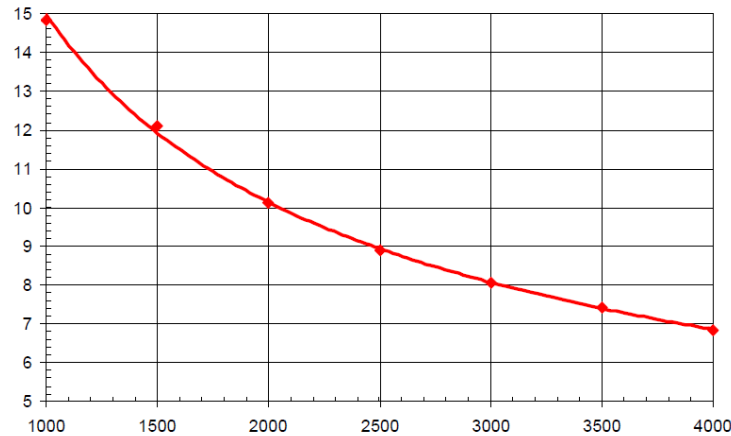
THICKNESS microns	EXPOSURE ENERGY mJ/cm ²	RELATIVE DOSE	THICKNESS microns	DEVELOPMENT TIME minutes
0.5 - 2	60 - 80	Silicon 1X	0.5 - 2	1
3 - 5	90 - 105	Glass 1.5X	3 - 5	1
6 - 15	110 - 140	Pyrex 1.5X	6 - 15	2 - 3
16 - 25	140 - 150	Indium Tin Oxide 1.5X	16 - 25	3 - 4
26 - 40	150 - 160	Silicon Nitride 1.5 - 2X	26 - 40	4 - 5
		Gold 1.5 - 2X		
		Aluminum 1.5 - 2X		
		Nickel Iron 1.5 - 2X		
		Copper 1.5 - 2X		
		Nickel 1.5 - 2X		
		Titanium 1.5 - 2X		

AZ, Hemispherical Channels (Mostly Transparent Photomask = Positive Photoresist = Keep UV Unexposed)

1. Get out AZ P4620 and pour ~5mL into a vial to remove bubbles so it can warm up to Room Temp for 1hr before using (No more than 3 hours)
2. Clean Chrome coated Si wafer with AZ® Kwik Strip heated to 60°C in the hood for 10 min
3. Turn on UV Source to warm up
4. Preheat hot plates to 65°C
5. Check that spin coater is clean (clean with acetone)
6. Rinse Si wafer with Ultrapure water and dry with compressed N₂
7. Place wafer in oven at 100°C for 20 min then let cool in clean hood
8. Turn on vacuum pump
9. Place Si wafer on spin coater and press Vac and then open N₂ cylinder (side small valve)
 - a. Vac should read >18 on the upper right
10. Pour ~3-4mL (fill inner ½) of AZ onto center of wafer and close lid
11. Set the spin coater to program A, then Press F1 to change the method and use the arrows to move through the method then press F1 again to enter it
 - a. Spin at _____ rpm (use spin graph to determine) for 17sec at 300 RPM/sec
12. Open the lid slowly to prevent dripping
13. Soft bake the wafer, covered, on the hot plate for 2 min at 65°C and then ramp to 95°C and hold for 2 min then ramp to 120°C and hold for 4 min and let cool covered in clean hood for 20 min
14. Use the power meter on the UV light (10sec exposure) and record the value in mW/cm²
15. Calculate the seconds needed using the dose requires as 630mJ/cm² (1W=1J/sec)
16. Clean off photomask with N₂ gas and clean quartz block with tape
17. Align mask on the wafer then place quartz block on top

18. Expose the mask for ___ sec for mask aligner exposure (Turn away to reduce exposure of your eyes to UV light)
19. Let sit covered for 10min
20. Develop in 1:4 AZ developer with gentle swirling and verify with Ultrapure water once complete-takes 3-5min
 - a. Be careful as the channels are very fragile
21. Dry with N₂ gas <50kPa
22. Place on hot plate at 120°C for 4 min

AZ P4620 Spin Speed vs Thickness



Make IEF PDMS Devices

1. Make 10:1 PDMS by weighing 9 g PDMS and 0.9 g Curing Agent
2. Stir with coffee stirrer for 1-2 min until well mixed
3. Place in vacuum for 30 min to remove bubbles
4. Add 5uL Xylenes +HTMD to the AZ master as a release agent
5. Pour the 10:1 PDMS on the AZ master with a plastic frame to create thickness in the oven for 30min
6. Clean the spin coater with acetone immediately
7. After 1hr 30min remove the device and take to the clean hood
8. Remove the plastic frame, by cutting around the edges with a small scalpel then slowly and carefully with minimal pressure pull off the PDMS (you can crack the master if not careful)
9. Trim the edges and then punch the reservoirs with the yellow punch (3mm)
 - a. Press straight down, make sure edge is in channel
 - b. Twist and then remove center with wire then twist to remove
10. Use tape to clean the channel and PDMS to seal to a glass slide
11. Place the two pieces together and remove any bubbles by slightly pulling up and then smoothing down carefully
12. Cover the top with tape and label the tape with date of creation (Always label the tape to keep track of use of the chips)

Make PDMS Covered Glass Slides

1. Make 10:1 PDMS by weighing 5 g PDMS and 0.5 g Curing Agent
2. Stir each with coffee stirrer for 1-2 min until well mixed
3. Place in vacuum for 30 min to remove bubbles
4. Clean ~7 glass slides by placing them in the sonicator a beaker with a small amount of Alcanox for 15min
5. Then rinse the slides in the sonicator in ultrapure water for 25min
6. Dry the slides with compressed N₂
7. Spin coat small amounts of the 5g PDMS on the glass slides glass slide (32sec, 2000 RPM)
8. Place the slides in an oven set at 80°C for 1 hr 30min
9. Cover the glass slides with tape and store

Appendix C: Mass Spectrometry Results for Serpin2 Co-IP

Experiments

5/20/2016					95% Peptide TH		95% Peptide TH
Name	Identified Proteins	Accession Number	Molecular Weight	Unique Peptide	Amino Acids	Total Amino Acids	% Coverage
Paralogue to CLIPC3,D1,C10,C5 ,C9,C4,C6	AGAP012946-PA	gi 333468851	35.46	1			3%
CLIPA14	AGAP011788-PA	gi 116117255	30 kDa	3	45	281	16%
CLIPA5	AGAP011787-PA	gi 347972680	43.49	1			4%
CLIPA6	AGAP011789-PA	gi 333469696	46 kDa	5	65	427	15%
CLIPA9	AGAP010968-PA	gi 347972523	39.61	1			3%
CLIPB12	AGAP009217-PA	gi 333469689	38 kDa	3	49	341	14%
CLIPB13	AGAP004855-PA	gi 58385954	45 kDa	3	36	410	9%
CLIPB5	AGAP004148-PA	gi 347971337	41 kDa	3	45	379	12%
CLIPB8	AGAP003057-PA	gi 30177147	45 kDa	5	45	405	11%
CLIPC7	AGAP003691-PA	gi 347970404	94 kDa	2	22	831	3%
CLIPC7	AGAP003689-PA	gi 333468916	67 kDa	3	39	594	7%
CLIFE4	AGAP010530-PA	gi 116127990	33.95	1			6%
CLIFE5	AGAP010545-PA	gi 158293179	98 kDa	3	35	876	4%
CLIFE5	AGAP010547-PA	gi 116128005	42 kDa	3	42	373	11%
PPO1	pro-phenol oxidase subunit 1	gi 2654527	78 kDa	10	142	688	21%
PPO3	AGAP004975-PA	gi 55239677	79 kDa	6	132	686	19%
PPO6	AGAP004977-PA	gi 31212181	79 kDa	8	96	687	14%
PPO9	prophenoloxidase 9	gi 20803453	78.01	1			2%
serine protease- like protein	serine protease-like protein	gi 8250039	25 kDa	2	22	219	10%
Serpin 2	serpin 2	gi 116041593	47 kDa	7	110	409	27%
Serpin11	serpin 11	gi 116041609	57 kDa	7	87	508	17%
Serpin11	serpin 11 non-inhibitory serine protease inhibitor	gi 240270550	30 kDa	2	68	259	26%
Serpin14	serine protease 14	gi 224038103	40 kDa	7	104	360	29%
Serpin16	serpin 16	gi 116041617	61 kDa	6	95	553	17%
Serpin3	AGAP006910-PA	gi 158286633	47 kDa	5	62	418	15%
Serpin4	AGAP009670-PA	gi 157013934	69 kDa	5	55	623	9%
Serpin4	AGAP009670-PB	gi 158298542	62 kDa	3	43	547	8%
Serpin8	serpin 8	gi 116041605	49 kDa	2	24	434	6%
Serpin9	serpin 9	gi 116041607	50 kDa	2	27	447	6%
SP14D1	AGAP013252-PA	gi 347970973	67 kDa	3	38	597	6%
TEP12	AGAP008654-PA	gi 347972960	96.28	1			1%
TEP15	AGAP008364-PA	gi 333469487	164 kDa	16	221	1476	15%
TEP4	AGAP010812-PA	gi 347972485	149 kDa	2	19	1335	1%

Figure C.1: Mass spectral from the final experiment to identify Co-IP Serpin2 binding partners.

Identified protein	Protein Name	Interesting Proteins		Non Specifically Bound Proteins			8/28/2014	1/14/2015
		2/25/2013	4/16/2013	5/2/2013	7/22/2014	7/22/2014 Control		
AGAP009217-PA	CLIPB12				x			
AGAP004148-PA	CLIPB5							x
AGAP003689-PA	CLIPC7				x			x
CLIPB1 protein, partial	CLIPB1							x
AGAP009844-PA	CLIPB15	x			/x			
serine protease 14D	CLIPB4	x			x		x	x
AGAP011788-PA	CLIPA14	x	x	x	x		x	x
AGAP011781-PA	CLIPA12							
AGAP011791-PA	CLIPA1							
AGAP011789-PA	CLIPA6	x		x	x			x
AGAP011792-PA	CLIPA7	x	x	x	x		x	x
serpin 11	Serpin 11			x	x		x	x
serpin 2	Serpin 2	x	x	x	x		x	x
serpin 4A	Serpin 4A							x
serpin 9	Serpin 9				x			x
TEP1, partial	TEP1				x		x	x
AGAP008364-PA	TEP15			x	x		x	x
AGAP010812-PA	TEP4							x
AGAP009146-PA	AgamP3			x				x
APOII/I, partial	APO II/I				x		x	
AGAP012045-PA	ATP-dependent RNA helicase DDX5/DBP2		x				x	x
AGAP013509-PA	Carboxylesterase clade H, member 1			x				x
APL1C	Complex with TEP 1							x
dopachrome conversion enzyme	dopachrome conversion enzyme				x			x
AGAP002564-PA	fructose-bisphosphate aldose				x		x	x
AGAP011369-PA	gelsolin				x			x
AGAP003873-PA	Notch signaling pathway phenoloxidase inhibitor protein							x
phenoloxidase inhibitor protein	phenoloxidase inhibitor protein							x
prophenoloxidase	PPO				x			
pro-phenol oxidase subunit	PPO1				x			x
AGAP004977-PA	prophenyloxidase							x
AGAP010750-PA	ryanodine receptor 2		x					x
SGS3	Salivary Gland Surface Protein							x
serine protease	serine protease							x
AGAP000376-PA	Transferrin				x			x
AGAP003691-PA	Tryp_SPC- Trypsin like serine protease				x			
AGAP012966-PA		x						x
AGAP000651-PB	Actin 5C				x	x	x	
AGAP007406-PA	elongation factor 1 alpha				x	x	x	x
AGAP003911-PA	histone H2A				x	x	x	
AGAP012558-PA	histone H4				x	x		
AGAP001826-PA	Lipophorin (Lg)			x	x	x	x	x

Figure C.2: Mass spectral results from multiple Co-IP experiments for the determination of Serpin2 binding partners

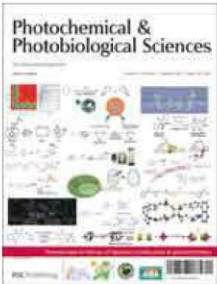
Pink labeled identifications are non-specifically bound peptides that elute from the Protein A beads used to preclear the hemolymph. All other colors indicate possible biological classes of compounds or possible biological relevance.

Appendix D: Figure Permissions

Figure 2.1 Permission

5/3/2018 Rightslink® by Copyright Clearance Center

  [Home](#) [Create Account](#) [Help](#) 



Title: Nanoplatforams for highly sensitive fluorescence detection of cancer-related proteases

Author: Hongwang Wang, Dinusha N. Udukala, Thilani N. Samarakoon, Matthew T. Basel, Mausam Kalita, Gayani Abayaweera, Harshi Manawadu, Aruni Malalasekera, Colette Robinson, David Villanueva, Pamela Maynez, Leonie Bossmann, Elizabeth Riedy, Jenny Barriga, Ni Wang, Ping Li, Daniel A. Higgins, Gaohong Zhu, Deryl L. Troyer, Stefan H. Bossmann

Publication: Photochemical & Photobiological Sciences

Publisher: Royal Society of Chemistry

Date: Sep 24, 2013

Copyright © 2013, Royal Society of Chemistry

LOGIN

If you're a **copyright.com** user, you can login to RightsLink using your copyright.com credentials. Already a **RightsLink** user or want to [learn more?](#)

Quick Price Estimate

The reuse of up to three figures is granted free of charge for academic/educational requestors. Payment is required for the reuse of four or more figures.

I would like to... ?	<input type="text" value="reuse in a thesis/dissertation"/>	No content delivery. This service provides permission for reuse only. Once licensed, you may copy and paste the text-only portion of the content according to the terms of your license.
I am a/an... ?	<input type="text" value="academic/educational"/>	
The portion I would like to use is... ?	<input type="text" value="figures/tables/images"/>	
Number of figures/tables/images requested ?	<input type="text" value="1"/>	
My format is... ?	<input type="text" value="print and electronic"/>	
My distribution is ?	<input type="text" value="100"/>	
I will be translating... ?	<input type="text" value="no"/>	
My currency is...	<input type="text" value="USD - \$"/>	
Quick Price	0.00 USD	

[QUICK PRICE](#) [CONTINUE](#)

To request permission for a type of use not listed, please contact Royal Society of Chemistry contracts-copyright@rsc.org.

Copyright © 2018 [Copyright Clearance Center, Inc.](#) All Rights Reserved. [Privacy statement](#). [Terms and Conditions](#). Comments? We would like to hear from you. E-mail us at customercare@copyright.com

Figure 2.4 Permission

5/3/2018

Author FAQ | PNAS

Can others (nonauthor third parties) use my original figures or tables in their works without asking PNAS for permission?

PNAS automatically permits others to use original figures or tables published in PNAS for noncommercial and educational use (i.e., in a review article, in a book that is not for sale), provided that the full journal reference is cited and, for articles published in volumes 90–105 (1993–2008), "Copyright (copyright year) National Academy of Sciences." Commercial reuse of figures and tables (i.e., in promotional materials, in a textbook for sale) requires permission from PNAS. Please see [PNAS Rights and Permissions](#).

Figure 4.1 Permission



Image Reuse Terms and Conditions

Most images found in the [Public Health Image Library \(PHIL\)](http://phil.cdc.gov/) (<http://phil.cdc.gov/>) are royalty-free and available for personal, professional and educational use in electronic or print media, with appropriate citation. Please credit CDC and the individual photographer if his/her name is given. If used in electronic media, please link back to the [PHIL site](http://phil.cdc.gov/) (<http://phil.cdc.gov/>).

Images other than those in the PHIL may have been licensed for use by CDC from a stock photography service or other copyright holder and the license holder may prohibit republication, retransmission, reproduction or other use of the images. Please [contact us](#) with any other questions about reuse of specific images.

Get Email Updates

To receive email updates about this page, enter your email address:

What's this? (<https://www.cdc.gov/emailupdates/>)

Submit (javascript:quickssubscribe();return false;)

Page last reviewed: March 19, 2014

Page last updated: March 19, 2014

Content source: Centers for Disease Control and Prevention (<https://www.cdc.gov/>)

Page maintained by: Office of the Associate Director for Communication, Division of Public Affairs

Figure 4.2 Permission

5/3/2018 Rightslink® by Copyright Clearance Center



[Home](#) [Create Account](#) [Help](#)



Title: Serpin Structure, Mechanism, and Function
Author: Peter G. W. Gettins
Publication: Chemical Reviews
Publisher: American Chemical Society
Date: Dec 1, 2002
Copyright © 2002, American Chemical Society

LOGIN

If you're a copyright.com user, you can login to RightsLink using your copyright.com credentials. Already a **RightsLink user** or want to [learn more?](#)

PERMISSION/LICENSE IS GRANTED FOR YOUR ORDER AT NO CHARGE

This type of permission/license, instead of the standard Terms & Conditions, is sent to you because no fee is being charged for your order. Please note the following:

- Permission is granted for your request in both print and electronic formats, and translations.
- If figures and/or tables were requested, they may be adapted or used in part.
- Please print this page for your records and send a copy of it to your publisher/graduate school.
- Appropriate credit for the requested material should be given as follows: "Reprinted (adapted) with permission from (COMPLETE REFERENCE CITATION). Copyright (YEAR) American Chemical Society." Insert appropriate information in place of the capitalized words.
- One-time permission is granted only for the use specified in your request. No additional uses are granted (such as derivative works or other editions). For any other uses, please submit a new request.

If credit is given to another source for the material you requested, permission must be obtained from that source.

[BACK](#)

[CLOSE WINDOW](#)

Copyright © 2018 Copyright Clearance Center, Inc. All Rights Reserved. [Privacy statement](#). [Terms and Conditions](#). Comments? We would like to hear from you. E-mail us at customer@copyright.com

Figure 4.16 Permission



11200 Rockville Pike
Suite 302
Rockville, Maryland 20852

August 19, 2011

American Society for Biochemistry and Molecular Biology

To whom it may concern,

It is the policy of the American Society for Biochemistry and Molecular Biology to allow reuse of any material published in its journals (the Journal of Biological Chemistry, Molecular & Cellular Proteomics and the Journal of Lipid Research) in a thesis or dissertation at no cost and with no explicit permission needed. Please see our copyright permissions page on the journal site for more information.

Best wishes,

Sarah Crespi

[American Society for Biochemistry and Molecular Biology](#)

11200 Rockville Pike, Rockville, MD

Suite 302

240-283-6616

[JBC](#) | [MCP](#) | [JLR](#)